8-2024

Degradation Products and Microbial Communities Associated with the Conversion of Five Long-chain Fatty Acids Relevant for Anaerobic Co-digestion of FOG with Sludge

Claire Funk
Clemson University, cefunk@clemson.edu

DEGRADATION PRODUCTS AND MICROBIAL COMMUNITIES ASSOCIATED WITH THE CONVERSION OF FIVE LONG-CHAIN FATTY ACIDS RELEVANT FOR ANAEROBIC CO-DIGESTION OF FOG WITH SLUDGE

A Thesis
Presented to
the Graduate School of
Clemson University

In Partial Fulfillment
Of the Requirements for the Degree
Master of Science
Environmental Engineering and Science

By
Claire Funk
August 2024

Approved by:

Dr. Sudeep Popat, Committee Chair
Dr. Kevin Finneran, Committee Member
Dr. David Freedman, Committee Member

Abstract

Anaerobic digestion is a technology that allows wastewater treatment plants to convert sludge to energy by recovering the biogas produced during the breakdown of proteins, carbohydrates, and lipids. Furthermore, adding fats, oils, and greases (FOG) through co-digestion with wastewater sludge can increase energy production as lipids have a higher methane yield than proteins and carbohydrates. However, adding FOG can also lead to operational problems in the digester due to the potential accumulation of certain long-chain fatty acids (LCFAs). Current research is limiting in the degradation pathways of prominent LCFAs in FOG and the microbial communities responsible for their degradation

The objective of this research is to investigate the degradation pathways and intermediates of five LCFAs prevalent in municipal wastewater sludge and analyze the microbial communities involved in their degradation.

This study was completed using batch assays. Each acid chosen was analyzed at 2, 4, and 6 g/L COD. The study employed the use of a gas chromatograph (GC) for the analysis of biogas produced in the assays, a GC flame ionizing detector for the analysis of LCFAs, a high-performance liquid chromatograph for the analysis of volatile fatty acids, a third party for sequencing data, and qiime2 for sequencing analysis.

The results of this study revealed a correlation between lag time in methane production and saturation as the unsaturated acids had much longer lag times when compared to the saturated acids. There was no apparent correlation between chain length of saturated acids and lag time. In the unsaturated assays and myristic 6 g/L COD, the pH dropped significantly due to acetate accumulation. The pH dropped below the optimum of 6.8 for methanogens, causing more acetate to accumulate. *Syntrophomonas*, the suspected beta oxidizer, has an optimal pH of 6.5. pH levels

below 6.5 could have been the cause of palmitic acid accumulation in the unsaturated assays since some of these assays had pHs below this value.

For the saturated acids, the anticipated LCFA intermediates that should have formed through beta-oxidation were not observed and did not accumulate. Both unsaturated acids had palmitic acid accumulate at high concentrations and stearic acid accumulate at low concentrations. The degradation pathway for unsaturated acids can be concluded to be either hydrogenation followed by beta-oxidation or simultaneous hydrogenation and beta-oxidation. There was no inhibitor identified for the saturated acids. The inhibitor for the unsaturated acids was palmitic acid.

Based on the degradation kinetics calculations for the saturated acids, myristic acid degraded the fastest followed by palmitic and stearic acid. Of the unsaturated acids, oleic acid degraded faster than linoleic acid. Both unsaturated acids degraded faster than the three saturated acids.

Acetate was the only volatile fatty acids observed at a high concentration. Acetate accumulated in varying degrees in all assays except the stearic acid assays. Propionate and butyrate were present in most assays and controls, but production and degradation did not correspond to lag phases or periods of inhibition. In all instances of a low pH, the cause can be linked to acetate accumulation.

Based on sequencing data, different microbial communities were present in unsaturated acid assays when compared to saturated acid assays. Also, the unsaturated acid assays also had differing microbial communities when compared to each other. In the saturated acid assays, the microbial communities associated with each concentration of each saturated acid was similar. However, in the unsaturated acids, the microbial communities at each concentration of each acid varied significantly.

Acknowledgements

First and foremost, I would like to thank my advisor Dr. Sudeep Popat for helping me develop my research project and for asking critical questions along the way. His guidance has helped to broaden my understanding of the wastewater field and has encouraged me to pursue a career in wastewater treatment design. I am also thankful for my undergraduate students, Julia Shashok and Hughes Clark, who assisted me in lab. They were both extremely helpful over the last year in preparing samples.

I would also like to thank the Environmental Engineering and Earth Sciences department for providing me with a teaching assistantship that allowed me to continue my education at Clemson. I have loved the experience of teaching undergraduate students. In addition, I am very grateful for this department and all of the professors who have contributed to my education, specifically my advisor and committee members, Dr. Sudeep Popat, Dr. David Freedman, and Dr. Kevin Finneran. Thank you for always pushing me to do my best and for helping me to become the Environmental Engineer I am today.

I would also like to express my deepest appreciation to my sister and lab buddy, Julia Ann Funk-Morris, for her help and guidance this last year. Thank you for taking time to teach me how to use all of the instruments in lab and for answering my millions of questions. I also thank you for your willingness to listen and talk through my data with me to help me better understand the results.

Lastly, I would like to thank my family and fiancé for their constant support and encouragement. Thank you for always being willing to let Julia Ann and I talk about wastewater at the dinner table. I would also like to specifically thank my dad and Papa for instilling in me the desire to problem solve. I am proud to be a third generation Clemson Engineer.

Table of Contents

List of Tables

List of Figures

Abbreviations

Fats, Oils, and Grease (FOG)

Long Chain Fatty Acid (LCFA)

Volatile Fatty Acid (VFA)

Denaturing Gradient Gel Electrophoresis (DGGE)

Maximum Substrate Utilization Rate (*k)*

Anaerobic Digestion Model No.1 (ADM1)

Chemical Oxygen Demand (COD)

Distilled De-ionized (DDI)

Gas Chromatograph (GC)

Methyl Tert-Butyl Ether (MTBE)

Fatty Acid Methyl Ester (FAME)

Flame Ionizing Detector (FID)

Polyvinylidene Filter (PVDF)

High-performance Liquid Chromatograph (HPLC)

Polymerase Chain Reaction (PCR)

National Center for Biotechnology Information (NCBI)

Quantitative Insights into Microbial Ecology (QIIME)

Water Resource Recovery Facility (WRRF)

Electron Milliequivalents (meeq)

Apparent Degradation Constant (k)

Maximum Methane Production Rate (k_p)

continuously stirred tank reactor (CSTR

Principle Coordinate Analysis (PCoA)

1. Research Significance

Anaerobic digestion is a technology that allows wastewater treatment plants to convert sludge to energy by recovering the biogas produced during the breakdown of proteins, carbohydrates, and lipids. Furthermore, adding fats, oils, and greases (FOG) through co-digestion with wastewater sludge can increase energy production as lipids have a higher methane yield than proteins and carbohydrates.[1] However, adding FOG can also lead to operational problems in the digester due to the potential accumulation of certain long-chain fatty acids (LCFAs). The successful operation of anaerobic co-digestors requires fundamental research, specifically into degradation pathways and microbial communities involved in beta-oxidation. This thesis was designed to understand better the degradation pathways and intermediates of five specific LCFAs dominant in FOG co-digestion and analyze the microbial communities involved in their degradation.

2. Background and Literature Review

2.1 Biochemistry of Anaerobic Digestion

The anaerobic digestion of organic waste consists of five important microbially-mediated conversions—hydrolysis, fermentation, beta-oxidation, acetogenesis, and methanogenesis.[2] Figure 2.1 shows the degradation of complex organic matter ultimately to methane. During hydrolysis, particulate organic matter in the form of carbohydrates, proteins, and lipids are hydrolyzed into simple sugars, amino acids, and LCFAs, respectively.[3] Fermentation of simple sugars and amino acids produces CO_2, H_2, acetate, and other preliminary volatile fatty acids (VFAs). The preliminary VFAs, typically consisting of butyrate and propionate, are anaerobically oxidized into CO_2, H_2, and acetate. LCFAs are beta-oxidized to CO_2, H_2, and acetate. Through methanogenesis, methanogenic archaea use acetate, CO_2/H_2, or secondary alcohols as carbon and energy sources to produce methane as their metabolic end-product.[4] Acetolactic methanogens utilize acetate, while hydrogenotrophic methanogens utilize CO_2 and H_2. A syntrophic environment must be maintained between methanogens, fermenters, and bacteria employing beta- and anaerobic oxidation. Hydrogenotrophic methanogens maintain a low partial pressure of H_2 (e.g., ~10^{-4} atm), which results in thermodynamically favorable conditions for fermentation and oxidation.[5] Anaerobic

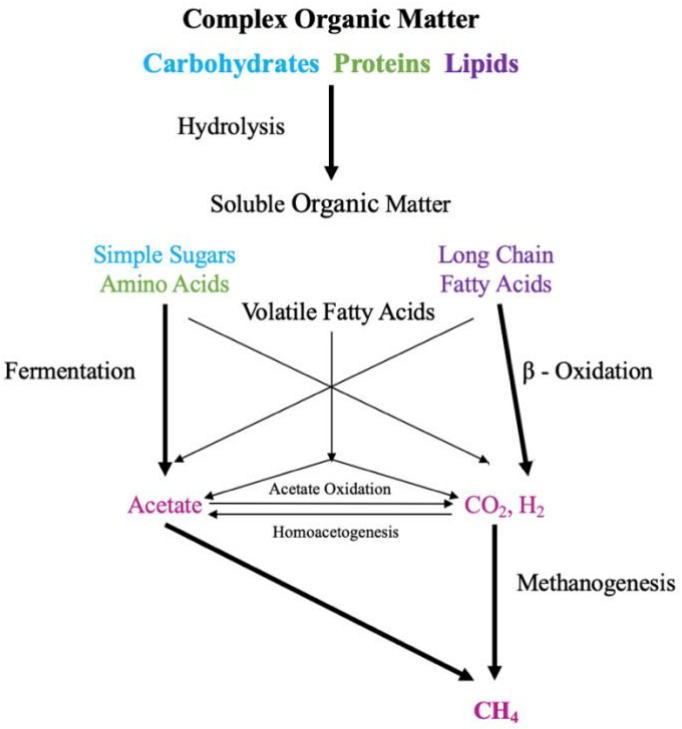

Figure 2.1: Illustration of biochemical processes occurring in anaerobic digestion

digestion is thus a complex system of microbial communities sensitive to environmental changes; therefore, additional research is required to ensure digesters optimally operate to maximize methane production, especially when specific constituents are increasingly fed as part of co-digestion approaches (see below).

2.2 Anaerobic Co-digestion and Lipid Hydrolysis

Anaerobic co-digestion of FOG is the simultaneous digestion of solids generated at a wastewater treatment plant and FOG accumulated in grease traps at restaurants and factories.[6] Lipids are more attractive substrates for co-digestion due to their higher methane yield than proteins and carbohydrates.[1] Therefore, the co-digestion of FOG as a renewable energy source should be further explored. FOG primarily comprises lipids, which rapidly hydrolyze to glycerol and free acids or LCFAs.[6] If LCFAs accumulate, they can be toxic and detrimental to microorganisms, thus impeding overall digester performance. The accumulation of LCFAs can lead to sludge flotation and eventual unwanted biomass washout, affecting the operational efficiency of the digester.[7] LCFAs also physically affect microorganisms as the acids impact cell membrane functions. At high concentrations, LCFAs lead to macromolecular crowding and disruptions to the proton motive force, DNA-docking, and ATP-chemosynthesis.[8] LCFAs also reduce substance transport efficiency and nutrient uptake by coating the cell wall.[9] While LCFAs have been reported to be acutely toxic to hydrogenotrophic and acetolactic methanogens, the inhibition has been proven to be reversible, creating opportunities for the digestion of waste with high lipid content.[10] Since lipid hydrolysis of LCFAs is rapid and these LCFAs are microbially toxic in co-digestion, understanding the kinetics of LCFA degradation is necessary. The principal LCFAs resulting in municipal wastewater are myristic, palmitic, stearic, oleic, and linoleic acids. These acids comprise over 90% of the fatty acids in municipal wastewater sludge, and their

degradation must be further studied to understand their degradation pathways and ensure methane recovery is optimized.[11]

2.3 Beta-oxidation

Fatty acids are carboxylic acids with a hydrophilic head and a hydrophobic aliphatic tail. Typically, carboxylic acids with greater than 12 carbons are considered LCFAs, and the absence or presence of double bonds in the aliphatic tail determines if the molecule is saturated or unsaturated.[12] Myristic, palmitic, and stearic acid are saturated molecules (i.e., no double bonds) with 14, 16, and 18 carbons, respectively. Oleic and linoleic acid are 18-carbon unsaturated molecules with one and two double bonds, respectively. Figure 2.2 displays each of these acids with their respective carbon length and saturation.[13]

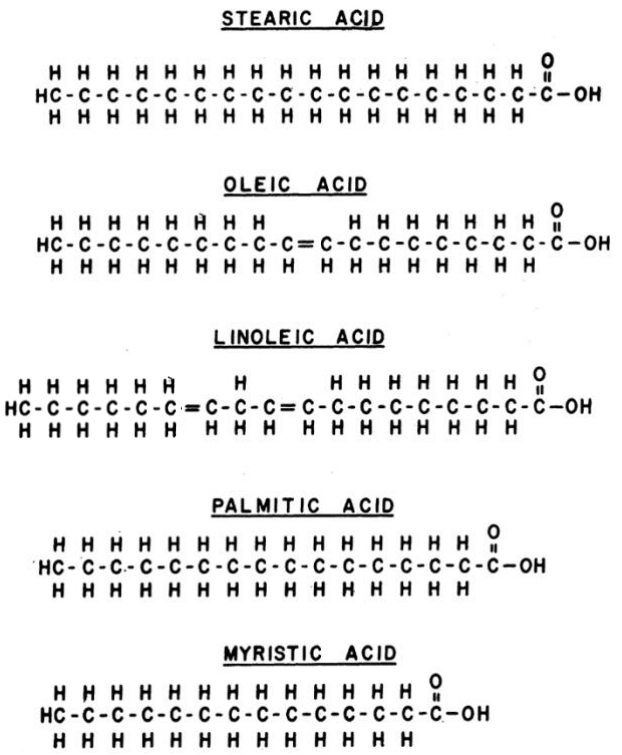

Figure 2.2: Molecular structure of the five LCFAs most prevalent in municipal wastewater.[13]

Hwu et al. [14] have proposed a four-phase description explaining the inhibition and oxidation of LCFAs in anaerobic digesters. First, LCFAs rapidly disappear from the aqueous phase upon addition to wastewater because they adsorb to biomass. The coating of the LCFAs on the cell's surface inhibits nutrient uptake and is ultimately toxic to the cell.[9] During this time, little to no methane is produced as the cells lack nutrients for metabolic functions. Slowly, the aqueous phase LCFA concentration will increase as LCFAs desorb from the surface of the cell. As LCFAs desorb, methane begins to be produced. Thirdly,

the LCFA concentration decreases in the aqueous phase as beta-oxidation occurs, and nutrients can begin to pass through the cell membrane. Finally, methane will be recovered once the adsorbed LCFA concentration is low, and the substrate can flow freely through the cell membrane.[14]

LCFAs are biologically degraded by obligate syntrophic communities of proton-reducing acetogenic bacteria that convert LCFAs to acetate and H_2 via beta-oxidation, as described in the third phase above.[4] Both saturated and unsaturated molecules are degraded via beta-oxidation. Saturated molecules enter directly into beta-oxidation, while the degradation of unsaturated acids may require hydrogenation before beta-oxidation.[6] Figure 2.3 shows the cycle of beta-oxidation.[15] Beta-oxidation is initiated by LCFA transport through the cellular membrane via the transport/acyl-activation mechanism, forming fatty acyl-CoA. For example, palmitic acid will be transported into the membrane and form palmityl-CoA. As the fatty acyl-CoA goes through beta-oxidation, 2-carbon acetate groups will be removed in each round until acetyl-CoA is produced. All saturated molecules enter this cycle immediately, but how unsaturated molecules enter the cycle is still unclear. Hydrogen is produced in the cycle when $NADH + H^+$ and $FADH_2$ return to NAD^+ and FAD, respectively. The current understanding of the microorganisms responsible for beta-oxidation and the kinetics of degradation of myristic, palmitic, stearic, oleic, and linoleic acid is discussed below.

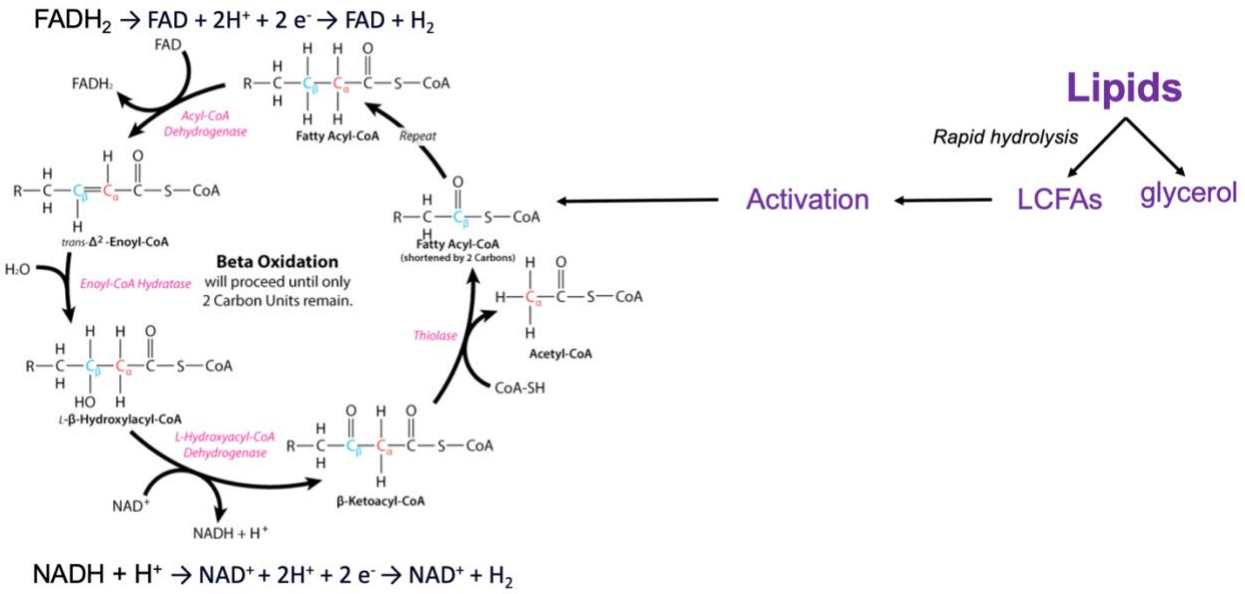

Figure 2.3: Visual representation of lipid hydrolysis, activation, and beta-oxidation.[15]

2.4 Microbial Communities of Interest

Beta-oxidizers convert LCFAs to acetate, using NAD^+ and FAD as electron acceptors. Hydrogen is also formed during beta-oxidation to convert NADH and $FADH_2$ back to NAD^+ and FAD, respectively. In a study by Ziels et al.,[16] syntrophic LCFA-degrading bacteria were monitored during anaerobic FOG co-digestion using qPCR. The beta-oxidizing genus *Syntrophomonas* increased to 15% in the digester fed with FOG and stayed below 3% in the control that was not fed FOG. In a study that sampled thermophilic anaerobic digesters fed with manure and LCFAs, 16S rDNA denaturing gradient gel electrophoresis (DGGE) profiling was used to characterize the microbial communities.[17] The DNA sequencing of predominant DGGE bands showed affinity to characteristics of *Syntrophomonas* and *Clostridium*, two beta-oxidizing microorganisms.[17] Ziels et al.[16] found that high *Syntrophomonas* biomass levels are ideal for efficient co-digestors as this ensures LCFA levels are kept low. The partial pressure of H_2 must also be kept low for beta-oxidization to remain thermodynamically feasible. Balance is critical for an efficient digester as other microbial communities, such as fermenters and methanogens, are also

affected by high H_2 partial pressure. An unbalanced digester will have a high partial pressure of H_2, causing the digester to stall, LCFAs to accumulate, and methane production to be minimal.[16] *Syntrophomonas* is considered a slow grower, leading to an initial lag time when FOG is first introduced to a digester.[16] Inhibition and LCFA accumulation in anaerobic co-digesters could be due to the sensitivity and slow growth of beta-oxidizers, specifically *Syntrophomonas*. Therefore, this thesis focuses on characterizing microbial communities in batch bottles to understand further the microbial communities involved in the beta-oxidation of varying LCFAs. **One evaluated hypothesis is that different microbial communities will be seen in bottles spiked with saturated and unsaturated acids.**

2.5 Saturated Long-Chain Fatty Acid Degradation

Saturated acids directly enter the beta-oxidation cycle, as shown in Figure 2.3. The only variation in the degradation of saturated fatty acid is found in the activation step.[18] There are mixed conclusions in the results of prior research surrounding the kinetics of degradation of myristic, palmitic, and stearic acids, some of the most prevalent in FOG.

2.5.1 Myristic Acid

Novak and Carlson [13] completed a study analyzing the degradation pathways of saturated and unsaturated fatty acids in municipal wastewater. A continuously fed laboratory digester was used, and the LCFA of interest was added as the sole organic carbon source. Inorganic nutrients were added in sufficient concentrations to understand the impacts of the individual LCFAs clearly. The sludge for this experiment was obtained from a municipal plant in Seattle, Washington. This study observed that the maximum substrate utilization rate (*k)* for myristic, palmitic, and stearic acids are equal, indicating that the rate-controlling step may be identical for these acids.[13] The rate *k* was calculated using a model relating solids retention time (SRT) to substrate concentration in

mixed liquor. For myristic acid, the concentration began to rapidly decrease at an SRT of 10 days and no acetate accumulated.[13] The intermediates of each of the LCFAs were not measured. Cirne et al.[19] completed a buffered batch reactor study observing the kinetics of myristic acid degradation. Varying concentrations of LCFAs were added to the buffered bottles to demonstrate the impact of concentration. Myristic acid concentrations were steady throughout the experiment, indicating that the conversion of myristic acid was not limiting.[19]

2.5.2 Palmitic Acid

In a study by Usman et al.,[20] 500 mL batch reactors were inoculated with saturated and unsaturated fatty acids. The inoculum was retrieved from a domestic biogas plant running on agricultural waste and manure, and the reactors were made with a 30% inoculum ratio. An inoculum ratio is the volumetric percentage of sludge from an active anaerobic digester in a reactor. Palmitic acid degradation was rapid and direct as palmitic acid was degraded through beta-oxidation to shorter-chain fatty acids like myristic acid.[20] The concentration of palmitic acid decreased over time; however, accumulation of VFAs like propionate and acetate did occur during the initial, rapid degradation of palmitic acid.[20] In contrast, Cirne et al. [19] observed an accumulation of palmitic acid, leading to methanogenesis inhibition. The results from Cirne et al. [19] dispute Novak and Carlson's [13] results. Novak and Carlson [13] observed that myristic and palmitic acids degrade at a similar rate, while Cirne et al. [19] observed palmitic acid accumulation and rapid myristic acid degradation. Funk et al.[21] studied FOG co-digestion in a semicontinuous reactor. Palmitic acid accumulated in the unbuffered reactor; however, methane production proceeded when the reactor was buffered. In the unbuffered reactor, palmitic acid accumulated with propionate. The results of this study suggest palmitic acid degradation is sensitive to pH, and any experiment should be buffered to a circumneutral pH.

2.5.3 Stearic Acid

In the study mentioned previously by Usman et al.,[20] degradation of stearic acid was also observed. Stearic acid was degraded directly to palmitic acid, but this reaction was much slower than palmitic acid degradation.[20] Their study concluded that stearic acid directly degrades into palmitic acid via beta-oxidation. The palmitic acid and remaining stearic acid eventually accumulated in the reactor. Palmitic acid was slowly converted to VFAs such as propionate and acetate, which also accumulated.[20] Novak and Carlson's study [13] results disagree with the findings by Usman et al.[20] as Novak and Carlson [13] cite that stearic and palmitic acid degrade at a similar rate. Funk et al.[21] found that in a buffered semicontinuous reactor, stearic acid does not accumulate, but in a non-buffered reactor, stearic acid accumulates with propionate. Cirne et al.[19] also found that in a buffered reactor, the conversion of stearic acid to palmitic acid was not rate-limiting.[19]

2.6 Unsaturated Long Chain Fatty Acid Degradation

The degradation of unsaturated LCFAs is highly debated, and four main theories surround their degradation. The first theory is that the fatty acid chain is hydrogenated to a saturated form and then proceeds through beta-oxidation.[22] The second theory is that the unsaturated acids directly enter the beta-oxidation pathway and are converted to shorter chain fatty acids.[23] A third possibility is that hydrogenation and beta-oxidation occur synchronously. The fourth theory is fractionation, which occurs at the double bonds of the unsaturated acids, reducing the length of the fraction and making the compound more easily degradable.[24]

2.6.1 Oleic Acid

In the study mentioned previously by Usman et al.,[20] degradation of oleic acid was also observed. Oleic acid was degraded into stearic acid and then palmitic acid, following the first theory described above.[20] However, oleic acid decreased more rapidly than the degradation time

for stearic acid, suggesting that oleic acid has faster degradation.[20] In contrast, Beccari et al.[25] observed the saturation of oleic acid to stearic acid as a limiting step, meaning the degradation took time to proceed. Cirne et al. [19] observed an accumulation of oleic acid in the first two days and then a decrease in oleic acid, which correlated to the accumulation of palmitic acid. Similarly, in a study by Lalman and Bagley,[23] oleic acid was degraded to form palmitic acid, but stearic acid was never observed, suggesting initial beta oxidation without hydrogenation. In the study by Novak and Carlson, [13] the unsaturated acids, oleic and linoleic acid, were degraded faster than the saturated acids, suggesting that a different mechanism controls the degradation of these two LCFAs. Novak and Carlson [13] suggest that the first theory of hydrogenation followed by beta-oxidation is unlikely as the degradation rate of the saturated and unsaturated acids would need to be similar for the theory to be valid. To explain the rate differential between saturated and unsaturated acids, Novak and Carlson [13] proposed the fractionation theory.

2.6.2 Linoleic Acid

In the study mentioned previously by Usman et al., [20] degradation of linoleic acid was also observed. Linoleic acid was first converted to palmitic acid and then to shorter carbon chains, unlike oleic acid, which was first converted to stearic acid.[20] Linoleic acid was observed to degrade faster than oleic and stearic acid. Novak and Carlson [13] also observed that linoleic acid has a higher *k* value than oleic acid and, therefore, degrades at a more rapid rate. In a study by Lalman and Bagley, [23] linoleic acid was degraded, but stearic acid was never observed, suggesting theories two or three described above.

How these degradation reactions proceed can depend on various factors, including the presence of specific microorganisms and the resulting thermodynamics. *Syntrophomonas* has been identified as the key genus involved in the degradation of these fatty acids. The thermodynamic

favorability of degradation is shown in Table 2.1 by the standard Gibbs energy of formation, as adapted from Sousa et al[26] and Zinder.[26,27] As the positive values show, none of these reactions are thermodynamically favorable at standard conditions, with a H_2 partial pressure of 10^5 Pa. When the partial pressure is decreased to 1 Pa, the Gibbs free energies are all negative, indicating the reactions are thermodynamically favorable. Ideally, the partial pressure would remain below 10.1 Pa to ensure thermodynamically favorable conditions.[28] The impact of H_2 partial pressure on thermodynamics reemphasizes the importance of balance within a digester. The Gibbs free energies imply that if the partial pressure of H_2 is low enough, linoleic will degrade the fastest and palmitic will degrade the slowest. This implication assumes thermodynamics is the primary cause of inhibition. However, realistically, thermodynamics and the microbial community both have the potential to impact the accumulation of LCFAs in anaerobic co-digesters. A comparison of the degradation rates for each of the acids related to the Gibbs free energies of the acids will be important in understanding the impact of thermodynamics on kinetics. **Two hypotheses were thus evaluated: First, lag times and responses of both unsaturated acids will be similar and lag times and responses of the three saturated acids will be similar. And secondly, microbial community composition and the Gibbs free energy of each reaction will impact kinetics.**

Table 2.1: Summary of Gibbs free energy at standard conditions and depleted partial pressure. Shows the free energies for linoleic, oleic, stearic, and palmitic acid.[26]

Reactant	$\Delta G^{0'}$* (kJ per reaction)	$\Delta G'$** (kJ per reaction)
Linoleic	+272	-152
Oleic	+338	-110
Stearic	+404	-68
Palmitic	+353	-59

* Gibbs free energies (at 25 °C) calculated at standard conditions (solute concentrations of 1 M and gas partial pressure of 10^5 Pa).

**Gibbs free energies (at 25 °C) for fatty acids concentrations of 1 mM with H_2 depletion to a partial pressure of 10^{-4} atm and acetate accumulation to 9 mM.

Many of the studies discussed above vary in experimental protocol and goals; however, they contribute valuable information to the current studies on the degradation of saturated and unsaturated LCFAs. Analysis of the kinetics, intermediates, and microbial communities involved in the degradation of five LCFAs (myristic, palmitic, stearic, oleic, and linoleic acids) in batch reactors has not been done.

3. Overview of Research Objectives

Three research objectives for this thesis are outlined below, based on the hypotheses mentioned above.

I. Evaluate biogas yield potential, length of lag phase, and the maximal biogas generation rate of five different LCFAs. Use methane production data to model using Gompertz model to analyze methane production mathematically to obtain these parameters.

II. Obtain a clearer understanding of the degradation pathways of LCFA, using LCFA and VFA data. Determine the apparent first-order kinetics of LCFA degradation which can be used in Anaerobic Digestion Model No.1 (ADM1).

III. Link microbial community composition to LCFA degradation by analyzing overall microbial communities. The key groups that will be monitored are hydrogenotrophic and acetoclastic methanogens and beta-oxidizers.

The research hypotheses that were described above based on literature and previous studies are outlined again below. Each of these hypotheses will be explored through the execution of each of the objectives.

I. Different microbial communities will be seen in bottles spiked with saturated and unsaturated acids.

II. Lag times and responses of both unsaturated acids will be similar and lag times and responses of the three saturated acids will be similar

III. Microbial community composition and the Gibbs free energy of each reaction will impact kinetics.

4. Materials and Methods

4.1 Execution of Objective I: Analysis of methane production in batch bottles

4.1.1 Assay Preparation

The first task included setting up batch bottles with three concentrations each of myristic, palmitic, stearic, oleic, and linoleic acid. The concentrations were represented in units of mg chemical oxygen demand (COD)/L to allow for consistency in electron equivalent loadings for each of the acids. The three concentrations were 2, 4, and 6 g COD/L. Choosing this range of concentrations allowed for observation of the impact of LCFA concentration on degradation pathways and microbial communities. For each acid batch bottles were made with the three concentrations in triplicates. To achieve 2 g/L COD, the actual concentration of linoleic, oleic, stearic, palmitic, and myristic acids added was 2.50, 2.45, 2.40, 2.72, and 3.13 mM, respectively. To achieve 4 g/L COD, the actual concentration of linoleic, oleic, stearic, palmitic, and myristic acids added was 5.00, 4.90, 4.81, 5.44, and 6.25 mM, respectively. To achieve 6 g/L COD, the actual concentration of linoleic, oleic, stearic, palmitic, and myristic acids added was 7.5, 7.35, 7.21, 8.15, and 9.38 mM, respectively. A control also was created in triplicate for each round of batch bottles. The LCFA-amended bottles contained inoculum, mineral medium (Table 4.1), trace metals described by Shelton and Tiedje[29], phosphate buffer (3 g/L as $CaCO_3$), and LCFA stock solution (see below). The control bottles had the same components but without the LCFA stock solution. A phosphate buffer was chosen instead of a carbonate buffer because phosphate buffers

are more effective at maintaining a neutral pH. The concentration was chosen to equal the alkalinity of the inoculum, mimicking the conditions of a well operating digester. 250 mL media bottles were used, but only 180 mL were filled with solution to allow for a 70 mL headspace. The inoculum was collected from the anaerobic co-digestion tank at Renewable Water Resources in Greenville, SC. The LCFA stock solution for palmitic was made with palmitic acid sodium salt with 98% purity from Thermoscientific. The LCFA stock solution for stearic was made with free stearic acid from MP Biomedicals, water, and sodium bicarbonate. Stearic acid is not soluble in water at a neutral pH, and therefore, the pH was raised to 11 with sodium hydroxide for stearic to dissolve. The LCFA stock solution for linoleic was made with 99% pure linoleic acid from Thermoscientific, water, and sodium bicarbonate. Solutions for myristic and oleic acid were formulated from sodium myristate and sodium oleate from Thermoscienfic.

Table 4.1: Composition of mineral media used in assay preparation.[29]

Components	Goal Conc. In bottles (g/L)
NH_4Cl	0.53
$CaCl_2 \cdot 2H_2O$	0.08
$MgCl \cdot 6H_2O$	0.05
$FeCl_2 \cdot 4H_2O$	0.02
$NaHCO_3$	1.20
$Na_2S \cdot 9H_2O$	0.50
DDI (mL)	-

Once all components were added to each bottle, the entire bottle was sparged for 10 minutes with argon to remove any oxygen in the solution. The sparging changed the pH; therefore, the pH was adjusted to 7.2 with hydrochloric acid. The volumes of each of the bottles were then brought to 180 mL with the addition of distilled de-ionized (DDI) water. Next, the headspace was sparged for 5 minutes with argon and the bottles were immediately sealed and capped with rubber septa

and aluminum crimp caps. The bottles were placed on an incubator/shaker set at 35 °C and 150 rpm. Anaerobic digesters typically have a temperature ranging between 30 °C to 38 °C.

4.1.2 Monitoring and Quantifying Biogas Production

Biogas volume and methane content samples were taken daily. The volume of biogas was measured via a 100 mL syringe with a needle attached. Methane content was measured using a gas chromatography unit (Shimadzu GC 2014). For this procedure, 250 µL of gas was collected from the batch bottle with a Hamilton Gastight® GC Syringe and injected into the GC. The samples ran for 5 minutes at a flow rate of 10 mL/min with ultra-high purity argon as the carrier gas at a pressure of 415 kPa. The injector and thermal conductivity detector were set to 150 ºC, and the column was set to 120 ºC.

A calibration curve for the GC was created to determine the percent volume of methane. The calibration curve was created by running the GC with four known methane volumes (0%, 10%, 30%, and 50%) in triplicate. The different methane volumes were created using a known 50% methane (Airgas) volume. These dilutions were conducted inside the gastight GC syringe. The averages of the triplicate measurements of each volume were plotted, and the slope of the curve was calculated. This slope was the reference factor. The reference factor was then used to calculate a methane percentage from a peak area of biogas produced from the batch bottles.

4.1.3 Gompertz Model

Using the biogas volume and methane composition in each bottle, a mathematical model known as the modified Gompertz model was used to determine parameters such as biogas yield potential, length of lag phase, and the maximal biogas generation rate.[30] Zwietering et al. considered three sigmoidal models, Gompertz, Logistic, and Richards models, to describe microbial growth in biochemical methane potential tests. The conclusion was that Gompertz best

fit the data.[31] Since methane is a terminal product in anaerobic digestion, the microbial growth curve will be like the methane production curve. Therefore, the modified Gompertz model was used to predict biogas potential, length of lag phase, and the maximal biogas generation rate. The solver tool in Excel was used to predict these values based on the biogas volume and methane content data.

4.2 Execution of Objective II: Chemical analysis and determination of kinetic constants for LCFA degradation

Samples were taken from the batch bottles twice daily for chemical and biological analysis. Each sample was 0.5 mL in volume. The chemical samples were stored in 2 mL microcentrifuge tubes in a freezer set at -20 °C. The biological samples were stored in 2 mL RNA-free microcentrifuge tube in a freezer set at -20 °C.

4.2.1 pH

pH was measured daily because microbial communities in anaerobic digesters are sensitive to pH. Methanogens only function in a pH range between 6.5 and 7.5.[32] As acetate and other VFAs form in the bottles, the pH decreases causing methanogens to stop using the acetate to produce methane. Therefore, the pH is another data point that was used to understand the reactions occurring in the bottles. pH was measured in raw sludge samples using a pH probe on every sample. The probe was re-calibrated once a month using set pH samples to ensure accurate readings on samples.

4.2.2 Long-chain Fatty Acid Analysis

For LCFA analysis, stored batch bottle chemical samples were thawed at room temperature, and then 0.25 mL of the sample was transferred to a 10 mL falcon tube. LCFAs in the samples were then extracted and trans-esterified using known methods derived by Ziels et al.

and Burja et al. as further described below.[33,34] Before extractions, 100 µL of 10 g/L pentadecanoic acid dissolved in methanol was added to the sample as the recovery standard. The recovery standard shows if any degradation of LCFAs occurred during the extraction and transesterification processes. A percent recovery was calculated from the final concentration of pentadecanoic acid and then used to calculate the original concentration of other LCFAs in the sample. During the LCFA extraction phase of this procedure, 200 µL of 250 g/L sodium chloride in MilliQ water, 10 µL of 50% sulfuric acid, 1 mL of hexane, and 1 mL of methyl tert-butyl ether (MTBE) were added to the sample and vortexed to mix. Samples were vortexed in a tabletop vortex for 20 minutes. The samples were then centrifuged at 3200 x *g* for 10 minutes. 1 mL of organic supernatant was extracted from the falcon tubes and placed in a clean glass vial, where the samples were dried using N_2 gas and capped immediately. Only dried LCFAs remained at the bottom of the vial. Next, the samples were trans-esterified by adding 2.5 mL of methanol, 250 µL of hydrochloric acid, and 250 µL of chloroform to the dried samples. The now liquid samples were vortexed for 10 seconds to ensure adequate mixing and then heated at 90 ºC for 120 minutes. After samples were removed from heat and cooled to room temperature, 1 mL of DDI water was added, and samples were again vortexed. The final step of the protocol was fatty acid methyl ester (FAME) extraction, in which 1.6 mL of hexane and 400 µL of chloroform were added to the sample and vortexed for 10 seconds. The solution settled before moving forward. This process was repeated three times with a total of 4.8 mL of hexane and 1.2 mL of chloroform added to maximize FAME extraction. After the solution was vortexed for the final time, the solution was allowed to settle until an organic supernatant formed. 1 mL of this supernatant was removed and added to a glass vial for analysis. Before analysis, 50 µL of 2 mg/mL pentadecane: hexane was added as the internal standard. The internal standard was used to determine the concentrations of other LCFAs in solution by

calculating a response factor. These prepared samples were analyzed using a GC flame ionization detector (FID) fitted with an Rt-2560 column (Restek). The carrier gas for this instrument was helium. The injector and detector temperatures remained at 240 ºC. The column temperature remained at 100 ºC for 5 minutes followed by an incremental temperature increase at 3 ºC/min until the temperature reached 240 ºC.

4.2.3 Volatile Fatty Acid Analysis

Using the chemical samples taken daily from each batch bottle, the concentration of VFAs was measured. For VFA analysis, 0.25 mL of sample was diluted in a microcentrifuge tube. The dilution factor ranged from 2x to 4x dilution depending on the sample. Once the dilution was made, the diluted sludge was centrifuged at 10,000 x *g* for 1 minute. Using a clean BD syringe and 18G needle, the supernatant was collected from the centrifuged sample and filtered through a 0.2-micron polyvinylidene (PVDF) filter. The filtrate was then placed in a high-performance liquid chromatography (HPLC) vial. If samples were not analyzed immediately after preparation, they were stored at -20ºC and then thawed at room temperature when the analysis was ready to be performed.

After the samples were prepared, an HPLC unit fitted with an Aminex® HPX-87H Ion Exclusion column was used to analyze VFA concentrations in reactor samples. The carrier fluid was 5 mM H_2SO_4 with a flowrate of 0.6 mL/min and a wavelength on the UV/Vis detector of 210 nm. All samples were processed in 120-minute runs at a column temperature of 30 ºC.

To quantify the concentration of VFAs in the samples, a calibration curve was required for each of the potential acids present within the sample, including lactate, formate, acetate, propionate, isobutyrate, butyrate, isovalerate, and valerate. Known concentrations of each VFA were prepared in duplicates. The concentrations were 0.1, 0.5, 1, 5, 10, and 20 mM. Also, two

mixed samples, with each VFA at the same concentration were prepared in duplicate to identify the individual retention times. The HPLC was used to analyze these samples. The peak areas and retention times were recorded, and the duplicates were averaged. These averages were plotted, and the slope of the line connecting the different concentrations provided the reference factor. The known retention times were used to identify which peak belongs to which VFA, and the reference factor allowed for the quantification of concentration from the peak area.

4.3 Execution of Objective III: Analyzing microbial communities and differences in communities present after degradation

Biological samples were collected daily and stored in 2 mL RNA-free microcentrifuge tubes in a freezer set at -20ºC. When the samples were ready to be analyzed, they were taken out of the freezer and thawed on ice to preserve sample integrity. DNA is fragile, and thawing at room temperature can damage it. Before any specific DNA analysis occurred, DNA was extracted from the biological sample taken from each batch bottle. Extractions were performed using the DNeasy Power Soil kit (Qiagen, Valencia, CA, USA) according to the manufacturer's instructions. DNA concentrations were quantified using a Qubit high sensitivity DNA assay kit on a Qubit 3.0.

DNA extracted from biological samples from the batch bottles were stored in a freezer at -20 °C. The samples were sent to MR DNA (Shallowater, TX, US) for sequencing. MR DNA sequenced the DNA using the 515F/806R primer pair specific to the V4 variable region of the 16S rRNA gene. This primer was used for both eubacterial and archaeal gene identification. Polymerase chain reaction (PCR) was run using the HotStarTaq Plus Master Mix Kit (Qiagen). Cycling conditions were as follows: 95 ºC for 5 minutes, 30-35 cycles of 95 ºC for 30 seconds, 53 ºC for 40 seconds, and 72 ºC for 1 minute, and a final elongation step at 72 ºC for 10 minutes. Following amplification, amplicons were loaded into a 2% agarose gel and separated via gel

electrophoresis. Individual PCR products were then compared using the size and intensity of the bands. Based on concentration and molecular weight, multiplexed samples were pooled in equal proportions and then purified using calibrated Ampure XP beads. A DNA library was created using purified samples. DNA libraries were sequenced on an Illumina MiSeq following the manufacturer's protocols. MR DNA processed sequences by removing sequences that were less than 150 bp or that contained ambiguous base readings. A maximum expected error threshold equal to 1 was used to quality filter the sequences before removing replicated sequences. Filtered sequences were denoised and taxonomy was assigned from a curated National Center for Biotechnology Information (NCBI) database using BLASTn. Taxonomic classification, sequence counts assigned to each zOTU (zero-radius operational taxonomic unit), and relative percentage of each zOTU were reported by MR DNA. Bioinformatic analyses were performed using Quantitative Insights into Microbial Ecology (QIIME) 2 2018.8 for identification and taxonomy classification.[35]

5. Objective I and II Results and Discussion: Saturated Acids

The three saturated acids evaluated in anaerobic co-digestion were stearic, palmitic, and myristic acid, with 18, 16, and 14 carbons, respectively. The inoculum was obtained from Mauldin Road Water Resource Recovery Facility (WRRF) (ReWa-Greenville, SC) a day before preparing the assays. Three cycles of assays were prepared, and the inoculum characteristics are summarized in Table 5.1.

Table 5.1: Summary of inoculum characteristics for the three batches of assays prepared for saturated acids.

	Stearic Assay	Palmitic Assay	Myristic Assay
pH	7.9	7.6	7.6
Alkalinity (mg/L $CaCO_3$)	2,700±110	3,700±140	2,800±110
Total Solids (mg/L)	15,300±2,900	10,800±2,800	13,400±5,700
Volatile Solids (mg/L)	11,200±2,000	8,000±2,200	10,000±4,200

5.1 Objective I

Objective I aimed to analyze methane production of anaerobic co-digestion batch bottles spiked with five different LCFAs at varying concentrations. This analysis included experimental data from sampling the assays and determination of parameters for methane production from a mathematical model, the Gompertz model. The following results describe the methane production of only the saturated acids.

5.1.1 Biogas Production

Biogas was measured daily while bottles were in operation, and the amount of biogas was recorded as mL of methane produced daily. The total volume of methane was calculated by adding the daily volume produced together. The volume (mL) of methane was then converted to electron milliequivalents (meeq) to allow for consistent comparison among all experiments. Shown in Figure 5.1, are the total amount of methane produced in meeq from stearic, palmitic, and myristic

acid, respectively, at three different concentrations of each LCFA. The control for each set of batch bottles is displayed in the figures in addition to the three concentrations of each of the acids.

S-curves are characteristic for methane production in anaerobic co-digestion assays as these would describe a lag phase, a phase of increasing methane production, and a phase of plateau

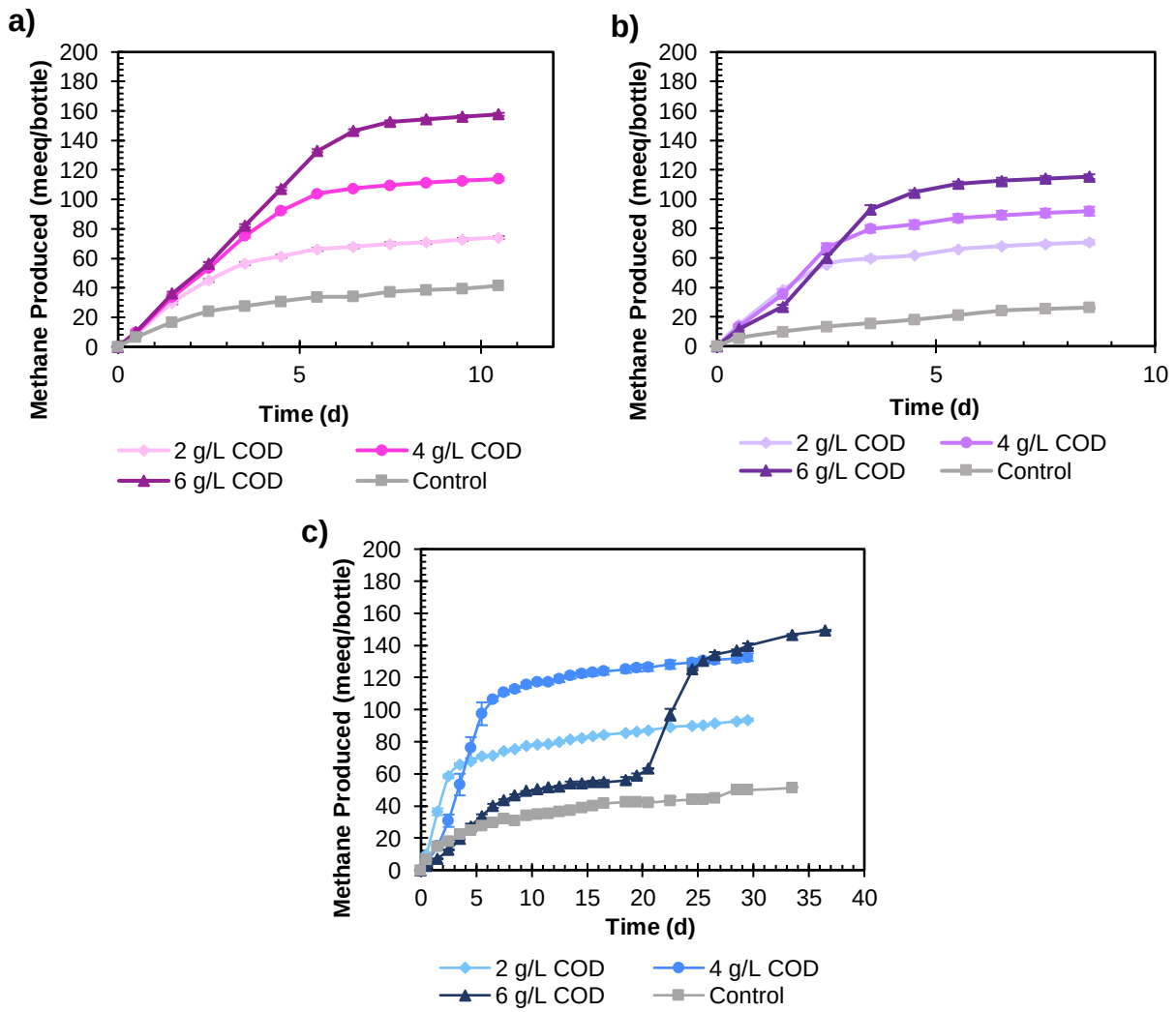

Figure 5.1: Total production of methane in milliequivalents (meeq/bottle) of assays spiked with 2, 4, and 6 g/L COD of a) stearic acid, b) palmitic acid, c) myristic acid.

in methane production. The methane production curves for the assays spiked with stearic and palmitic acid shown in Figure 5.1 a and b display a characteristic s-curve with a short lag phase that was less than one day followed by a time of large and consistent methane production and then a plateau at a maximum methane yield. This trend is also seen in myristic acid assays with 2 and

4 g/L COD of myristic acid, as shown in Figure 5.1 c. However, at a higher concentration of myristic acid (6 g/L COD) there was a much longer lag phase followed by a steady rise in methane production and then a plateau at a maximum methane production volume. The curve for 6 g/L COD myristic acid is very different from the other myristic concentrations and other acids. This curve would be classified as a double S-curve, while the other curves are single S-curves. Since the lag phase from day 0 to day 15 for myristic 6 g/L COD produced more methane than the control, not all methane production was inhibited by adding this acid at a high concentration.

Based on acetolactic and hydrogenotrophic methanogenesis, the total amount of methane expected was calculated based on the concentration of acids being added in mg/L COD. Based on the expected methane production, 2% of the methane produced was from hydrogenotrophic methanogens and 80% of the methane produced was from acetoclastic methanogens. The percentages were calculated with the total methane predicted and the total methane produced in each saturated acid assay, excluding the methane produced in the control. An example of the calculations is shown in Appendix A. For assays with stearic acid added at 2, 4, and 6 g/L COD, it was predicted that 30.1, 60.2, and 90.3 meeq of methane would be produced, respectively. The assays with stearic acid added produced on average 90% (2 g/L) and 99% (4 g/L) of the predicted methane. The stearic acid assay with 6 g/L COD produced 6% more methane than predicted. For assays with palmitic acid added at 2, 4, and 6 g/L COD, it was predicted that 30.3, 60.4, and 90.8 meeq of methane would be produced, respectively. The assays with palmitic acid added produced on average 80% (2 g/L), and 90% (4 g/L) of the predicted methane. The assays with 6 g/L COD of palmitic acid added produce 21% more methane that was predicted. For assays with myristic acid added at 2, 4, and 6 g /L COD, it was predicted that 30.4, 61.0, and 91.1 meeq of methane would be produced, respectively. The actual assays with myristic acid added produced on average

58% (2 g/L), 32% (4 g/L), and 0.6% (6 g/L) more methane than predicted. Five of the assays produced more methane than predicted. This result can be attributed to the control. The control was subtracted when calculating produced methane, but the control assays did not experience the same pH drop as the saturated assays. Therefore, the control assays might have had more methane production potential which was observed in five of the saturated assays.

Appendix B Figure B.1 a, b, and c show the H_2 partial pressures present in the stearic, palmitic, and myristic acid assays. At some points during the experiment, the partial pressures H_2 of the assays did exceed 10^{-4} atm which is denoted by the dashed red line. However, 10^{-4} atm is just an approximation and all of the instances in which 10^{-4} atm was exceeded was by a small amount. Therefore, the short lag in methane production observed in the saturated acid assays is likely not a result of elevated H_2 partial pressure.

5.1.2 Gompertz Model

Gompertz model was used to determine biogas yield potential, length of lag phase, and the maximum biogas generation rate. Appendix C Figure C.1 a, b, and c display the methane production curves fitted with Gompertz model to display the fit. All curves were calculated with $R^2 \geq 0.94$. Table 5.2 shows the average lag times in days for each of the saturated acids. Stearic acid had longer lag times than palmitic acid for all concentrations except the highest concentration. At the highest concentration, the lag times are almost equal. Stearic acid has two more carbons than palmitic acid and due to its size, it may cause more inhibition as shown by the lag times. Palmitic acid had shorter lag times compared to myristic acid. Myristic acid had a shorter lag time than stearic acid at the lowest concentration, but as the concentration increased, myristic acid had the highest lag time compared to both stearic and palmitic acid. Myristic acid has 14 carbon and is the shortest carbon chain being evaluated. Therefore, the hypothesis that longer chain length

leads to greater lag times cannot be confirmed. Since the highest concentration of myristic displayed a double S-curve in its methane production curve, Gompertz model cannot be applied. The control had a lag phase of 0 ± 0 days. Table 5.3 shows the maximum methane production rate (mL/d) [k_p] for each of the saturated acids. The methane production rate was calculated excluding the methane produced in the control. Palmitic and stearic acid maintain the highest and lowest k_p, respectively, for all concentrations. For palmitic and stearic acid, k_p increases as concentration increases; however, this is not the trend for myristic acid. Of the two k_p values calculated for myristic acid, the lower concentration had a slightly higher k_p. Based on an analysis of variance (ANOVA) statistical test and post- ANOVA analysis there is no statistical different in the lag times of the saturated acids. Calculations for this ANOVA analysis are shown in Appendix D.

Table 5.2: Average lag phase (d) and standard deviation calculated using the Gompertz model for each of the saturated acids.

	Stearic Acid	Palmitic Acid	Myristic Acid
2 g/L COD	0.41±0.07	0.19±0.03	0.37±0.07
4 g/L COD	0.77±0.06	0.54±0.17	1.77±0.21
6 g/L COD	1.09±0.03	1.10±0.05	

Table 5.3: Average maximum methane production rate (mL/d) and standard deviation calculated using the Gompertz model for each of the saturated acids, excluding the methane produced in the control.

	Stearic Acid	Palmitic Acid	Myristic Acid
2 g/L COD	35.26±0.58	75.90±1.64	73.93±2.98
4 g/L COD	59.84±4.27	95.75±4.90	72.06±4.57
6 g/L COD	77.32±2.83	116.42±2.72	

5.2 Objective II

Objective II aimed to analyze pH, VFAs, and LCFAs in the assays. The LCFA data was used to determine the apparent first-order degradation kinetics of each LCFA analyzed and intermediate

LCFAs that form during saturated LCFA degradation. The VFA data was used to understand the intermediates that form and accumulate during saturated LCFA degradation.

5.2.1 pH

The pH was recorded daily and is shown in Figure 5.2 a, b, and c. All assays began at a pH of 7.2 since adjusting the pH with hydrochloric acid was part of assay preparation. A 20 mM phosphate buffer was also added to resist changes in pH due to the production and consumption of acetate and other by-products in the degradation process. The assays with stearic acid added had a pH ranging from 7.34 to 6.87. The assays with palmitic acid added had a pH ranging from 7.28 to 6.95. For these acids, the pH did not change drastically during the experiment. The 2 and 4 g/L COD assays with myristic acid added had pH trends similar to stearic and palmitic acid, as their pH ranged from 7.41 to 6.89. The highest concentration of myristic acid had a pH range from 7.28 to 6.11. This pH of 6.11 is the lowest observed in the experiment, and methanogens only function in a pH range between 6.5 and 7.5, and the optimum pH is 6.8.[32] Processes have been observed to fail below a pH of 6.1.[36] However, methane was produced following this drop in pH as shown in Figure 5.1 c; therefore, the system was able to recover from the low pH. The lowest pH values occurred during the long lag between days 10 and 20 for myristic 6 g/L COD. The buffer added was 3 g/L as CaCO3 which is around the same level as the alkalinity in the inoculum. However, the phosphate buffer, along with the alkalinity in the inoculum, was not high enough to resist the significant change in pH and, in the future, should be added at a higher concentration. The low pH most likely impacted the Gibbs free energy values for the reaction and microbial function since most microbes have a narrow pH range in which they can function.[37]

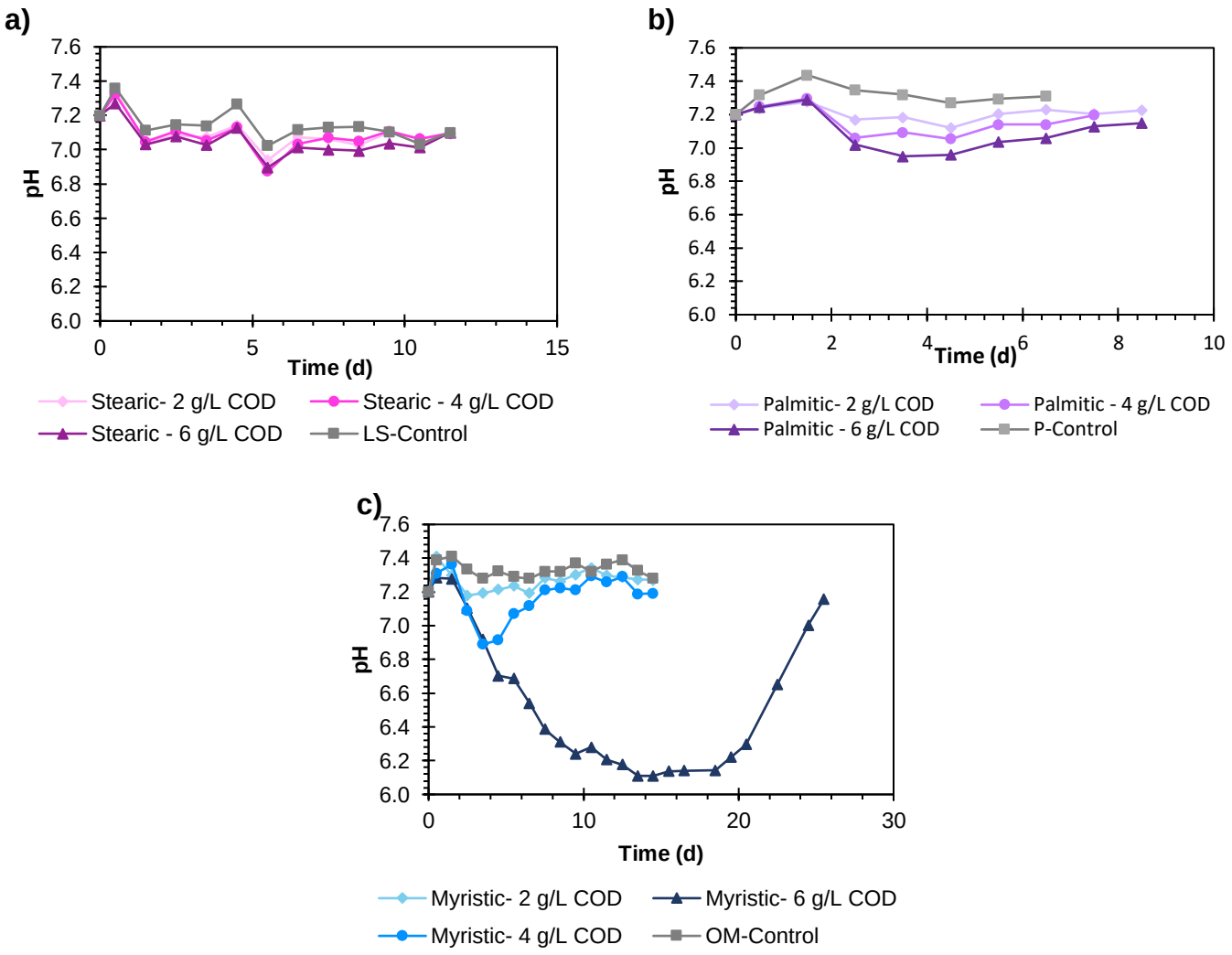

Figure 5.2: Change in pH versus time in assays with a) stearic acid, b) palmitic acid, and c) myristic acid added.

5.2.2 Long-chain Fatty Acid Analysis

LCFAs were measured for each saturated acid at every concentration on varying days throughout the experiment. LCFAs were measured in mM and converted into meeq/L to allow for consistent comparison across all LCFA, VFA, and biogas data.

The LCFA data for the control prepared for the stearic acid assays is shown in Figure 5.3 a. The LCFA data for the three concentrations of stearic acid, 2, 4, and 6 g/L COD, is shown in Figure 5.3 b, Figure 5.3 c, and Figure 5.3 d, respectively. The LCFA data for the stearic acid assays

shows that stearic acid degraded slowly over the course of the experiment, but no other LCFA accumulated during its degradation. Typical beta oxidation indicates that stearic acid would form palmitic acid after the first cycle. Palmitic acid was observed at low concentrations; however, it was also observed at the same concentration in the control, as shown more clearly in Appendix E Figure E.1. Therefore, the presence of palmitic acid can be attributed to the control. The results do not confirm that microorganisms do not convert stearic acid to palmitic acid through beta-oxidation because the microbial communities could be doing this conversion internally or converting palmitic acid to a form that is not detectable by the GC used (i.e., palmitoyl-CoA).

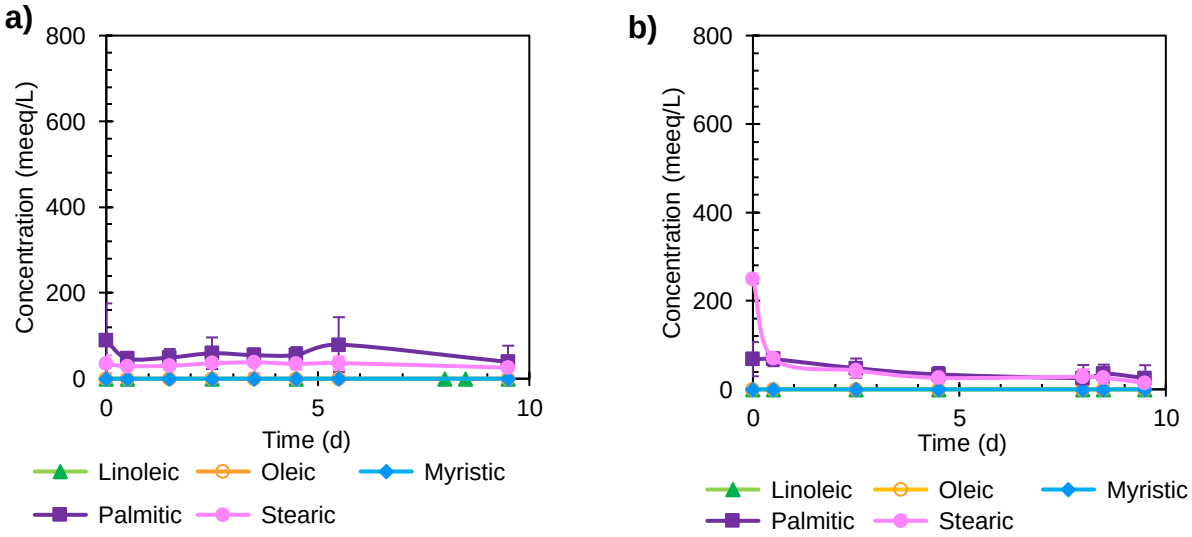

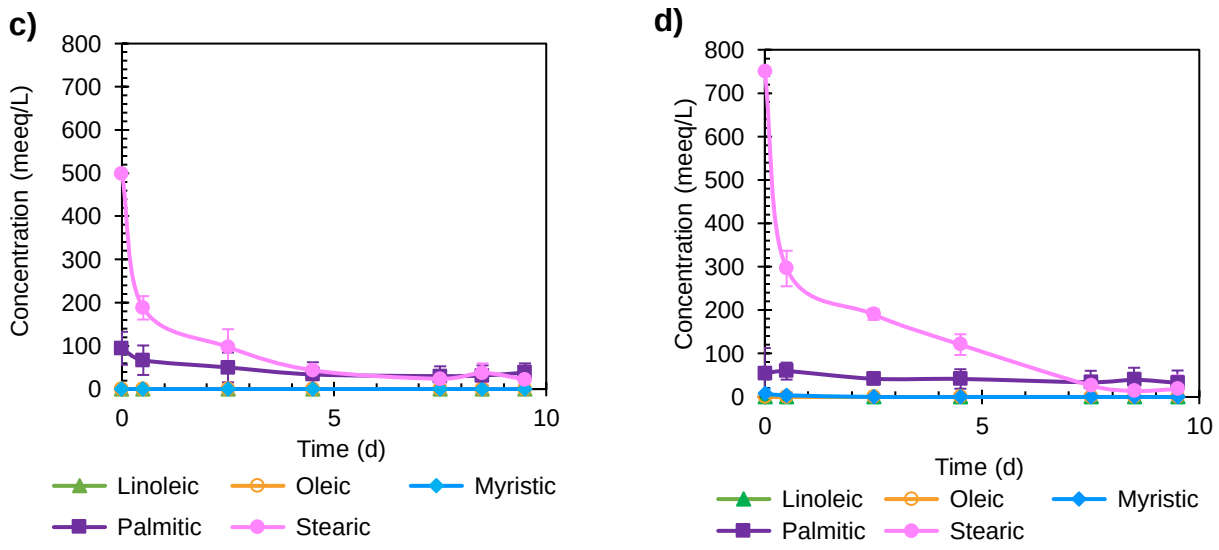

Figure 5.3: LCFA data for a) the control and stearic acid assays with b) 2 g/L COD, c) 4 g/L COD, and d) 6 g/L COD of stearic acid added. The acids are shown in different colors in units of meeq/L.

The LCFA data for the control prepared for the palmitic acid assays is shown in Figure 5.4 a. The LCFA data for the three concentrations of palmitic acid, 2, 4, and 6 g/L COD, is shown Figure 5.4 b, Figure 5.4 c, and Figure 5.4 d, respectively. Each of the palmitic acid assays show that palmitic acid degraded slowly over the course of the experiment, but no other LCFAs accumulated during its degradation. These results were expected since the palmitic acid assays had a short lag time, as shown in Figure 5.1 b and Table 5.2. Likely, palmitic acid quickly degraded through beta-oxidation, forming acetate, and ultimately, methane was produced within the first five days. By day five, the biogas curve shown in Figure 5.1 b had reached a peak for all concentrations, and at the same time, all of the palmitic acid was consumed from the assays. Beta-oxidation suggests that 16-carbon palmitic acid would lose two carbons in the first cycle and form 14-carbon myristic acid. Myristic acid was not detected in any assays; however, this conversion could happen internally inside the cells, or myristic acid might be in a form that the GC does not detect (i.e., myristoyl-CoA).

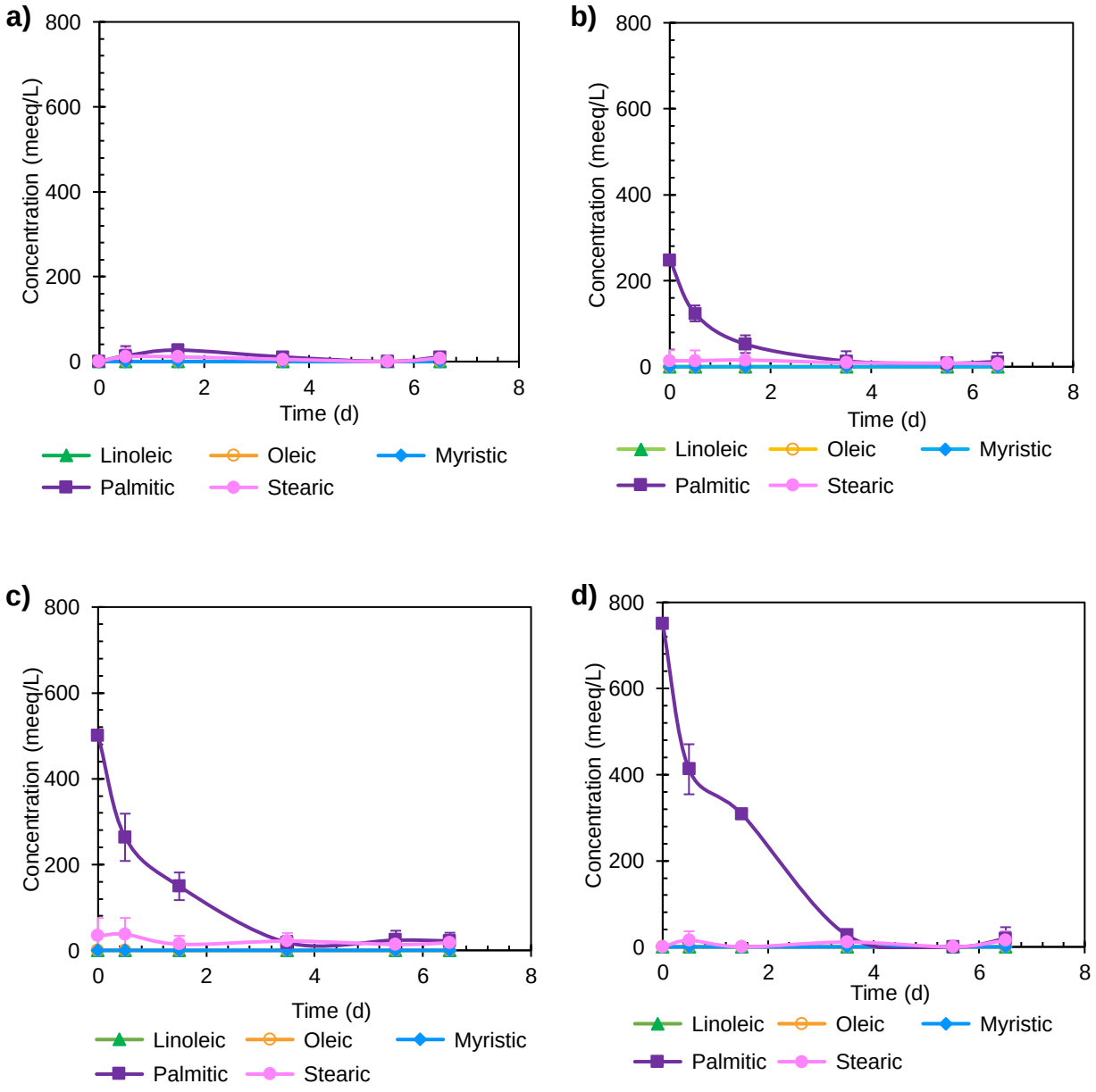

Figure 5.4: LCFA data for a) the control and palmitic acid assays with b) 2 g/L COD, c) 4 g/L COD, and d) 6 g/L COD of palmitic acid added. The acids are shown in different colors in units of meeq/L.

The LCFA data for the control prepared for the myristic acid assays is shown in Figure 5.5 a. The LCFA data for the three concentrations of myristic acid, 2, 4, and 6 g/L COD, is shown in Figure 5.5 b, Figure 5.5 c, and Figure 5.5 d, respectively. Each of the myristic acid assays show that myristic acid degraded by day 4 in each of the assays, but no other LCFA accumulated during

its degradation. The myristic concentrations of 2 and 4 g/L COD degraded in the first 2 and 3 days, respectively. This observation coincides with when peak methane production was reached in biogas analysis, as shown in Figure 5.1 c. Peak methane production was reached within 3 days of myristic acid being completely consumed. The highest concentration of myristic acid did not show this same trend. Myristic acid was consumed in the first seven days; however, peak methane production was not reached until day 25. Therefore, myristic acid degradation was not the inhibitor for methane production at the high concentration. For the highest concentration of myristic acid, more methane was produced in the 6 g/L COD assay than in the control by day 7 as shown in Figure 5.1 c. This observation indicates that some myristic acid degraded in the first seven days could go through beta-oxidation and methanogenesis to ultimately form methane. However, most of the carbon potential was inhibited until day 25.

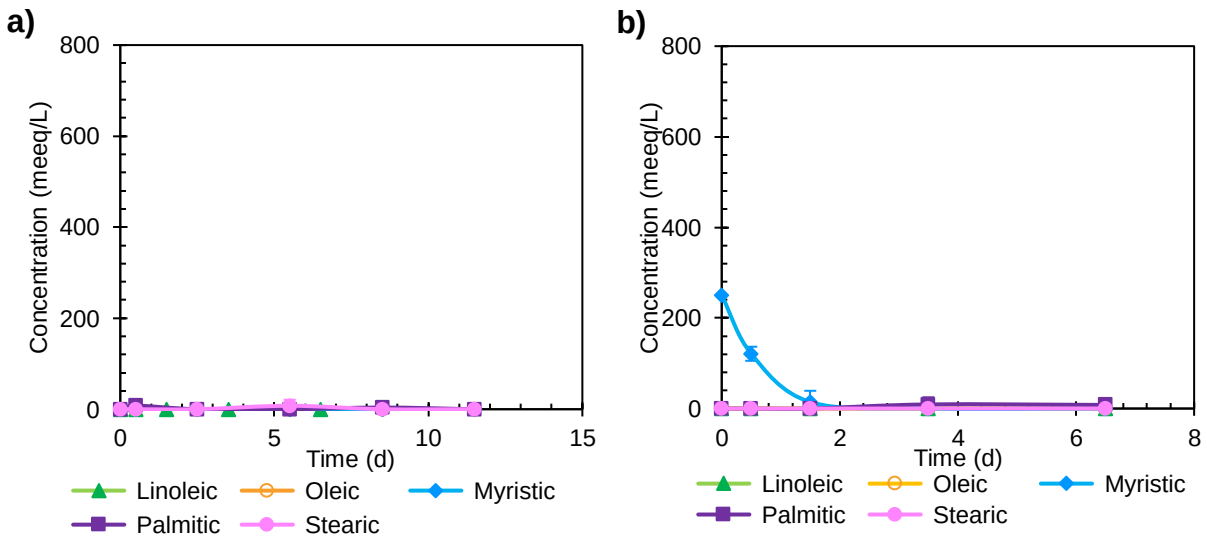

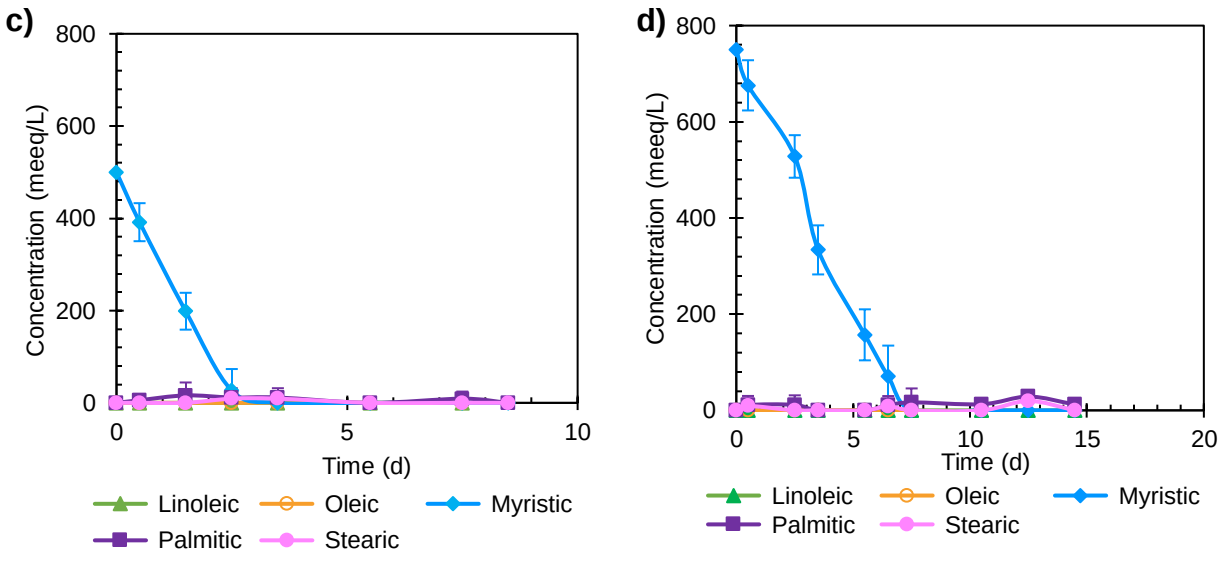

Figure 5.5: LCFA data for a) the control and myristic acid assays with b) 2 g/L COD, c) 4 g/L COD, and d) 6 g/L COD of myristic acid added. The acids are shown in different colors in units of meeq/L.

To better understand the degradation rates and allow for comparison, a kinetic evaluation was completed, and the apparent degradation constants normalized to g VS fed are shown in Table 5.4. These values are considered apparent because the acid could be adsorbing to biomass and not actually degrading. The apparent degradation constants show that myristic acid at low concentrations degraded the fastest, followed by palmitic acid first and then stearic acid. At a high concentration, myristic acid degraded the slowest. The decrease in the apparent degradation constants can most likely be attributed to the low pH experienced in 6 g/L COD myristic acid assays. *Syntrophomonas*, the suspected beta oxidizer for myristic acid, has a pH range for growth between 6.5 to 8.5, and its optimal range is 7 to 7.5.[38] Being outside of this range, such as in the 6 g/L COD myristic acid assays, would likely result in slow growth of the beta-oxidizers and, therefore, slow degradation of the acid. From a thermodynamic perspective, stearic acid has a more negative Gibbs free energy and would, therefore, be more thermodynamically favorable to degrade, as shown in Table 2.1; however, this did not lead to a faster degradation rate. Therefore,

while a reaction may be more thermodynamically favorable to proceed based on Gibbs free energy, it will not necessarily have a faster rate of reaction.

Table 5.4: Apparent degradation constants (k) [1/days/g VS] for the saturated acids.

	Stearic Acid	Palmitic Acid	Myristic Acid
2 g/L COD	0.21±0.05	0.58±0.2	1.07±0.39
4 g/L COD	0.24±0.03	0.66±0.13	0.63±0.21
6 g/L COD	0.20±0.05	0.66±0.01	0.19±0.04

5.2.3 Volatile Fatty Acid Analysis

VFAs were measured for each saturated acid at every concentration on varying days throughout the experiment. VFAs were measured in mM and then converted into meeq/L to allow to consistent comparison across all LCFA, VFA, and biogas data.

The VFA data for the control prepared for the stearic acid assays is shown in Figure 5.6 a. The VFA data for the three concentrations of stearic acid, 2, 4, and 6 g/L COD, is shown in Figure 5.6 b, Figure 5.6 c, and Figure 5.6 d, respectively. Butyrate decreased after day 0 but remained present in all low concentration assays. The control shows that butyrate was present in the inoculum. Propionate was produced and degraded in all assays, including the control. The propionate and butyrate observed in the stearic acid assays are likely not the result of stearic acid degrading; rather, these VFAs were already present or were produced in the inoculum and slowly degraded during the experiment. At peak acetate accumulation, the fraction of electrons measured were 0.39±0.1%, 0.35±0.3%, and 0.56±0.3% of the 2, 4, and 6 g/L COD stearic acid added, respectively. Based on these low percentages, acetate did not accumulate in the stearic acid assays, explaining the minimal drop in pH and short lag time during stearic acid degradation (Figure 5.2 c and Table 5.2).

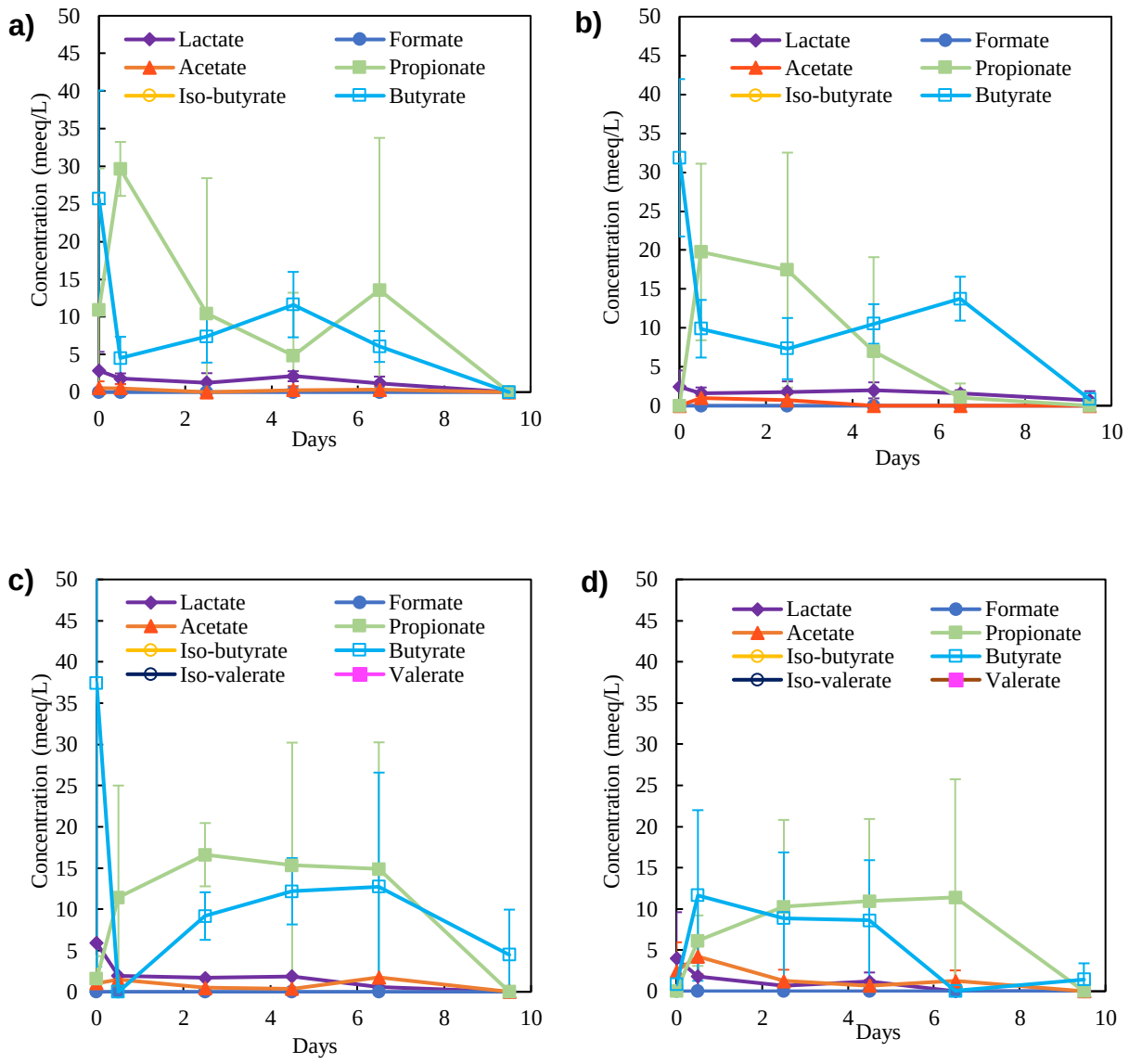

Figure 5.6: VFA data for a) the control and stearic acid assays with b) 2 g/L COD, c) 4 g/L COD, and d) 6 g/L COD of stearic acid added. The acids are shown in different colors in units of meeq/L.

The VFA data for the control prepared for the palmitic acid assays is shown in Figure 5.7 a. The VFA data for the three concentrations of palmitic acid, 2, 4, and 6 g/L COD, is shown in Figure 5.7 b , Figure 5.7 c, and Figure 5.7 d, respectively. Propionate and butyrate were present from day 0 in all assays and remained relatively constant at low concentrations throughout the experiment. The control shows that propionate and butyrate were present in the inoculum. The propionate and butyrate observed in the palmitic acid assays do not result from palmitic acid

degrading; rather, these VFAs were already present in the inoculum and slowly degraded in the assays. Acetate did accumulate in each of the assays. At peak acetate accumulation, the fraction of electrons measured were 1.36±0.2%, 0.79±0.3%, and 1.01±0.1% of the 2, 4, and 6 g/L COD palmitic acid added, respectively. The acetate concentration increased as the palmitic acid concentration added to each of the assays increased. This increase in acetate explains the larger drop in pH observed as the concentration of palmitic acid increased, as shown in Figure 5.2 b.

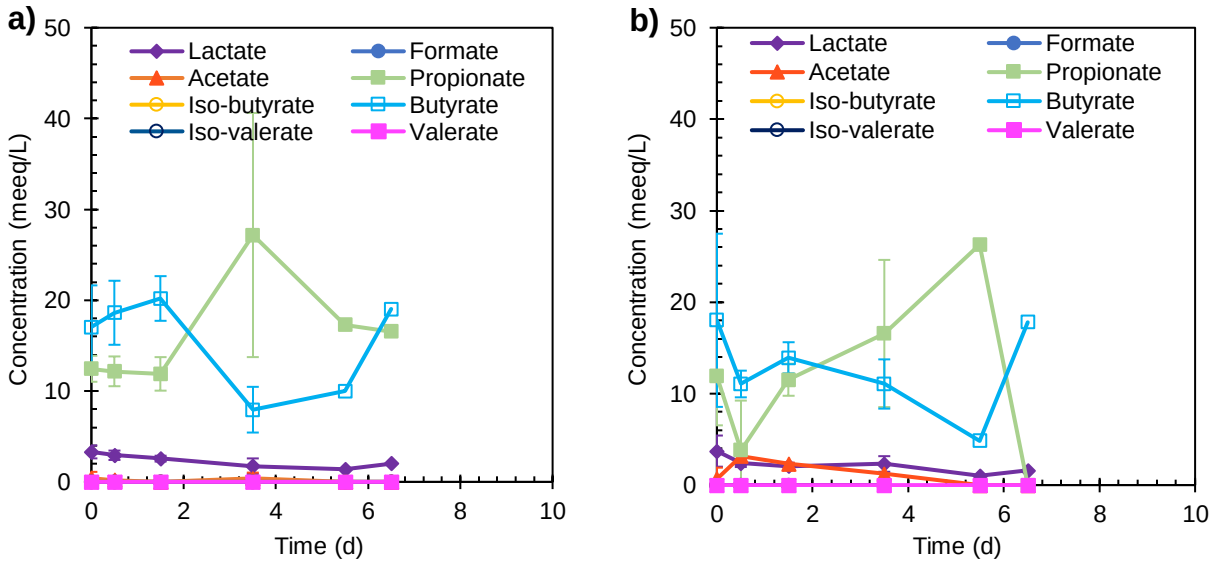

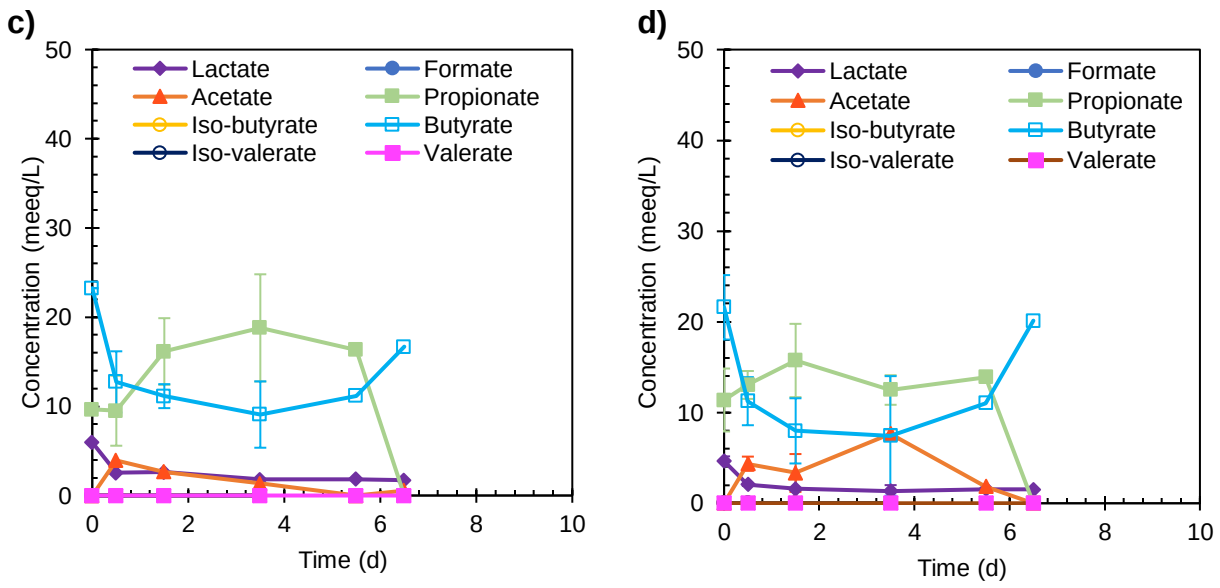

Figure 5.7: VFA data for a) the control and palmitic acid assays with b) 2 g/L COD, c) 4 g/L COD, and d) 6 g/L COD of palmitic acid added. The acids are shown in different colors in units of meeq/L.

The VFA data for the control prepared for the myristic acid assays is shown in Figure 5.8 a. The VFA data for the three concentrations of myristic acid, 2, 4, and 6 g/L COD, is shown in Figure 5.8 b, Figure 5.8 c, and Figure 5.8 d, respectively. Butyrate was present from day 0 in all assays except the control and degraded within the experiment's first days. The butyrate presence on day 0 suggests it was present in the LCFA stock solution used. After the initial degradation, butyrate remained relatively constant at low concentrations throughout the experiment. Low acetate concentrations were present in assays spiked with 2 and 4 g/L COD of myristic acid. At peak acetate accumulation, the fraction of electrons measured were 5.40±0.1% and 19.5±2.4% of the 2 and 4 g/L COD myristic acid added, respectively. In contrast, at peak acetate accumulation, the fraction of electrons measured were 72.1±9.8% of the 6 g/L COD myristic acid added. Therefore, a significantly greater acetate concentration was accumulated in the assays spiked with 6 g/L COD of myristic acid. The significant difference in acetate concentrations explains the large differences in pH of the 6 g/L COD compared to the 2 and 4 g/L COD as shown in Figure 5.2 c. As the pH decreased, methanogens were most likely unable to quickly utilize the acetate to produce

methane since methanogens only function in a pH range between 6.5 and 7.5 with an optimum of pH 6.8.[32] The assays spiked with 6 g/L myristic acid had a significantly different response than the 2 and 4 g/L COD assays because of the low pH. The low pH could have impacted the Gibbs free energy and/or microbial function.

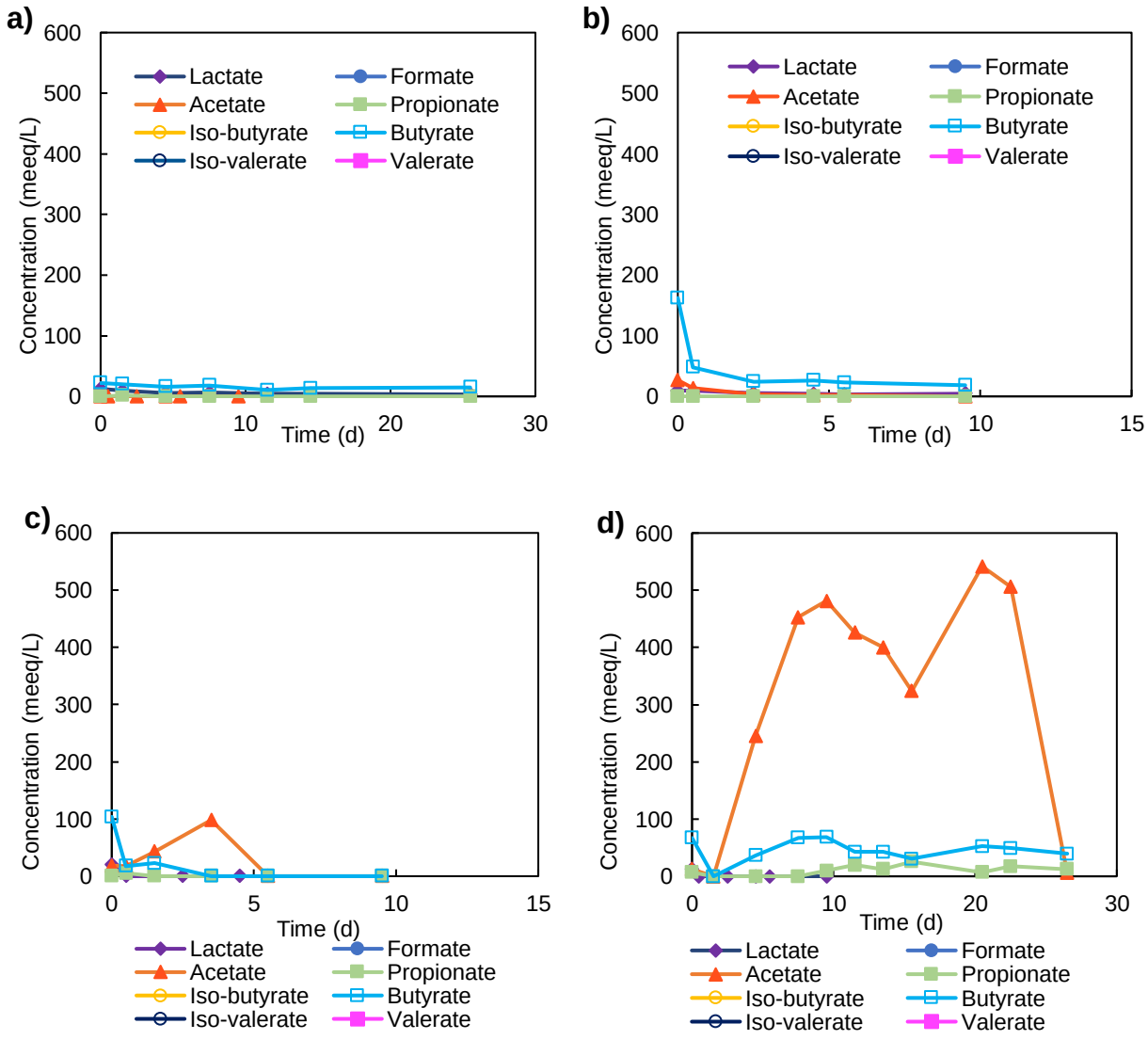

Figure 5.8: VFA data for a) the control and myristic acid assays with b) 2 g/L COD, c) 4 g/L COD, and d) 6 g/L COD of myristic acid added. The acids are shown in different colors in units of meeq/L.

To allow eeq/bottle to be tracked throughout the experiment, the methane, LCFA, and VFA graphs associated with stearic acid at every concentration are shown in Appendix F. These graphs

shown the eeq/bottle divided into methane, LCFA, and VFA eeq; however, to more clearly show the eeq/bottle trend, graphs with total eeq/bottle, summing eeq/bottle of methane, LCFA, and VFA, are included in Appendix G. The graphs in Appendix F serve as an example of how the graphs in Appendix G were calculated. The graphs in Appendix G show that all or almost all eeq added to the bottle on day 0 were converted to methane. All of the assays had a drop in eeq/bottle on day 1 which shows that the acid could have become insoluble during this time, or it could have adsorbed to biomass.

6. Objective I and II Results and Discussion: Unsaturated Acids

The two unsaturated acids evaluated in anaerobic co-digestion were linoleic and oleic acid with 18 carbons and two and one double bond, respectively. The inoculum was obtained from Mauldin Road Water Resource Recovery Facility (WRRF) (ReWa-Greenville, SC) a day before preparing the assays. Two cycles of assays were prepared, and the inoculum characteristics are summarized in Table 6.1.

Table 6.1: Summary of inoculum characteristics for the two batches of assays prepared for unsaturated acids.

	Linoleic Assay	Oleic Assay
pH	7.9	7.6
Alkalinity (mg/L $CaCO_3$)	2,700±110	2,800±110
Total Solids (mg/L)	15,300±2,900	13,400±5,700
Volatile Solids (mg/L)	11,200±2,000	10,000±4,200

6.1 Objective I

Objective I aimed to analyze methane production of anaerobic co-digestion batch bottles spiked with five different LCFAs at varying concentrations and saturation. This analysis included experimental data from sampling the assays and determination of parameters for methane

production from a mathematical model, the Gompertz model. The following results describe the methane production of only the unsaturated acids.

6.1.1 Biogas Production

Biogas was measured daily while bottles were in operation, and the amount of biogas was recorded as mL of methane produced daily. The total volume of methane was calculated by adding the daily volume produced together. The volume (mL) of methane was then converted to electron milliequivalents (meeq) to allow for consistent comparison among all experiments. Shown in Figure 6.1 a and b are the total amount of methane produced in meeq from the addition of linoleic and oleic acid, respectively, at three different concentrations of each LCFA. The control for each set of batch bottles is displayed in the figures in addition to the three concentrations of each of the acids.

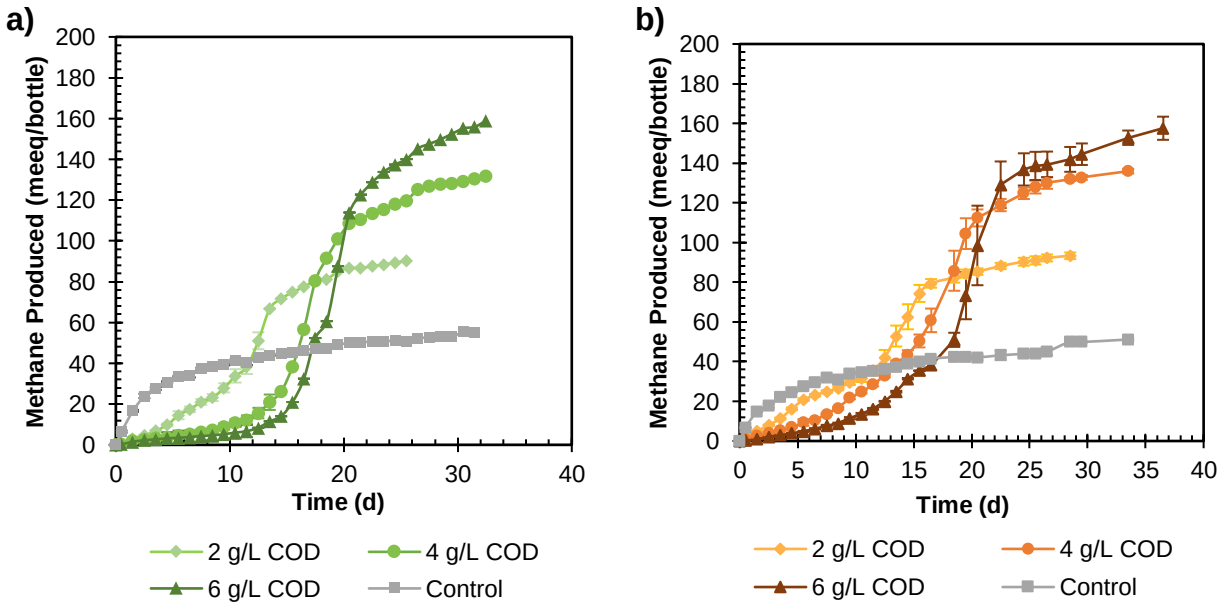

Figure 6.1: Total production of methane in milliequivalents (meeq/bottle) of assays spiked with 2, 4, and 6 g/L COD of a) linoleic acid and b) oleic acid.

The methane production curves for the assays spiked with linoleic and oleic acid shown in Figure 6.1 a and b display a characteristic S-curve with a long lag phase followed by large and

consistent methane production and then a plateau at a maximum methane yield. The curves for the unsaturated acids are similar; however, the bottles spiked with oleic acid had a more gradual increase in methane, while the bottles with linoleic acid had a longer phase where methane production was zero within the first days. While the two 18-carbon unsaturated acids had very similar methane production curves, the curves are different from the saturated 18-carbon (stearic acid) methane curve shown in Figure 5.1 a.

Based on acetolactic and hydrogenotrophic methanogenesis, the total amount of methane expected was calculated based on the concentration of acids being added in mg/L COD. Based on the expected methane production, 20% of the methane produced was from hydrogenotrophic methanogens and 80% of the methane produced was from acetoclastic methanogens. The percentages were calculated with the total methane predicted and the total methane produced in each saturated acid assay, excluding the methane produced in the control. An example of the calculations is shown in Appendix A. For assays with linoleic acid added at 2, 4, and 6 g COD/L, it was predicted that 31.3, 62.6, and 93.9 meeq of methane would be produced, respectively. The actual assays with linoleic acid added produced, on average, 3.3% (2 g/L) and 1.2% (4 g/L more methane than predicted. The linoleic acid 6 g/L assays produced 90% of the predicted methane. For assays with oleic acid added at 2, 4, and 6 g COD/L, it was predicted that 30.0, 60.1, and 90.1 meeq of methane would be produced, respectively. The actual assays with oleic acid added produced, on average, 58% (2 g/L), 36% (4 g/L), and 10% (6 g/L) more methane than predicted.

Appendix B Figure B.1 d and e show the H_2 partial pressures present in linoleic and oleic acid assays. At some points during the experiment, the partial pressures of all of the assays did exceed 10^{-4} atm, denoted by the dashed red line. However, 10^{-4} atm is just an approximation, and

all the instances in which 10^{-4} atm was exceeded were by a small amount. Therefore, the inhibition observed in the saturated acid assays does not result from elevated H_2 partial pressure.

6.1.2 Gompertz Model

The Gompertz model was used to determine biogas yield potential, length of lag phase, and the maximal biogas generation rate. Appendix C Figure C.1 d and e display the methane production curves fitted with the Gompertz model to display the fit. All curves were calculated with $R^2 \geq 0.98$. Figure C.1 e shows that the Gompertz Model did not fit the oleic acid methane production curve at a high concentration as well as the lower concentrations. This deviation can be attributed to lower pH observed in these assays which will be discussed in the following section. Table 6.2 shows the average lag times in days for each of the unsaturated acids. Linoleic acid had a longer lag time compared to oleic acid for all concentrations. Linoleic acid has two double bonds and oleic acid only has one which could contribute to linoleic acid having longer lag times. The control maintained a lag phase of 0 ± 0 days. Table 6.3 shows the maximum methane production rate (mL/d) [k_p] for each of the unsaturated acids. Linoleic maintained the highest k_p for all concentrations. As concentration increases, the k_p for linoleic acid and oleic acid increased.

Table 6.2: Average lag phase (d) and standard deviation calculated using the Gompertz model for each of the unsaturated acids.

	Linoleic Acid	Oleic Acid
2 g/L COD	11.45±0.2	10.37±0.5
4 g/L COD	15.74±0.4	13.58±0.3
6 g/L COD	17.91±0.1	17.65±0.1

Table 6.3: Average maximum methane production rate (mL/d) and standard deviation calculated using the Gompertz model for each of the unsaturated acids.

	Linoleic Acid	Oleic Acid
2 g/L COD	29.43±2.7	28.10±0.7
4 g/L COD	58.52±14.8	39.77±2.9
6 g/L COD	78.91±23.1	76.77±20.5

Figure 6.2 compares the lag times for each acid based on concentration, including both saturated and unsaturated acids. The bar chart shows that the unsaturated, linoleic and oleic acids had longer lag times than all the saturated acids. Based on an ANOVA test completed, the p-value was 8.8×10^{-6}, indicating that there is statistical difference among the mean lag times when comparing the acids. After a post-ANOVA assessment, the statistical difference was found to be between all saturated acids' when their mean lag times were compared to unsaturated acids' mean lag times. There was no statistical difference when the mean lag times of saturated acids were compared to other saturated acids or when linoleic acid was compared to oleic acid. The calculations used to make these statistical conclusions are shown in Appendix D. For all acids, the lag time follows a trend of increasing with increasing concentration. However, there is no statistical difference in lag times based on concentration (ANOVA p-value=0.8). Figure 6.3 shows a comparison of the methane production rate from all acids, based on concentration, including for both saturated and unsaturated acids. The bar chart shows that 18 carbon acids (linoleic, oleic, and stearic acid) have similar methane production rates at all three concentrations. Palmitic acid has the highest methane production rate for all concentrations compared to the other acids at the same

concentration. For all of the acids, excluding myristic acid, the methane production rate increases with increasing concentration.

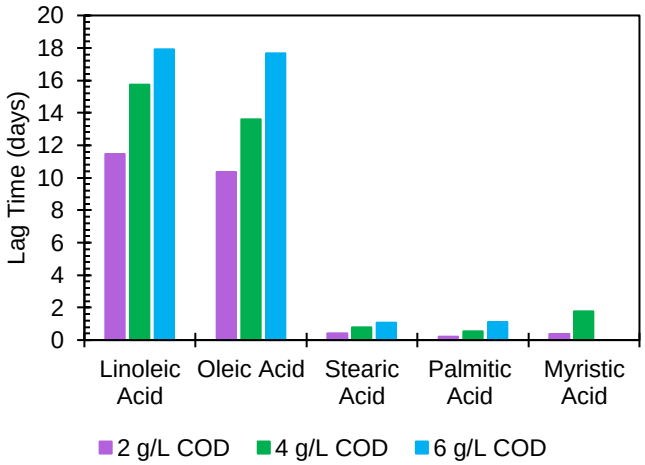

Figure 6.2: Lag times (days) of each of the acids, saturated and unsaturated as determined with the Gompertz model. Each concentration is distinguished by a different color.

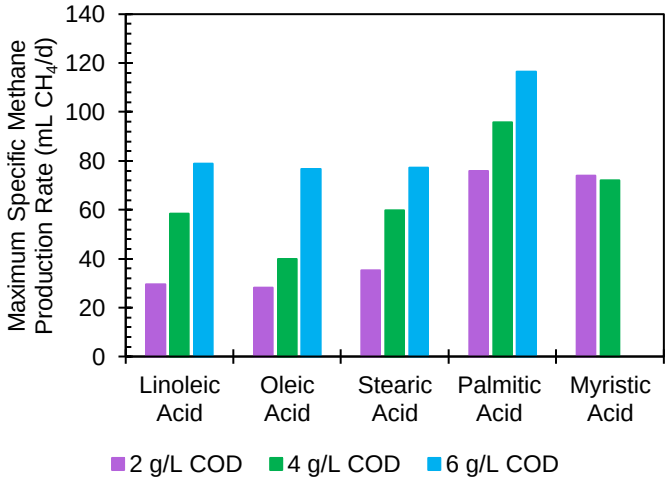

Figure 6.3: Maximum methane production rate (mL CH4/d) of each of the acids, saturated and unsaturated, as determined with the Gompertz model. Each concentration is distinguished by a different color.

6.2 Objective II

Objective II aimed to analyze pH, VFAs, and LCFAs in the assays. The LCFA data was used to determine the apparent first-order degradation kinetics of each LCFA and intermediate LCFAs

that form during unsaturated LCFA degradation. The VFA data was used to understand the intermediates that form and accumulate during unsaturated LCFA degradation.

6.2.1 pH

The pH was recorded daily and is shown in Figure 6.4 a and b. All assays began at a pH of 7.2 since adjusting the pH with hydrochloric acid was part of assay preparation. A 20 mM phosphate buffer was also added to resist changes in pH due to the production and consumption of acetate and other by-products in the degradation process. The assays with linoleic acid added had a pH ranging from 7.36 to 6.6. For linoleic acid, all of the concentrations had similar drops in pH. The assays with oleic acid added had a pH ranging from 7.41 to 6.47. For oleic acid, not all concentrations reached a pH of 6.47. The lowest concentration dropped to a pH of 6.88, the 4 g/L COD assays dropped to a pH of 6.56, and the highest concentration dropped to a pH of 6.47. The low pH can impact methanogenesis as methanogens have an ideal pH range between 6.5 and 7.5 and are optimized at a pH of 6.8.[36] *Syntrophomonas*, a suspected beta-oxidizer, are also impacted by low pH as its pH range for growth is between 6.5 and 8.5 and its optimal pH is between 7 and 7.5.[38] The buffer added was 3 g/L as CaCO3 which is around the same level as the alkalinity in the inoculum for the linoleic and oleic assays. However, the phosphate buffer, along with the alkalinity in the inoculum, was not high enough to resist the significant change in pH and, in the future, should be added at a higher concentration.

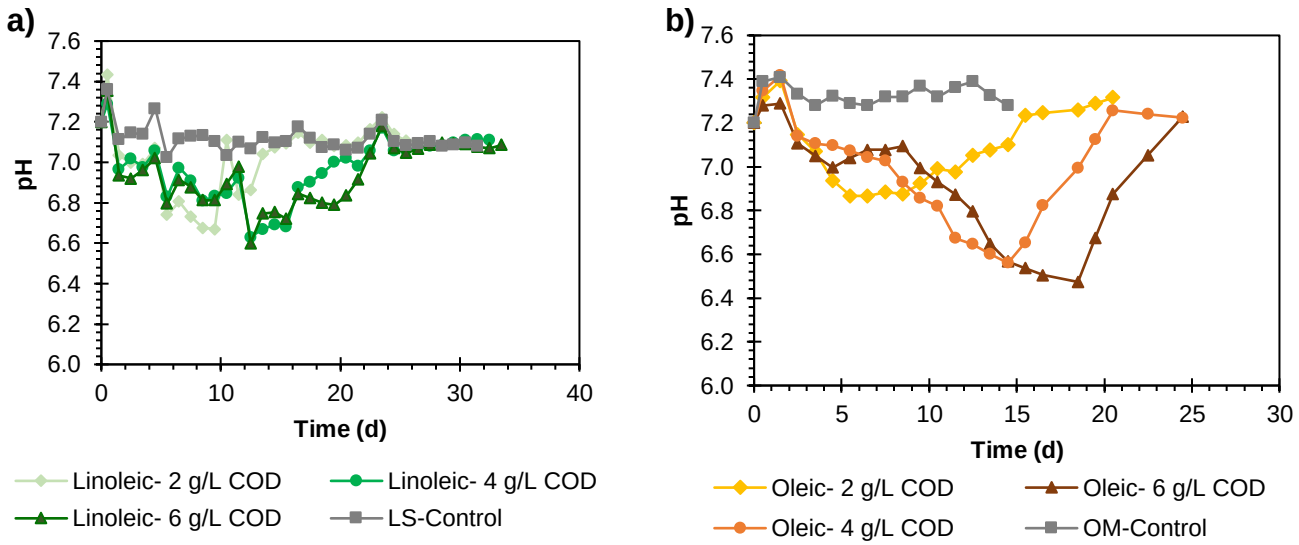

Figure 6.4: Change in pH versus time in assays with a) linoleic acid and b) oleic acid added.

6.2.2 Long-chain Fatty Acid Analysis

LCFAs were measured for each unsaturated acid at every concentration on varying days throughout the experiment. LCFAs were measured in mM and then converted into meeq/L to allow for consistent comparison across all LCFA, VFA, and biogas data.

The LCFA data for the control prepared for the linoleic acid assays is shown in Figure 6.5 a. The LCFA data for the three concentrations of linoleic acid, 2, 4, and 6 g/L COD, is shown in Figure 6.5 b, c, and d, respectively. Each of the linoleic assays shows that linoleic acid degraded rapidly in the first days of the experiment. After linoleic acid was degraded, stearic acid was observed at low levels, slightly higher than the control, as shown in Appendix E Figure E.2. At peak stearic acid accumulation, the fraction of electrons measured were 37.4±2.8%, 13.1±2.6% and 9.87±0.8% of the 2, 4, and 6 g/L COD linoleic acid added, respectively. Palmitic acid was formed at high concentrations and accumulated in all assays. At peak palmitic acid accumulation, the fraction of electrons measured were 79.11±3.6%, 68.4±5.8%, and 58.1±2.3% of the 2, 4, and 6 g/L COD linoleic acid added, respectively. Palmitic acid accumulation and subsequent degradation in the linoleic assays align with the lag phase observed in the biogas data shown in

Figure 6.1 a. Biogas was only observed after palmitic acid began to degrade in the assays. Myristic acid was also observed in low concentrations in each of the assays and increased in concentration as concentration of linoleic acid added increased. At peak myristic acid accumulation, the fraction of electrons measured were 24.7±13.3%, 25.1±1.7%, and 21.3±2.9% of the 2, 4, and 6 g/L COD linoleic acid added, respectively. This LCFA data suggests that the mode of degradation of the unsaturated LCFA is either hydrogenation followed by beta-oxidation or hydrogenation and beta-oxidation occurring simultaneously. Since stearic acid was not observed at concentrations significantly different than the control, it either was produced through hydrogenation and consumed immediately through beta-oxidation, or it was never produced, suggesting simultaneous hydrogenation and beta-oxidation. Another observation is that oleic acid was never detected. Therefore, hydrogenation of the two double bonds must occur simultaneously since the single, double-bonded compound (oleic acid) was never observed. Palmitic acid thus can be confirmed as the primary LCFA inhibitor for linoleic acid degradation. As discussed previously, palmitic acid did not greatly inhibit methane production in assays spiked with palmitic acid, as shown in Figure 5.1 b. However, in the bottles spiked with palmitic acid, the pH never went below 6.95, whereas in the assays spiked with linoleic acid, the pH was between 7 and 6.9 when palmitic acid began to accumulate but decreased to as low as 6.6. Therefore, the inhibition caused by an accumulation of palmitic acid could be partially attributed to decreased pH. Also, in the assays spiked with palmitic acid, no stearic acid was present. In contrast, palmitic acid accumulated alongside stearic acid in the linoleic assays. In these assays, stearic acid was at a much lower concentration than palmitic acid. Therefore, another possibility is that stearic acid inhibits palmitic acid degradation.

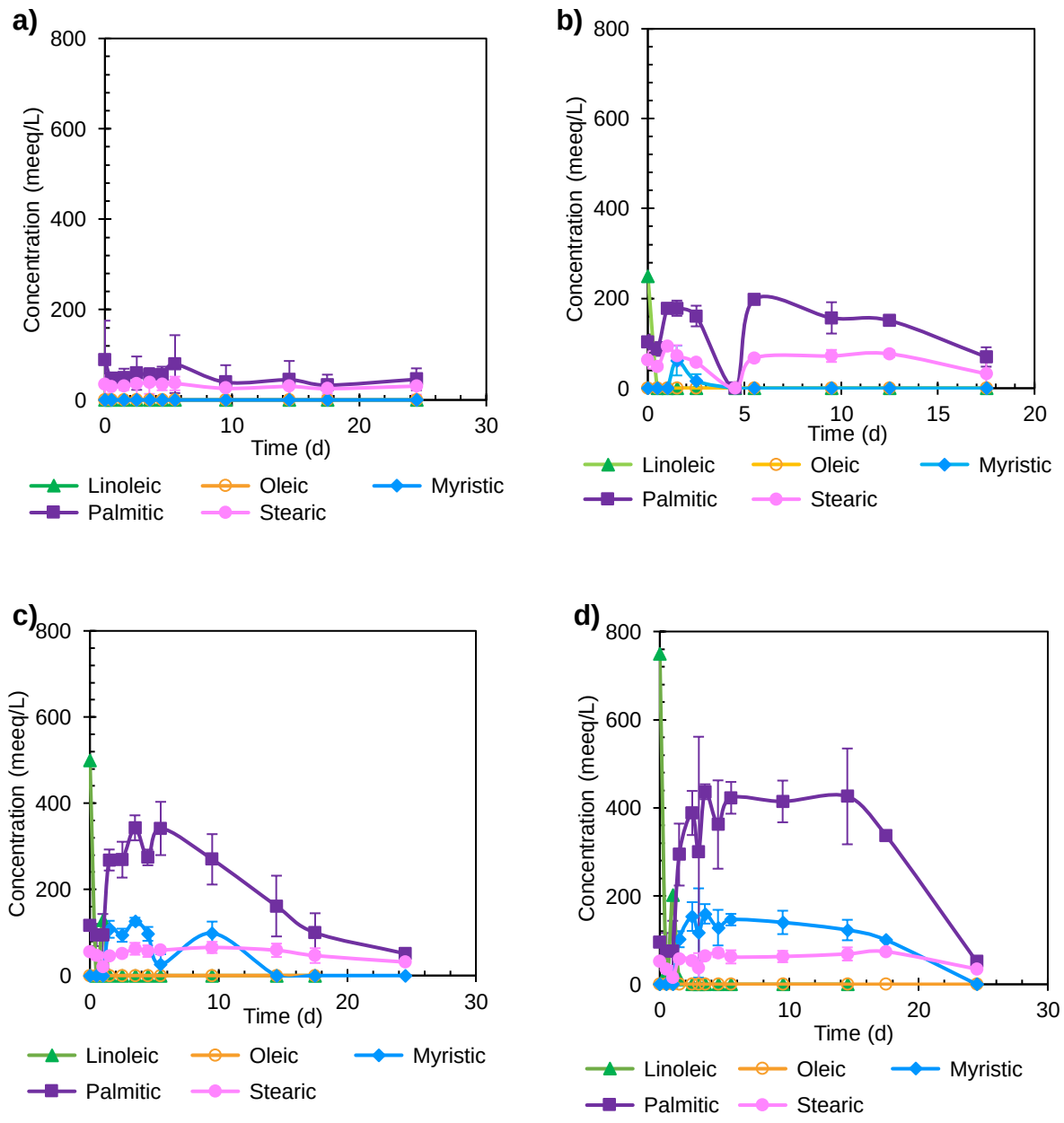

Figure 6.5: LCFA data for a) the control and linoleic acid assays with b) 2 g/L COD, c) 4 g/L COD, and d) 6 g/L COD of linoleic acid added. The acids are shown in different colors in units of meeq/L.

The LCFA data for the control prepared for the oleic acid assays is shown in Figure 6.6 a. The LCFA data for the three concentrations of oleic acid, 2, 4, and 6 g/L COD, is shown in Figure 6.6 b, c, and d, respectively. Each of the oleic assays shows that oleic acid degraded rapidly in the first days of the experiment. After oleic acid was degraded, stearic acid was observed at low levels,

slightly higher than the control, as shown in Appendix E Figure E.3. At peak stearic acid accumulation, the fraction of electrons measured were 16.4±15.6%, 9.22±8.5%, and 6.5±5.6% of the 2, 4, and 6 g/L COD oleic acid added, respectively. Palmitic acid was formed at high concentrations and accumulated in all the assays. At peak palmitic acid accumulation, the fraction of electrons measured were 36.8±20.8%, 37.5±8.4%, and 48.1±1.6% of the 2, 4, and 6 g/L COD oleic acid added, respectively. Palmitic acid did not accumulate as significantly in the lowest concentration assay, as shown in Figure 6.6 b. Palmitic acid accumulation and subsequent degradation in the oleic assays align with the lag phase observed in the biogas data shown in Figure 6.1 b. Biogas was only observed after palmitic acid was completely or almost completely degraded in each assay. Myristic acid was not detected in any of the assays. Similarly to the linoleic assays, this LCFA data suggests that the mode of degradation of the unsaturated LCFA is either hydrogenation followed by beta-oxidation or hydrogenation and beta-oxidation occurring simultaneously. Since stearic acid was not detected at large concentrations, it either was produced through hydrogenation and consumed immediately through beta-oxidation, or it was never produced, which would suggest simultaneous hydrogenation and beta-oxidation. Palmitic acid thus can be confirmed as the primary LCFA inhibitor for oleic acid degradation. As discussed previously, palmitic acid did not greatly inhibit methane production in assays spiked with palmitic acid, as shown in Figure 5.1 b. However, in the bottles spiked with palmitic acid, the pH never went below 6.95 and, in the assays spiked with oleic acid, the pH was between 7.1 and 7 when palmitic acid began to accumulate but dropped as low as 6.85, 6.55, and 6.45 for 2, 4, and 6 g/L COD, respectively. Therefore, the accumulation of palmitic acid can be partially attributed to the significant drop in pH. Once the pH dropped significantly, the system had to recover, leading to

the long lag phase caused by accumulation of palmitic acid. Similarly to the linoleic acid assays, the presence of stearic acid could be inhibiting palmitic acid degradation.

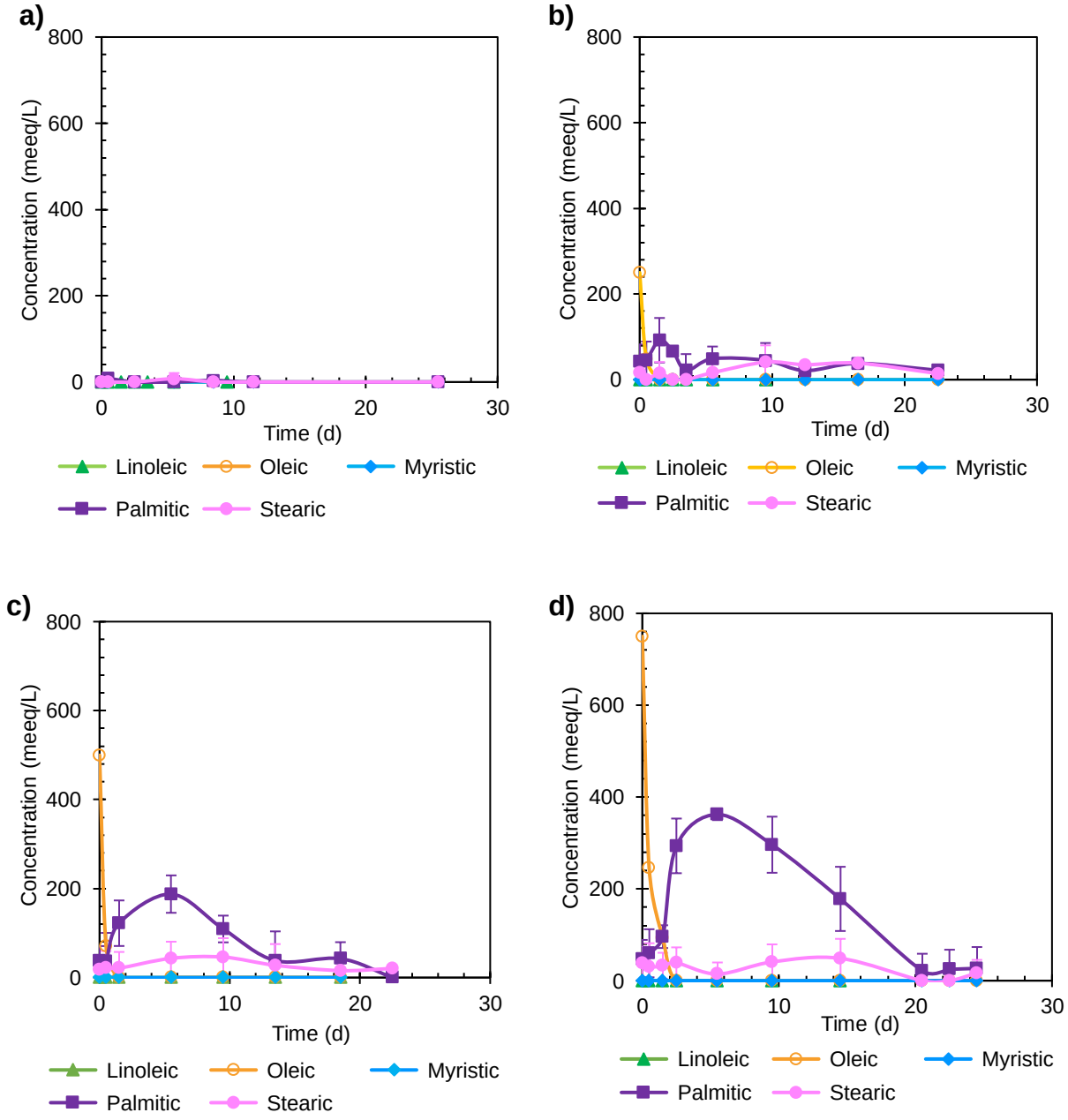

Figure 6.6: LCFA data for a) the control and oleic acid assays with b) 2 g/L COD, c) 4 g/L COD, and d) 6 g/L COD of oleic acid added. The acids are shown in different colors in units of meeq/L.

To better understand the degradation rates and allow for comparison, a kinetic evaluation was completed, and the apparent degradation constants normalized to g VS fed of all acids, including saturated and unsaturated acids are shown in Figure 6.7. The apparent degradation

constant was not calculated for the lowest concentration of linoleic acid because it degraded within the first 12 hours before the first sample was taken. Oleic acid degraded the fastest at 4 g/L COD and the slowest at 6 g/L COD. Inversely, linoleic acid degraded the slowest at 4 g/L COD and the fastest at 6 g/L COD. Based on the averages, oleic acid has a higher apparent degradation constant and, therefore, faster degradation when compared to linoleic acid. Both unsaturated acids had a greater apparent degradation constant than the saturated 18-carbon, stearic acid. From a thermodynamic perspective, linoleic acid has a more negative Gibbs free energy when compared to oleic acid and would, therefore, be more thermodynamically favorable to degrade, as shown in Table 2.1; however, the rate of degradation was slower than oleic acid. Therefore, while a reaction may be more thermodynamically favorable to proceed, it will not necessarily have a faster rate of reaction. However, both unsaturated acids have a more negative Gibbs free energy compared to the 18-carbon saturated compound and both unsaturated acids degrade faster than stearic acid, implying that Gibbs free energy does partially influence degradation kinetics. From the bar graph, it is clear that unsaturated acids degrade faster than saturated acids. Of the saturated acids, excluding myristic at 6 g/L COD, myristic acid degrades faster than palmitic acid, which degrades faster than stearic acid. An ANOVA test was used to determine the statistical variance between saturated vs unsaturated acid's degradation constants. A p-value of 0.03 was calculated and therefore suggests that one or more of the mean degradation constants are different from each other. A post-ANOVA assessment was completed to determine which groups are statistically different from each other. The assessment concluded that there was statistical different between the saturated and unsaturated acids but there was no statistical different within the saturated and unsaturated groups. The calculations used to make these statistical conclusions are shown in Appendix D.

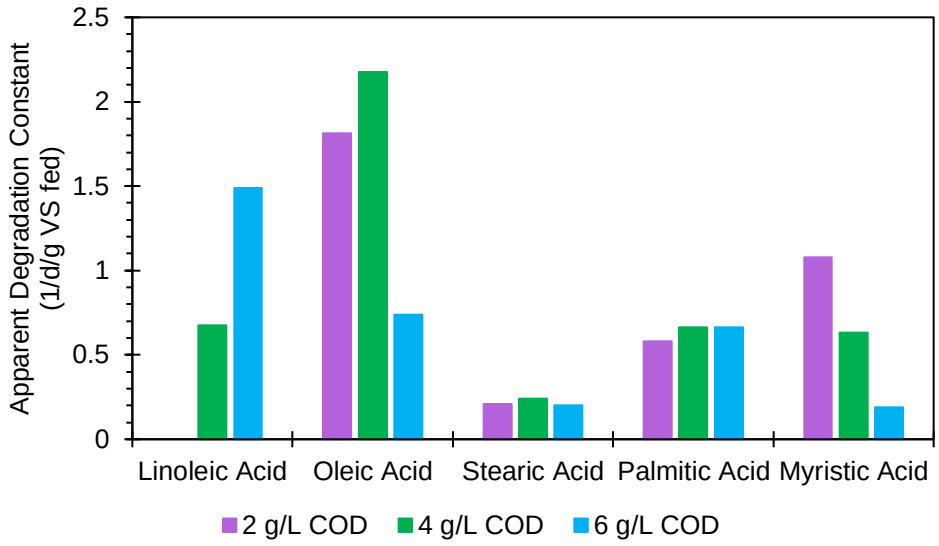

Figure 6.7: Bar graph showing the apparent degradation constants (1/d/g VS fed) of each acid at all concentrations.

6.2.3 Volatile Fatty Acid Analysis

VFAs were measured for each unsaturated acid at every concentration on varying days throughout the experiment. VFAs were measured in mM and then converted into meeq/L to allow to consistent comparison across all LCFA, VFA, and biogas data.

The VFA data for the control prepared for the linoleic acid assays is shown in Figure 6.8 a. The VFA data for the three concentrations of linoleic acid, 2, 4, and 6 g/L COD, is shown in Figure 6.8 b, c, and d, respectively. Butyrate is present on day 0 at a high concentration in all assays except for the control. Butyrate is present in the control but at a much lower concentration. The butyrate in the linoleic assays may be from the inoculum and the stock linoleic acid used in the experiment. Propionate was produced in all linoleic acid assays at low concentrations. At peak propionate accumulation, the fraction of electrons measured were 12.2±4.3%, 8.3±2.3%, and 7.7±1.3% of the 2, 4, and 6 g/L COD linoleic acid added, respectively. The propionate production could be attributed to the degradation mechanism of the unsaturated acid. Acetate was the VFA at

the highest concentration, and the maximum amount produced increased with the increase in linoleic acid concentration. At peak acetate accumulation, the fraction of electrons measured were 61.5±0.8%, 30.6±2.1%, and 18.8±1.9% of the 2, 4, and 6 g/L COD linoleic acid added, respectively. The drop in pH and long lag phase experienced in the linoleic assays can be attributed to the increased acetate production and accumulation. The acetate accumulation also occurred during the same time as palmitic acid accumulation, as shown in Figure 6.6 b, c, and d.

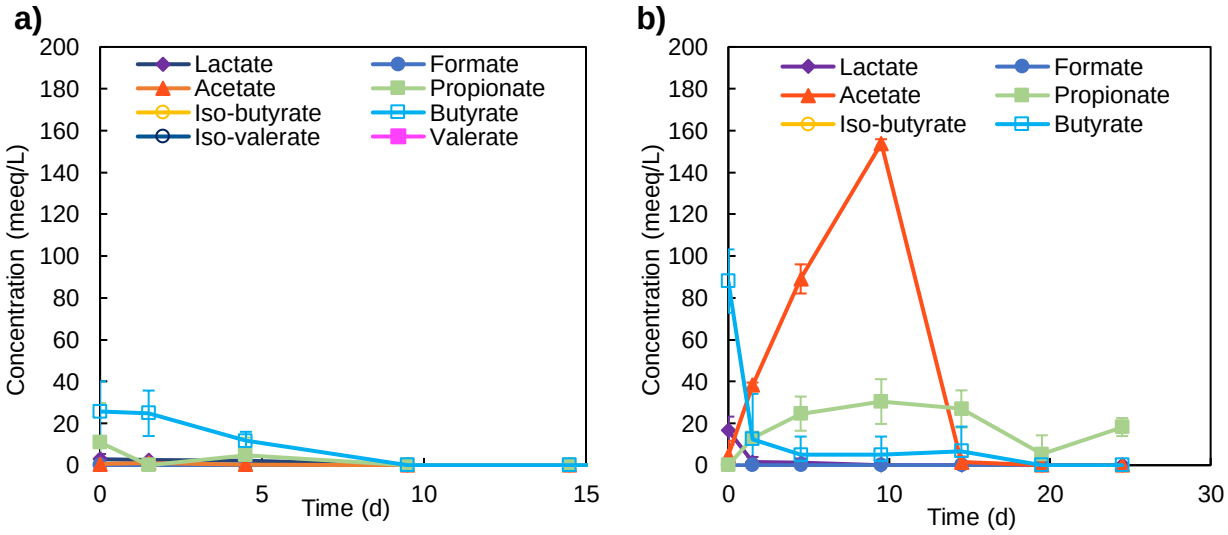

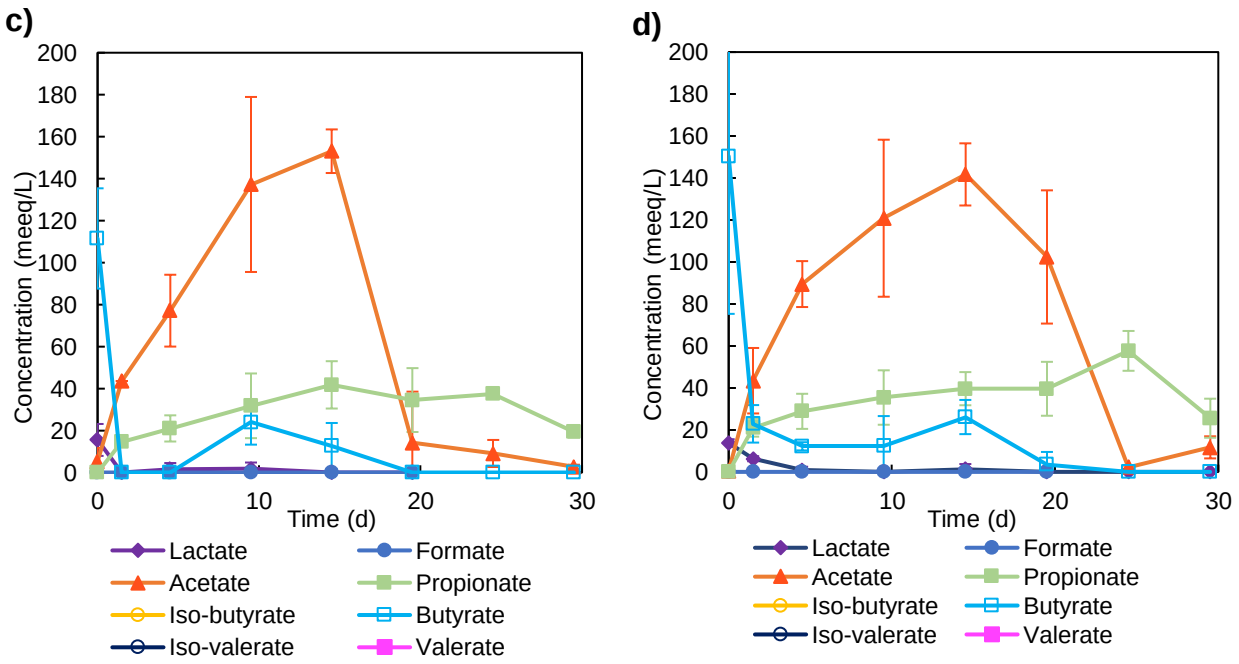

Figure 6.8: VFA data for a) the control and linoleic acid assays with b) 2 g/L COD, c) 4 g/L COD, and d) 6 g/L COD of linoleic acid added. The acids are shown in different colors in units of meeq/L.

The VFA data for the control prepared for the oleic acid assays is shown in Figure 6.9 a. The VFA data for the three concentrations of oleic acid, 2, 4, and 6 g/L COD, is shown Figure 6.9 b, c, and d, respectively. Butyrate is present on day 0 at a high concentration in all assays except for the control. Butyrate is present in the control but at a much lower concentration. The butyrate may, therefore, be from the stock oleic acid used in the experiment. Similarly to linoleic acid, propionate was produced in all oleic acid assays at low concentrations. At peak propionate accumulation, the fraction of electrons measured were 12.8±2.2%, 6.2±1.3%, and 21.7±3.3% of the 2, 4, and 6 g/L COD oleic acid added, respectively. The propionate production could be attributed to the degradation mechanism of oleic acid. Acetate was the VFA at the highest concentration, and the maximum amount produced increases with increasing oleic acid concentration, indicating a direct relationship between oleic degradation and acetate production. At peak acetate accumulation, the fraction of electrons measured were 82.7±1.3%, 57.9±2.7%, and 46.7±5.7% of the 2, 4, and 6 g/L COD oleic acid added, respectively. The decreases in pH and

long lag phase experienced in the oleic assays can be attributed to the increased acetate production and accumulation. The trend that pH becomes lower at higher oleic acid concentration as seen in Figure 6.4 b can be attributed to the increased acetate production and accumulation as oleic acid concentration increases in the assays. The acetate accumulation also occurred during the same time as palmitic acid accumulation as shown in Figure 6.6 b, c, and d.

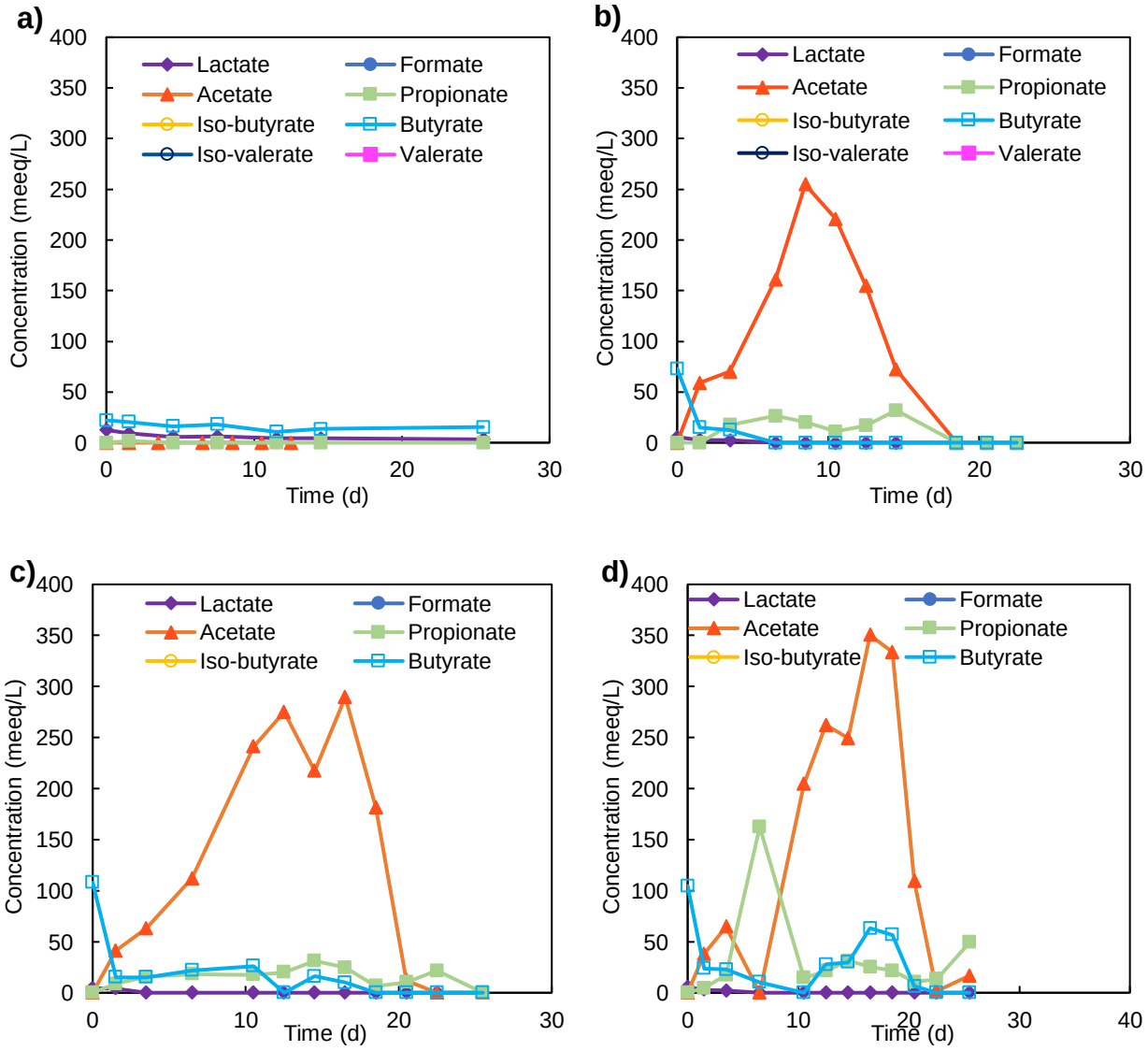

Figure 6.9: VFA data for a) the control and oleic acid assays with b) 2 g/L COD, c) 4 g/L COD, and d) 6 g/L COD of oleic acid added. The acids are shown in different colors in units of meeq/L.

To clearly show the eeq/bottle trend, graphs with total eeq/bottle, summing eeq/bottle of methane, LCFA, and VFA, are included in Appendix G. The graphs in Appendix G show that all or almost all eeq added to the bottle on day 0 were converted to methane. All of the assays had a drop in eeq/bottle on day 1 which shows that the acid could have become insoluble during this time, or it could have adsorbed to biomass.

7. Objective III Results and Discussion: Saturated and Unsaturated Acids

7.1 Objective III

The purpose of the third objective was to compare microbial community composition between the saturated and unsaturated acid assays. Within this objective, the microbial communities were analyzed through 16S rRNA sequencing. The inoculum obtained for this experiment was from an operating anaerobic digester. Since digesters are operated as a continuously stirred tank reactor (CSTR), there could have been an impact on the initial microbial community when they were spiked with LCFAs in this experiment. In typical anaerobic digesters much lower concentrations of LCFAs are maintained unless there is an upset. Also, the use of batch reactors most likely impacted the kinetics of growth of microbes in the system. In CSTRs, the reactors are continuously fed which promotes stable and continuous growth. In batch reactors, the reactors are spiked with nutrients at the beginning of operation which leads to variable growth rate of microbes in the system due to changes in substrate availability. Growth rate of microbes in batch reactors can be slowed down due to lack of substrate or inhibition.

7.1.1 Sequencing: Inoculum

DNA samples were sequenced by a third party (MRDNA) and analyzed using qiime2. The inoculum, which represents the initial microbial communities, and end samples for each of the batch assays were analyzed. Three different inocula were used in the experiment. The archaea and

bacterial abundance for each of the inocula is shown in Figure 7.1 a and b, respectively. Each inoculum contained similar percentages of all archaea and bacteria; therefore, differences in response to the LCFAs cannot be attributed to differences in the microbial communities in the inoculum. The archaea present mainly belong to *Methanosaeta*, *Methanospirillum*, and *Methanofastidiosum*, which are all methanogens. *Methanosaeta* use VFAs as a carbon source and is an acetolactic methanogen.[39] *Methanospirillum* is a hydrogenotrophic methanogen that uses hydrogen as an electron donor to produce methane.[40] *Methanofastidiosum* was previously uncharacterized, but a recent genome study reveals that acetate, propionate, and malonate are potential carbon sources. In addition, *Methanofastidiosum* lacks genes for acetoclastic and hydrogenotrophic methanogenesis and most likely is restricted to methylated thiol reduction for methane production.[41] The bacteria present mainly belong to *Cloacimonas* and *Rikenellaceae DMER64*. *Cloacimonas* is a dominant bacterium in anaerobic digestion and is believed to be a hydrogen-producing syntroph. The bacterium is also suspected to acquire carbon and energy through fermentation of amino acids, carboxylic acids, and sugars.[42] *Rikenella* is a fermenting genus which produces propionate and occasionally acetate.[21] *Syntrophomonas* has been previously identified as an LCFA beta-oxidizer in anaerobic digestion; however, *Syntrophomonas* is not shown in Figure 7.1 b because it had a relative abundance of less than 5% in all inoculum samples. In the inoculum used in linoleic and stearic acid assays, *Syntrophomonas* was on average 0.3% (±0.1%) of the total bacteria present. In the inoculum used in oleic and myristic acids, *Syntrophomonas* was on average 0.18% (±0.02%) of the total bacteria present and in the inoculum used in palmitic acid assays, it was 0.06% (±0.03%) of the total bacteria present.

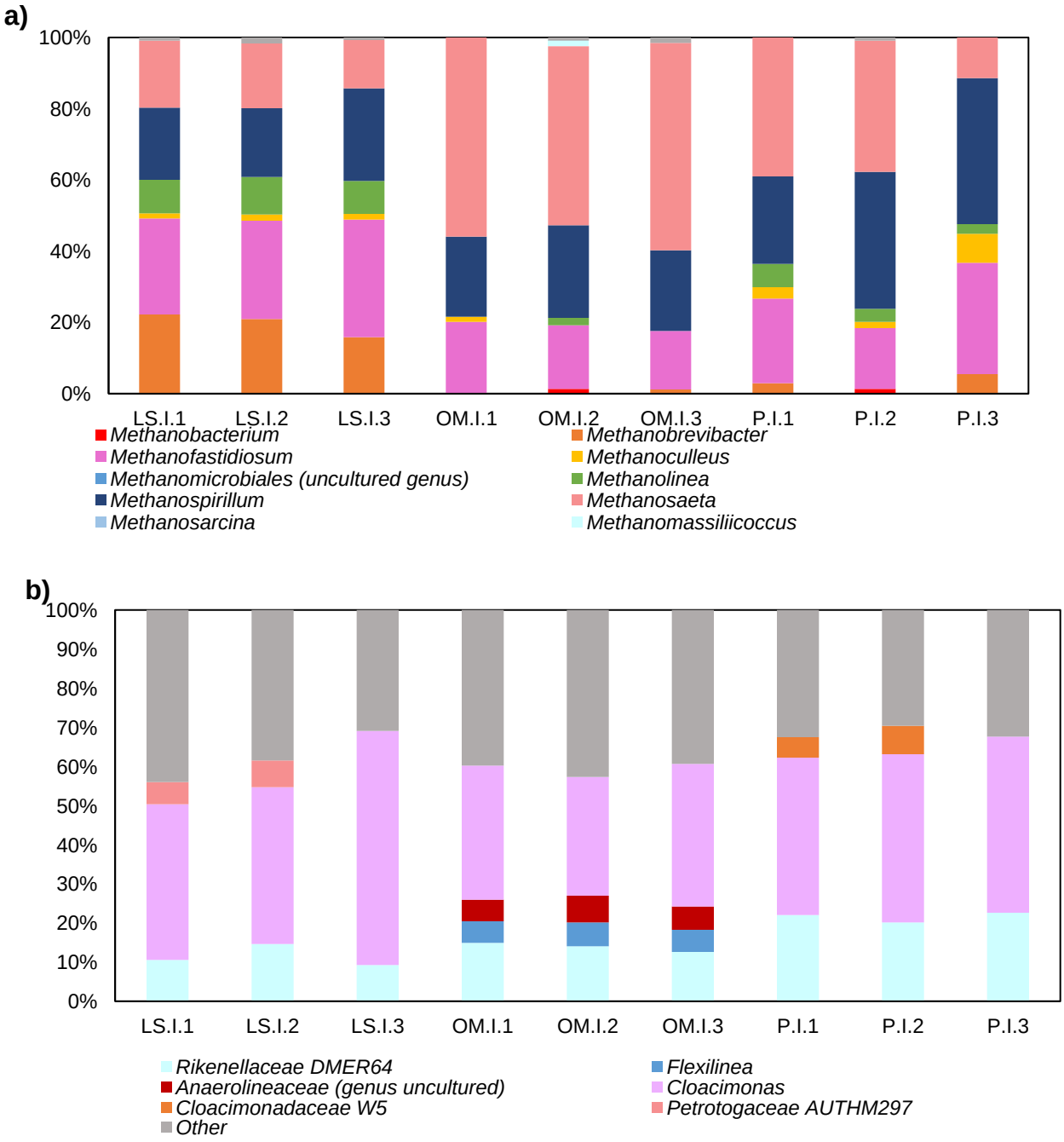

Figure 7.1: a) Archaeal and b) bacterial genera present in the inoculum used in each of the batch assays. LS represents the inoculum used in linoleic and stearic assays. OM represents the inoculum used in oleic and myristic assays. P represents inoculum used in palmitic assays. The inoculum samples were run in triplicate. Only archaea present above 1% are included in the chart. Only bacteria present above 5% are included in the chart.

7.1.2 Sequencing: 2 g/L COD Samples

The sequencing data showing percentages of various archaea and bacteria in the assays with 2 g/L COD of the LCFAs added are shown in Figure 7.2 a and b, respectively. Compared to

the inoculum, *Methanospirillum* was more dominant in the assays after LCFAs had been added and subsequently degraded. Since the degradation of LCFAs produces hydrogen, this increase is expected for the hydrogenotrophic methanogenic genus. *Methanosaeta* remained present at high percentages and most likely can be linked to acetate consumption as it is an acetoclastic methanogenic genus. The bacteria present in each of the different acid assays varied; however, *Cloacimonas* remained abundant in all assays. *Anaerolineaceae* was observed in both unsaturated LCFAs as well as two palmitic acid bottles. *Anaerolineaceae* has previously been observed to be dominant in the anaerobic digestion of LCFAs, but its role (if any) in unsaturated LCFA degradation has not been determined.[43] *Flexilinea* was only observed above 5% abundance in the unsaturated acid assays. This genus' growth has been shown to be enhanced when co-cultivated with hydrogenotrophic methanogens such as *Methanospirillum*; however, there has not been a link to the degradation of unsaturated LCFAs.[44] *Rikenella* remained present at a low abundance in the saturated acid assays and significantly decreased in abundance in the unsaturated acid assays. *Syntrophomonas* remained below 5% in all samples. In the linoleic and oleic acid assays, *Syntrophomonas* was, on average, present at 1.4% (±0.2%) and 0.64% (±0.2%), respectively. In the stearic, palmitic, and myristic acid assays, *Syntrophomonas* was, on average, present at 0.83% (±0.2%), 0.30% (±0.02%), and 0.50% (±0.1%), respectively. Compared to the inoculum percentages, the percentage of *Syntrophomonas* present did increase, but this does not necessarily mean that *Syntrophomonas* grew.

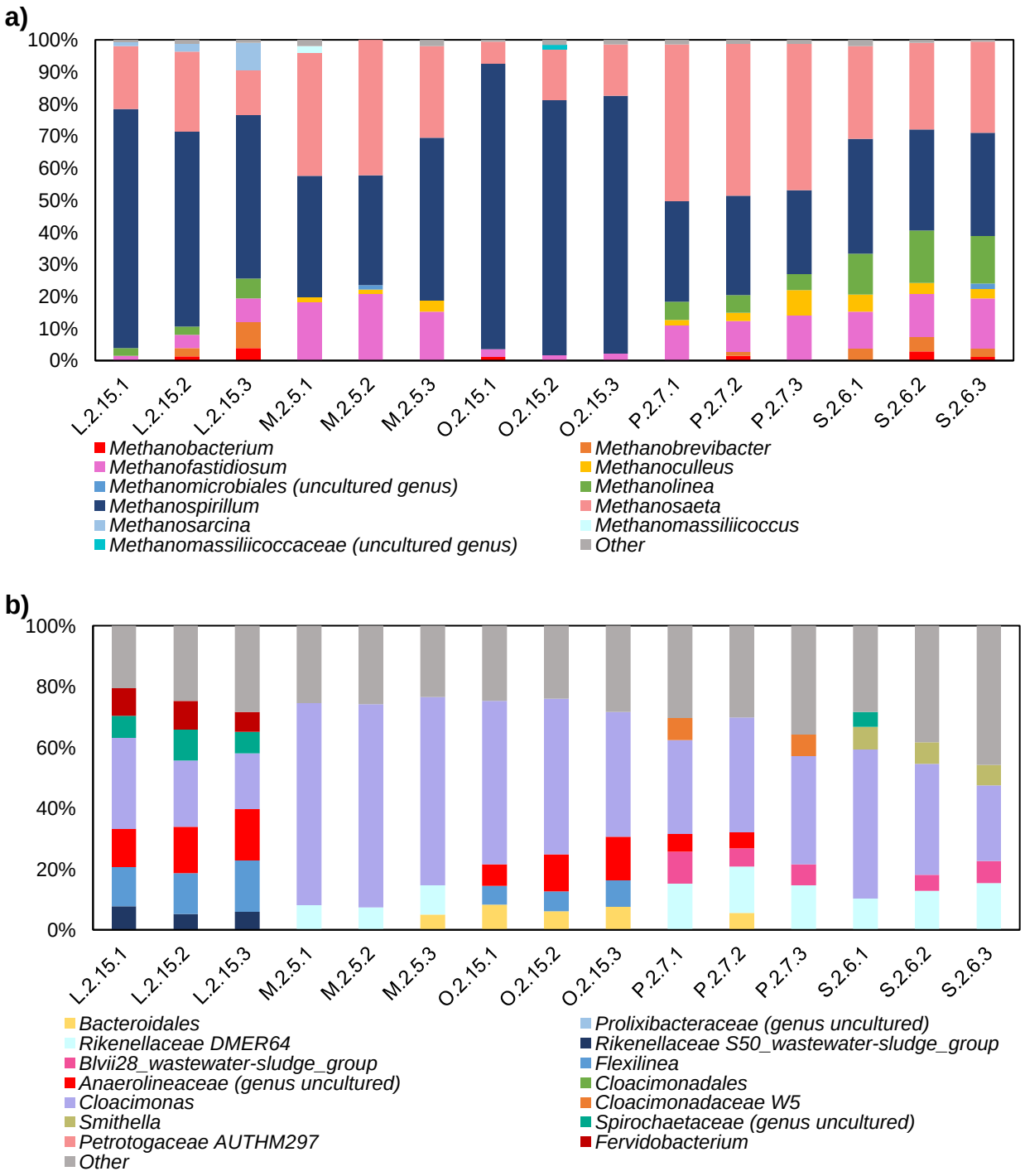

Figure 7.2: a) Archaeal and b) bacterial genera present in the end point samples taken from each of the 2 g/L COD batch assays. LS represents the inoculum used in linoleic and stearic assays. OM represents the inoculum used in oleic and myristic assays. P represents inoculum used in palmitic assays. The inoculum samples were run in triplicate. Only archaea present above 1% are included in the chart. Only bacteria present above 5% are included in the chart.

7.1.3 Sequencing: 4 g/L COD Samples

The sequencing data showing percentages of various archaea and bacteria in the assays with 4 g/L COD of the LCFAs added are shown in Figure 7.3 a and b, respectively. Compared to the inoculum, *Methanospirillum* became a more dominant genus in the 4 g/L COD unsaturated acid samples after the LCFA had been degraded. In the saturated samples, *Methanospirillum* and *Methanosaeta* became the most abundant genus present. *Methanospirillum* can most likely be linked to the low hydrogen partial pressure that was maintained throughout the experiment, as it is a hydrogenotrophic methanogen.[45] The *Methanosaeta* percent abundance was suppressed in the unsaturated acid samples but remained high in the saturated samples. *Methanosarcina* was only abundant in the unsaturated acid samples. *Methanosarcina* can use three methanogenic pathways: acetoclastic, hydrogenotrophic, and methylotrophic methanogenesis. As discussed previously, the unsaturated acids had the longest lag times observed, which could have allowed this metabolically versatile archaeal genus to grow. *Cloacimonas* remained abundant in the saturated acid samples and was suppressed in the unsaturated acid samples, indicating that it does not play a role in unsaturated acid degradation and metabolism. Similarly to the 2 g/L COD unsaturated samples, *Flexilinea* was abundant in small percentages, which correlates to the high percentage of a hydrogenotrophic methanogen genus, *Methanospirillum*. *Anaerolineaceae* was observed in large abundance in oleic acid assays and in smaller abundance in linoleic acid and palmitic acid assays. The genus' abundance in the unsaturated acid end samples suggests that this genus could be important for degradation of unsaturated LCFAs or conversion of degradation products to acetate. *Peptostreptococcales-Tissierallales* was dominant in the linoleic acid assays. This genus, commonly found in human intestines, metabolizes peptone and amino acids to VFAs and has not been observed previously in degradation of LCFAs.[46] *Syntrophomonas* can be observed in the

chart for the linoleic acid assays, and it remained below 5% in all other acids. In the linoleic and oleic acid assays, *Syntrophomonas* was, on average, present at 8.97% (±1.4%) and 3.84% (±0.4%), respectively. In the stearic, palmitic, and myristic acid assays, *Syntrophomonas* was, on average, present at 2.08% (±0.5%), 1.19% (±0.2%), and 1.12% (±0.17%), respectively. Compared to the inoculum and 2 g/L COD percentages, the percentage of Syntrophomonas present did increase, but this does not necessarily mean that *Syntrophomonas* grew.

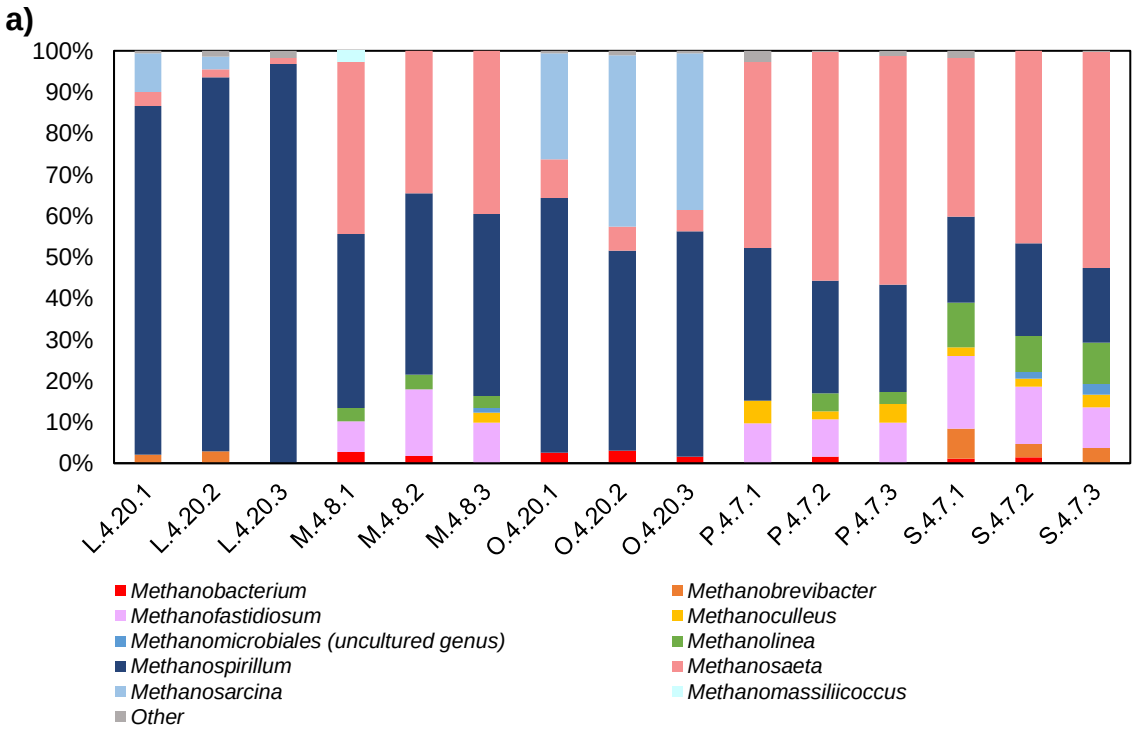

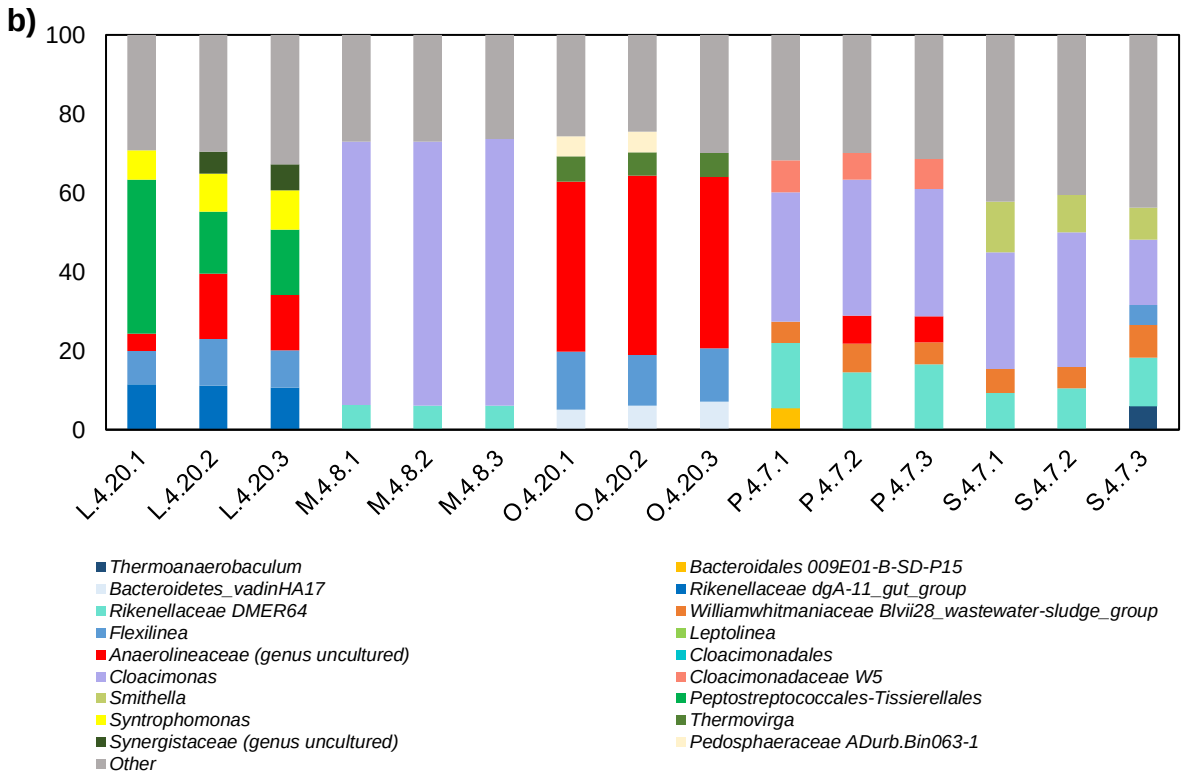

Figure 7.3: a) Archaeal and b) bacterial genera present in the end point samples taken from each of the 4 g/L COD batch assays. LS represents the inoculum used in linoleic and stearic assays. OM represents the inoculum used in oleic and myristic assays. P represents inoculum used in palmitic assays. The inoculum samples were run in triplicate. Only archaea present above 1% are included in the chart. Only bacteria present above 5% are included in the chart.

7.1.4 Sequencing: 6 g/L COD Samples

The sequencing data showing percentages of various archaea and bacteria in the assays with 6 g/L COD of the LCFAs added are shown in Figure 7.4 a and b, respectively. From an archaea perspective, both unsaturated acids have a similar dominance of *Methanospirillum* and *Methanosarcina* when compared to the 4 g/L COD sequencing data. As discussed previously, myristic acid at 6 g/L COD resulted a double S-curve in the methane production curve. Therefore, two sets of samples were sequenced from two different days to show the change in microbial abundance during the first curve and second curve. On day 15, both *Methanospirillum* and *Methanosaeta* were dominant, with *Methanospirillum* being at a higher percent abundance. On day 26, after the lag was overcome and peak methane was produced, *Methanosarcina*, which was

commonly observed in unsaturated acid samples, had a greater abundance than both *Methanospirillum* and *Methanosaeta*. Assays for myristic acid at 6 g/L, linoleic acid, and oleic acid all had long lags that can be observed in the methane curves. In each of these assays, the pH also decreased more than the other saturated acid assays (especially in myristic 6 g/L COD). The presence of *Methanosarcina*, a methanogen capable of utilizing all three pathways of methanogenesis, in all of these samples in which long lag times and low pHs were observed suggests that *Methanosarcina* was capable of growing at the low, non-favorable pH and used both acetate and H_2 and CO_2 to produce methane and bring the pH back to neutral. For the saturated acids, the dominant bacteria remain consistent from 2 and 4 g/L COD. Mostly *Cloacimonas* is dominant in the saturated acid bacteria sequencing data; however, in bottles 2 and 3 for stearic acid, there is no dominant bacteria as "other" is a large percent of the present bacteria, which indicates genera present at less than 5% abundance. The unsaturated acid bacteria sequencing results differ from 2 and 4 g/L results as different genera were abundant. *Clostridia* was dominant in the linoleic acid assays; however, little information is available for this genus with respect to LCFA degradation. *Clostridia* in general have a fermentative metabolism with the major end product being acetate.[47] The two unsaturated acids have two bacterium in common—*Acidobacteriae GoutB8* and *Hydrogenedensaceae*. *Acidobacteriae GoutB8* has not been characterized or connected with a prominent anaerobic digestion genus. *Hydrogenedensaceae* is a suspected hydrogen consumer.[48] *Caldilieaceae* appeared above 5% in day 26 myristic acid assays, one oleic acid assay, and two palmitic acid assays. *Caldilieaceae* is notable because its carbon sources for growth include carbohydrates, amino acids, and fatty acids, suggesting that *Syntrophomonas* is not the only bacteria present that may consume LCFAs.[49] *Syntrophomonas* can be observed in the bottle 2 oleic acid assay chart, and it remained below 5% in all other acids. In

the linoleic and oleic acid assays, *Syntrophomonas* was on average present at 0.43% (±0.4%) and 3.94% (±2.8%), respectively. In the stearic, palmitic, and myristic acid day 15 and 26 assays, *Syntrophomonas* was on average present at 0.16% (±0.2%), 0.67% (±0.01%), 1.33% (±0.01%), and 0.27% (±0.1%), respectively. Compared to the 4 g/L COD percentages, the percent of *Syntrophomonas* present decreased, but this does not necessarily mean that there was less *Syntrophomonas* growth or less *Syntrophomonas* present. This decrease only means that *Syntrophomonas* was less abundant in the assay than the other bacteria in the same assay.

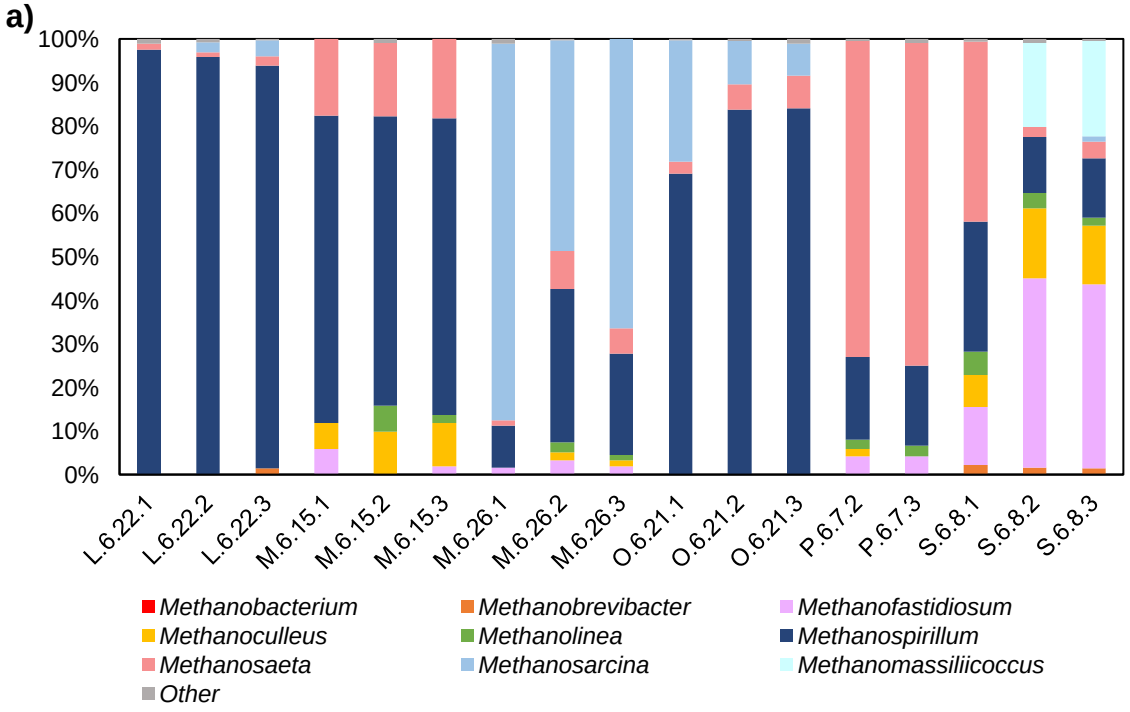

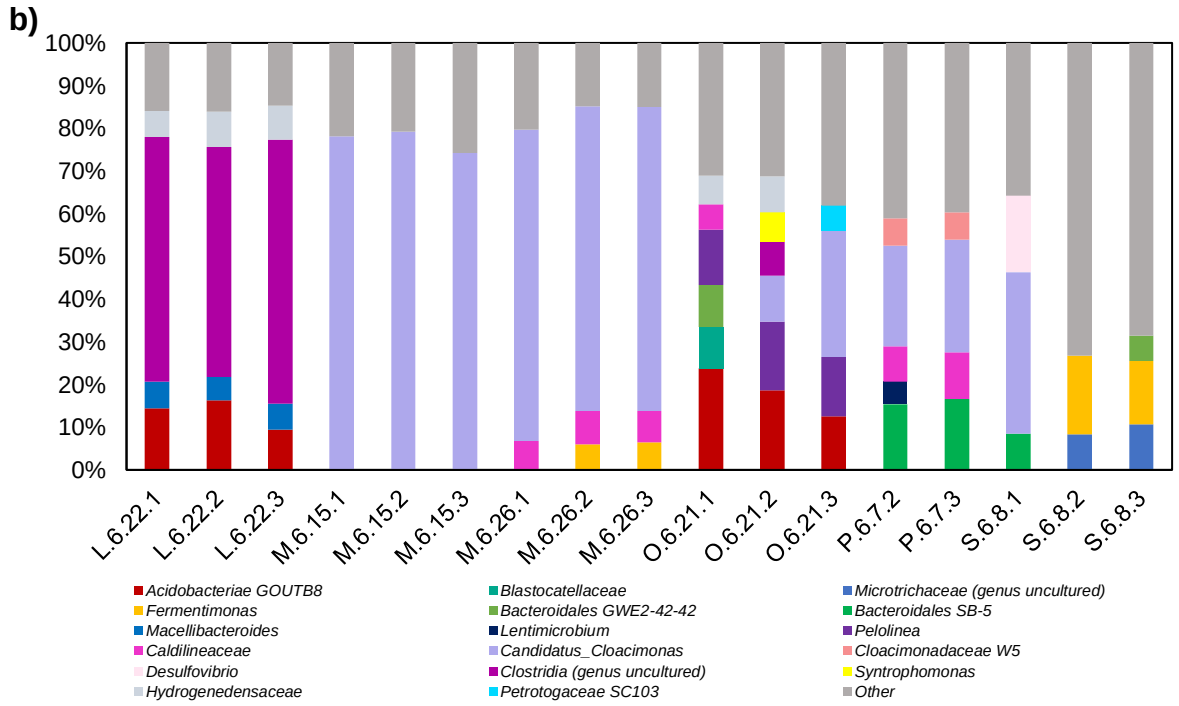

Figure 7.4: a) Archaeal and b) bacterial genera present in the end point samples taken from each of the 4 g/L COD batch assays. LS represents the inoculum used in linoleic and stearic assays. OM represents the inoculum used in oleic and myristic assays. P represents inoculum used in palmitic assays. The inoculum samples were run in triplicate. Only archaea present above 1% are included in the chart. Only bacteria present above 5% are included in the chart.

7.1.5 Principle Coordinate Analysis

Principle coordinate analysis (PCoA) is useful in determining relationships within sequencing data. This statistical tool is helpful in visualizing similarities and differences amongst sequencing data.[50] The PCoA plots for 2, 4, and 6 g/L COD are shown in Figure 7.5 a, b, and c, respectively. The distance metric used in these PCoA plots is weighted unifrac distances. As shown by the PCoA plots all of the inocula were similar to one another. Also, the saturated acids, specifically palmitic and stearic acid were similar to each other at every concentration. However, linoleic and oleic acid were different from the saturated acids and each other for all concentrations. While myristic acid day 15 and 26 had slight differences observed in the percent abundance graphs discussed above, the PCoA plots show that those differences were minimal.

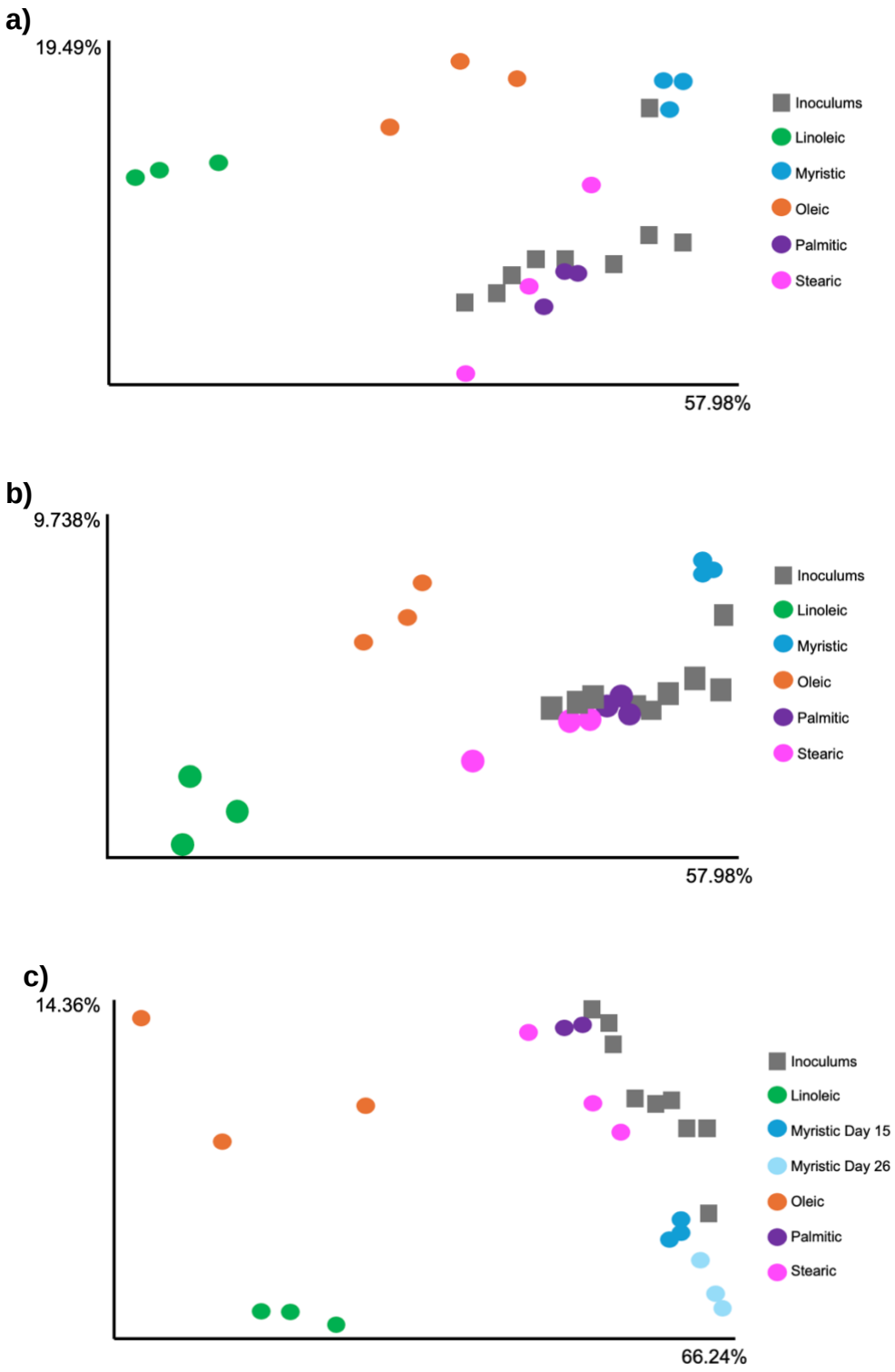

Figure 7.5: PCoA plot for all assays with a) 2 g/L, b) 4 g/L, and c) 6 g/L of LCFA added and the three sets of inocula.

PCoA plots were also created comparing all concentrations of unsaturated acids. This PCoA plot is displayed in Figure 7.6. This plot indicates that the 2 g/L COD unsaturated LCFA microbial communities are actually more similar to each other than the microbial communities from higher concentrations of unsaturated LCFAs. Linoleic acid 4 and 6 g/L COD have similar microbial communities, but the linoleic acid 2 g/L COD has a very different microbial community in comparison. Each concentration of oleic acid had very different microbial communities present. These results indicate that concentration of the unsaturated LCFA impacts the microbial communities present.

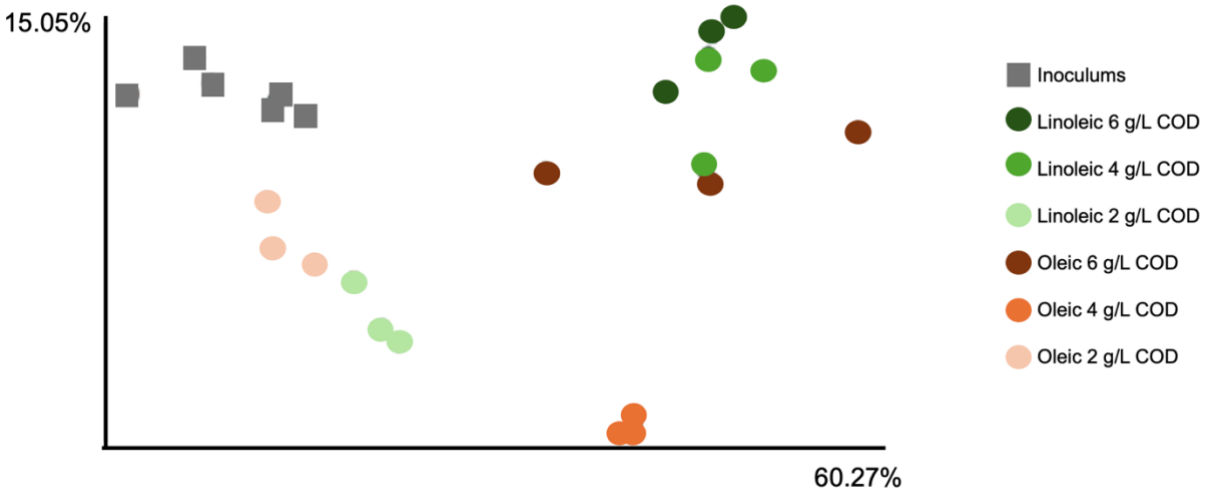

Figure 7.6: PCoA plot for all assays with unsaturated LCFAs added and the two sets of inocula associated with those assays.

In comparison, a PCoA plot was created comparing all concentrations of saturated acids. This PCoA plot is displayed Figure 7.7. Unlike the unsaturated acids, the microbial communities associated with each concentration of each saturated acid is similar. This similarity is shown by the clear clumps of each color in the PCoA plot. The microbial communities associated with each saturated acid is also different. The microbial communities in the palmitic and stearic acid assays appear to be more similar when compared to the microbial communities in the myristic acid assays. These results indicate that concentration of the saturated LCFAs does not impact the

microbial communities present. Also, the longer chain saturated acids (18 and 16-carbon) have more similar microbial communities than the shorter chain saturated acid (14-carbon).

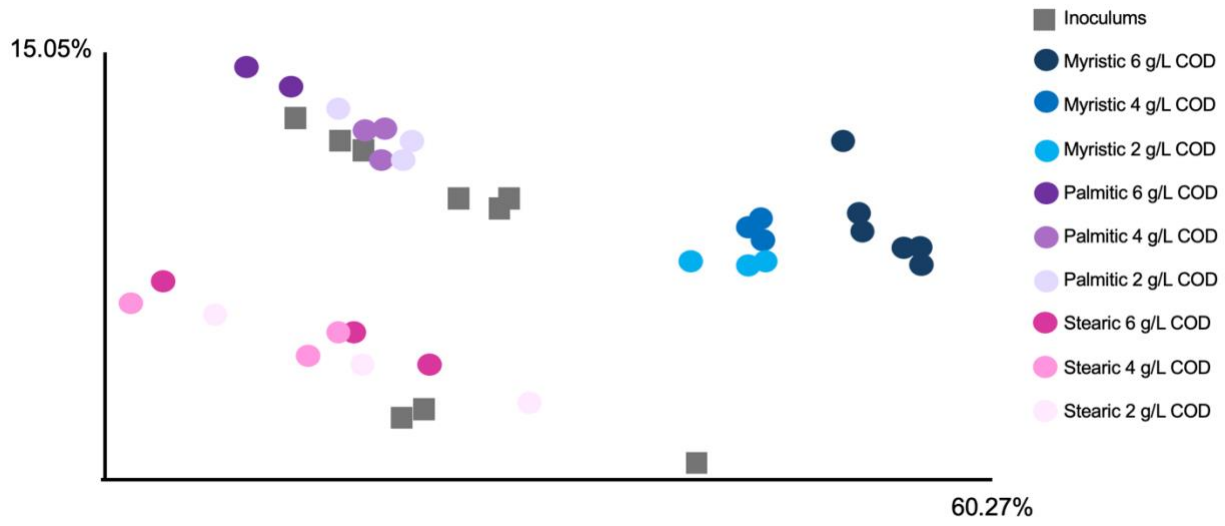

Figure 7.7: PCoA plot for all assays with saturated LCFAs added and the three sets of inocula associated with those assays.

8. Conclusions

In summary, this research was designed to better understand the degradation pathways and intermediates of five specific LCFAs dominant in FOG co-digestion and analyze the microbial communities involved in their degradation. Through preliminary research, three hypotheses were created:

I. Different microbial communities will be seen in bottles spiked with saturated and unsaturated acids.

II. Lag times and responses of both unsaturated acids will be similar and lag times and responses of the three saturated acids will be similar.

III. Microbial community composition and the Gibbs free energy of each reaction will impact kinetics.

Based on biogas data and Gompertz model, lag times for saturated LCFAs were much shorter than unsaturated LCFAs and the more unsaturated an acid was (i.e. the more double bonds) the longer the lag time becomes. The lag times shown in Table 5.2 and the ANOVA and post-ANOVA statistical analysis confirm that the second hypothesis shown above is correct—lag times and responses of both unsaturated acids were statistically similar and lag times and responses of the three saturated acids were statistically similar. While there is a correlation between lag times and saturation, there is no apparent correlation between chain length of saturated acids and lag time.

A possible impact on degradation kinetics that was not hypothesized was pH. As the pH dropped below the optimum pH of 6.8 for methanogens, acetate accumulated in many of the assays which led to an even larger pH drop and inhibition. Another possible pH implication is that *Syntrophomonas*, a LCFA beta-oxidizer, could have been inhibited or slowed when the pH was below its optimal pH of 6.5. This theory is supported by the accumulation of palmitic acid at low pHs; however, cannot be confirmed until more extensive microbial analysis is completed. In future experiments, a more concentrated buffer should be used to avoid pH being a factor in inhibition.

One purpose of this research was to increase understanding of the intermediates of the five LCFAs analyzed. For the saturated acids, the anticipated LCFA intermediates that should have formed through beta-oxidation were not observed and did not accumulate. However, this observation does not confirm that the intermediates did not form. The intermediates could have been in equilibrium and been consumed at the same rate they were produced. Since the three saturated acids had very short lag times, there was no specific inhibitor identified. The intermediates for the unsaturated acids were identifiable. Both unsaturated acid assays had palmitic acid accumulate. This acid was the only LCFA that accumulated in the assays. The degradation

pathway for the unsaturated LCFAs remains uncertain; however, it is either hydrogenation followed by beta-oxidation or simultaneous hydrogenation and beta-oxidation. For linoleic acid, the hydrogenation of the two double bonds occurred simultaneously since no oleic acid was observed. The LCFA inhibitor for these two unsaturated acids can be identified as palmitic acid.

The apparent degradation kinetics of the saturated acids did not align with what was most thermodynamically favorable to react based on Gibbs free energy. Myristic acid degraded the fastest followed by palmitic and stearic acid. If degradation was dependent on Gibbs free energy, the inverse would be true since of the saturated acids stearic acid has the most negative Gibbs free energy as shown in Table 2.1.The degradation kinetics of the unsaturated acids also did not follow what was thermodynamically favorable either. Oleic acid degraded faster than linoleic acid. Based solely on the Gibbs free energy values in Table 2.1, linoleic acid would degrade faster than oleic acid. The overall trend that the unsaturated acids degraded faster than the saturated acids can be explained with the Gibbs free energy values. However, thermodynamics did not impact kinetics as much as expected. Therefore, the third hypothesis that states thermodynamics will impact kinetics is incorrect. Gibbs free energy and thermodynamics have proven in previous studies to be a poor indicator of kinetics.[51]

From a volatile fatty acid perspective, acetate was the only impactful VFA observed. In the stearic acid assays, no VFAs accumulated. In the palmitic and myristic acid assays, acetate increased in concentration as the saturated acid concentration added increased. However, in the 6 g/L COD myristic acid assay, acetate accumulated for much longer and at a much higher concentration than palmitic acid 6 g/L COD. Acetate also accumulated in the unsaturated acid assays and aligned with times of palmitic acid accumulation. Acetate accumulation explains the large drops in pH experiences in myristic acid 6 g/L COD and the two unsaturated acids assays.

Propionate and butyrate were present in most assays, but production and degradation did not correspond to lag phases or periods of inhibition

Based on the sequencing data and PCoA plots, the first hypothesis described above is shown to be correct -- different microbial communities were seen in bottles spiked with saturated and unsaturated acids. However, it was not hypothesized that the two unsaturated acids would also have different microbial communities present. Based on the current data, it cannot be determined if the microbial communities impacted kinetics; therefore, the third hypothesis must be further researched.

9. Future Research

Syntrophomonas has been identified as the primary beta-oxidizer for palmitic acid and is suspected to degrade other saturated and unsaturated acids. Based on the sequencing data, the percent abundance of *Syntrophomonas* increased in the assays after the LCFAs were degraded. However, this sequencing data cannot be used to make any conclusions about *Syntrophomonas* growth. Future research will be important in determining if *Syntrophomonas* grew while the acids were being degraded which would indicate that the bacteria does degrade the given acid. If growth does occur, kinetics of growth can be determined and compared to the LCFA degradation rates calculated. The use of qPCR to quantify *Syntrophomonas* would also provide more answers to the third hypothesis above and possibly allow for a linkage between the microbial communities present and degradation kinetics.

Another area of future research would require spiking assays with two acids. In the unsaturated acid assays, palmitic acid accumulated at a high concentration while stearic acid was present at a much lower concentration. In the palmitic acid assays, palmitic did not accumulate but stearic acid was not present in these assays. The impact of stearic acid being present during

palmitic acid degradation is unclear and should be further explored. A future study would involve spiking assays with a constant, high concentration of palmitic acid and a lower, varying concentration of stearic acid and observing the results.

The final area of future research entails repeating this experiment except with carbon 14 versions of the saturated and unsaturated acids. Tagging the acids with carbon 14 would allow for easier identification of degradation products. This method would allow for more definitive conclusions to be made about the degradation pathways of linoleic and oleic acid. The use of carbon 14 would also assist in identifying which bacteria and archaea were involved in the degradation of the acids and their conversion to biogas. As bacteria and archaea consume the LCFAs enriched with caron 14, the carbon 14 will then be traceable in the biomass which will allow for easier identification of communities responsible for degradation.

10.References

(1) Hansen, K. H.; Ahring, B. K.; Raskin, L. Quantification of Syntrophic Fatty Acid-β-Oxidizing Bacteria in a Mesophilic Biogas Reactor by Oligonucleotide Probe Hybridization. *Appl Environ Microbiol* **1999**, *65* (11), 4767–4774. https://doi.org/10.1128/aem.65.11.4767-4774.1999.

(2) Grady, C. P. L.; Daigger, G. T.; Love, N. G.; Filipe, C. D. M. *Biological Wastewater Treatment: Third Edition*; 2011.

(3) Vavilin, V. A.; Rytov, S. V.; Lokshina, L. Y. A Description of Hydrolysis Kinetics in Anaerobic Degradation of Particulate Organic Matter. *Bioresour Technol* **1996**, *56* (2–3), 229–237. https://doi.org/10.1016/0960-8524(96)00034-X.

(4) Schink, B.; Friedrich, M. Energetics of Syntrophic Fatty Acid Oxidation. *FEMS Microbiol Rev* **1994**, *15* (2–3), 85–94. https://doi.org/10.1111/j.1574-6976.1994.tb00127.x.

(5) Mobilian, C.; Craft, C. B. Wetland Soils: Physical and Chemical Properties and Biogeochemical Processes. *Encyclopedia of Inland Waters, Second Edition* **2022**, *3*, 157–168. https://doi.org/10.1016/B978-0-12-819166-8.00049-9.

(6) Weng, C. nan; Jeris, J. S. Biochemical Mechanisms in the Methane Fermentation of Glutamic and Oleic Acids. *Water Res* **1976**, *10* (1), 9–18. https://doi.org/10.1016/0043-1354(76)90151-2.

(7) Rinzema, A.; Boone, M.; van Knippenberg, K.; Lettinga, G. Bactericidal Effect of Long Chain Fatty Acids in Anaerobic Digestion. *Water Environment Research* **1994**, *66* (1), 40–49. https://doi.org/10.2175/wer.66.1.7.

(8) Desbois, A. P.; Smith, V. J. Antibacterial Free Fatty Acids: Activities, Mechanisms of Action and Biotechnological Potential. *Appl Microbiol Biotechnol* **2010**, *85* (6), 1629–1642. https://doi.org/10.1007/s00253-009-2355-3.

(9) Salama, E. S.; Saha, S.; Kurade, M. B.; Dev, S.; Chang, S. W.; Jeon, B. H. Recent Trends in Anaerobic Co-Digestion: Fat, Oil, and Grease (FOG) for Enhanced Biomethanation. *Prog Energy Combust Sci* **2019**, *70*, 22–42. https://doi.org/10.1016/J.PECS.2018.08.002.

(10) Pereira, M. A.; Sousa, D. Z.; Mota, M.; Alves, M. M. Mineralization of LCFA Associated with Anaerobic Sludge: Kinetics, Enhancement of Methanogenic Activity, and Effect of VFA. *Biotechnol Bioeng* **2004**, *88* (4), 502–511. https://doi.org/10.1002/bit.20278.

(11) Viswanathan, C. V; Bai, B. M.; Pillai, S. C. Fatty Matter in Aerobic and Anaerobic Sewage Sludges. *J Water Pollut Control Fed* **1962**, *34* (2), 189–194.

(12) Sousa, D. Z.; Smidt, H.; Alves, M. M.; Stams, A. J. M. Ecophysiology of Syntrophic Communities That Degrade Saturated and Unsaturated Long-Chain Fatty Acids. *FEMS Microbiol Ecol* **2009**, *68* (3), 257–272. https://doi.org/10.1111/j.1574-6941.2009.00680.x.

(13) NOVAK JT; CARLSON DA. Kinetics of Anaerobic Long Chain Fatty Acid Degradation. *Journal of the Water Pollution Control Federation* **1970**, *42* (11), 1932–1943.

(14) Hwu, C. S.; Tseng, S. K.; Yuan, C. Y.; Kulik, Z.; Lettinga, G. Biosorption of Long-Chain Fatty Acids in UASB Treatment Process. *Water Res* **1998**, *32* (5), 1571–1579. https://doi.org/10.1016/S0043-1354(97)00352-7.

(15) Weng, C. nan; Jeris, J. S. Biochemical Mechanisms in the Methane Fermentation of Glutamic and Oleic Acids. *Water Res* **1976**, *10* (1), 9–18. https://doi.org/10.1016/0043-1354(76)90151-2.

(16) Ziels, R. M.; Karlsson, A.; Beck, D. A. C.; Ejlertsson, J.; Yekta, S. S.; Bjorn, A.; Stensel, H. D.; Svensson, B. H. Microbial Community Adaptation Influences Long-Chain Fatty

Acid Conversion during Anaerobic Codigestion of Fats, Oils, and Grease with Municipal Sludge. *Water Res* **2016**, *103*, 372–382. https://doi.org/10.1016/J.WATRES.2016.07.043.
(17) Palatsi, J.; Illa, J.; Prenafeta-Boldú, F. X.; Laureni, M.; Fernandez, B.; Angelidaki, I.; Flotats, X. Long-Chain Fatty Acids Inhibition and Adaptation Process in Anaerobic Thermophilic Digestion: Batch Tests, Microbial Community Structure and Mathematical Modelling. **2009**. https://doi.org/10.1016/j.biortech.2009.11.069.
(18) It MAHLER, B. H.; Wakil, S. J.; Bock, R. M. STUDIES ON FATTY ACID OXIDATION .
(19) Cirne, D. G.; Paloumet, X.; Björnsson, L.; Alves, M. M.; Mattiasson, B. Anaerobic Digestion of Lipid-Rich Waste—Effects of Lipid Concentration. *Renew Energy* **2007**, *32* (6), 965–975. https://doi.org/10.1016/J.RENENE.2006.04.003.
(20) Usman, M.; Zhao, S.; Jeon, B. H.; Salama, E. S.; Li, X. Microbial β-Oxidation of Synthetic Long-Chain Fatty Acids to Improve Lipid Biomethanation. *Water Res* **2022**, *213*, 118164. https://doi.org/10.1016/J.WATRES.2022.118164.
(21) Funk, J. A. *Evaluation of Two-Phase Anaerobic Digestion for Increased Sludge Handling Capacity and Energy Production at the F. Wayne Hill Water Resources Center*; 2021. https://tigerprints.clemson.edu/all_theses/3604.
(22) Heukelekian, A. H.; Mueller, P. Transformation of Some Lipids in Anaerobic Sludge Digestion. *Sewage Ind Waste* **1958**, *30* (9), 1108–1120.
(23) Lalman, J. A.; Bagley, D. M. Anaerobic Degradation and Inhibitory Effects of Linoleic Acid. *Water Res* **2000**, *34* (17), 4220–4228. https://doi.org/10.1016/S0043-1354(00)00180-9.
(24) NOVAK JT; CARLSON DA. Kinetics of Anaerobic Long Chain Fatty Acid Degradation. *Journal of the Water Pollution Control Federation* **1970**, *42* (11), 1932–1943.
(25) Beccari, M.; Majone, M.; Torrisi, L. Two-Reactor System with Partial Phase Separation for Anaerobic Treatment of Olive Oil Mill Effluents. *Water Science and Technology* **1998**, *38* (4–5), 53–60. https://doi.org/10.2166/wst.1998.0580.
(26) Sousa, D. Z.; Smidt, H.; Alves, M. M.; Stams, A. J. M. Ecophysiology of Syntrophic Communities That Degrade Saturated and Unsaturated Long-Chain Fatty Acids. *FEMS Microbiol Ecol* **2009**, *68* (3), 257–272. https://doi.org/10.1111/j.1574-6941.2009.00680.x.
(27) Zinder, S. Microbiology of Anaerobic Conversion of Organic Wastes to Methane: Recent Developments.
(28) Grady, C. P. L.; Daigger, G. T.; Love, N. G.; Filipe, C. D. M. *Biological Wastewater Treatment: Third Edition*; 2011.
(29) Shelton't And, D. R.; Tiedje12, J. M. *General Method for Determining Anaerobic Biodegradation Potentialt*; 1984; Vol. 47.
(30) Ben Khedher, N.; Lattieff, F. A.; Mahdi, J. M.; Ghanim, M. S.; Majdi, H. S.; Jweeg, M. J.; Baazaoui, N. Modeling of Biogas Production and Biodegradability of Date Palm Fruit Wastes with Different Moisture Contents. *J Clean Prod* **2022**, *375* (July), 134103. https://doi.org/10.1016/j.jclepro.2022.134103.
(31) Zwietering, M. H.; Jonegenburger, I.; Rombouts, F. M.; Van 'T Riets, K. Modeling of the Bacterial Growth Curve. *Appl Environ Microbiol* **1990**, *56* (6), 1875–1881. https://doi.org/10.1016/j.fm.2004.01.007.
(32) Inam, A.; Deniz, I. Introduction to Bioenergy; Current Status, Merits & Demerits. *Bioenergy Engineering: Fundamentals, Methods, Modelling, and Applications* **2023**, 1–15. https://doi.org/10.1016/B978-0-323-98363-1.00002-8.

(33) Ziels, R. M.; Beck, D. A. C.; Martí, M.; Gough, H. L.; Stensel, H. D.; Svensson, B. H. Monitoring the Dynamics of Syntrophic β-Oxidizing Bacteria during Anaerobic Degradation of Oleic Acidby Quantitative PCR. *FEMS Microbiol Ecol* **2015**, *91* (4), 1–13. https://doi.org/10.1093/femsec/fiv028.

(34) Burja, A. M.; Radianingtyas, H.; Windust, A.; Barrow, C. J. Isolation and Characterization of Polyunsaturated Fatty Acid Producing Thraustochytrium Species: Screening of Strains and Optimization of Omega-3 Production. *Appl Microbiol Biotechnol* **2006**, *72* (6), 1161–1169. https://doi.org/10.1007/s00253-006-0419-1.

(35) Caporaso, J. G.; Kuczynski, J.; Stombaugh, J.; Bittinger, K.; Bushman, F. D.; Costello, E. K.; Fierer, N.; Peña, A. G.; Goodrich, J. K.; Gordon, J. I.; Huttley, G. A.; Kelley, S. T.; Knights, D.; Koenig, J. E.; Ley, R. E.; Lozupone, C. A.; Mcdonald, D.; Muegge, B. D.; Pirrung, M.; Reeder, J.; Sevinsky, J. R.; Turnbaugh, P. J.; Walters, W. A.; Widmann, J.; Yatsunenko, T.; Zaneveld, J.; Knight, R. Correspondence QIIME Allows Analysis of High-Throughput Community Sequencing Data Intensity Normalization Improves Color Calling in SOLiD Sequencing. *Nature Publishing Group* **2010**, *7* (5), 335–336. https://doi.org/10.1038/nmeth0510-335.

(36) Lay, J.; Noike, T. *INFLUENCES OF PH AND MOISTURE CONTENT ON THE METHANE PRODUCTION IN HIGH-SOLIDS SLUDGE DIGESTION*; 1518; Vol. 31.

(37) Funk, J. A. The Importance of PH in Conversion of Long-Chain Fatty Acids (LCFA) During Anaerobic Co-Digestion of Municipal Solids with Fats, Oils, and Grease (FOG) Waste.

(38) Wu, C.; Liu, X.; Dong, X. Syntrophomonas Cellicola Sp. Nov., a Spore-Forming Syntrophic Bacterium Isolated from a Distilled-Spirit-Fermenting Cellar, and Assignment of Syntrophospora Bryantii to Syntrophomonas Bryantii Comb. Nov. *Int J Syst Evol Microbiol* **2006**, *56* (10), 2331–2335. https://doi.org/10.1099/ijs.0.64377-0.

(39) Sekiguchi, Y.; Kamagata, Y.; Harada, H. Recent Advances in Methane Fermentation Technology. *Curr Opin Biotechnol* **2001**, *12* (3), 277–282. https://doi.org/10.1016/S0958-1669(00)00210-X.

(40) Shukla, S. K.; Khan, A.; Rao, T. S. Microbial Fouling in Water Treatment Plants. *Microbial and Natural Macromolecules: Synthesis and Applications* **2021**, 589–622. https://doi.org/10.1016/B978-0-12-820084-1.00023-5.

(41) Nobu, M. K.; Narihiro, T.; Kuroda, K.; Mei, R.; Liu, W. T. Chasing the Elusive Euryarchaeota Class WSA2: Genomes Reveal a Uniquely Fastidious Methyl-Reducing Methanogen. *ISME Journal* **2016**, *10* (10), 2478–2487. https://doi.org/10.1038/ismej.2016.33.

(42) Pelletier, E.; Kreimeyer, A.; Bocs, S.; Rouy, Z.; Gyapay, G.; Chouari, R.; Rivière, D.; Ganesan, A.; Daegelen, P.; Sghir, A.; Cohen, G. N.; Médigue, C.; Weissenbach, J.; Le Paslier, D. "Candidatus Cloacamonas Acidaminovorans": Genome Sequence Reconstruction Provides a First Glimpse of a New Bacterial Division. *J Bacteriol* **2008**, *190* (7), 2572–2579. https://doi.org/10.1128/JB.01248-07.

(43) Nakasaki, K.; Nguyen, K. K.; Ballesteros, F. C.; Maekawa, T.; Koyama, M. Characterizing the Microbial Community Involved in Anaerobic Digestion of Lipid-Rich Wastewater to Produce Methane Gas. *Anaerobe* **2020**, *61*, 102082. https://doi.org/10.1016/J.ANAEROBE.2019.102082.

(44) Sun, L.; Toyonaga, M.; Ohashi, A.; Matsuura, N.; Tourlousse, D. M.; Meng, X. Y.; Tamaki, H.; Hanada, S.; Cruz, R.; Yamaguchi, T.; Sekiguchi, Y. Isolation and Characterization of Flexilinea Flocculi Gen. Nov., Sp. Nov., a Filamentous, Anaerobic Bacterium Belonging to

the Class Anaerolineae in the Phylum Chloroflexi. *Int J Syst Evol Microbiol* **2016**, *66* (2), 988–996. https://doi.org/10.1099/ijsem.0.000822.

(45) Zhou, L.; Liu, X.; Dong, X. Methanospirillum Psychrodurum Sp. Nov., Isolated from Wetland Soil. *Int J Syst Evol Microbiol* **2014**, *64* (PART 2), 638–641. https://doi.org/10.1099/ijs.0.057299-0.

(46) Könönen, E.; Jalava, J. Peptostreptococcus. In *Molecular Detection of Human Bacterial Pathogens*; CRC Press, 2011; pp 423–435. https://doi.org/10.1002/9781118960608.gbm00668.

(47) Yutin, N.; Galperin, M. Y. A Genomic Update on Clostridial Phylogeny: Gram-Negative Spore Formers and Other Misplaced Clostridia. *Environ Microbiol* **2013**, *15* (10), 2631–2641. https://doi.org/10.1111/1462-2920.12173.

(48) Rinke, C.; Schwientek, P.; Sczyrba, A.; Ivanova, N. N.; Anderson, I. J.; Cheng, J. F.; Darling, A.; Malfatti, S.; Swan, B. K.; Gies, E. A.; Dodsworth, J. A.; Hedlund, B. P.; Tsiamis, G.; Sievert, S. M.; Liu, W. T.; Eisen, J. A.; Hallam, S. J.; Kyrpides, N. C.; Stepanauskas, R.; Rubin, E. M.; Hugenholtz, P.; Woyke, T. Insights into the Phylogeny and Coding Potential of Microbial Dark Matter. *Nature* **2013**, *499* (7459), 431–437. https://doi.org/10.1038/nature12352.

(49) Speirs, L. B. M.; Rice, D. T. F.; Petrovski, S.; Seviour, R. J. The Phylogeny, Biodiversity, and Ecology of the Chloroflexi in Activated Sludge. *Frontiers in Microbiology*. Frontiers Media S.A. September 13, 2019. https://doi.org/10.3389/fmicb.2019.02015.

(50) CD Genomics. *Principal Component Analysis (PCA) and Principal Coordinate Analysis (PCoA) for Microbial Sequencing: Introduction and Procedures*. CD Genomics.

(51) Jin, Q.; Bethke, C. M. The Thermodynamics and Kinetics of Microbial Metabolism. *Am J Sci* **2007**, *307* (4), 643–677. https://doi.org/10.2475/04.2007.01.

A. Appendix A

Predicted methane production was calculated considering both acetoclastic and hydrogenotrophic methanogenesis. An example of how methane production was calculated for 2 g/L COD stearic acid is shown below. This method can also be applied to 4 and 6 g/L COD and 2, 4, and 6 g/L COD palmitic, myristic, linoleic, and oleic acid.

The following reaction is used to convert g/L COD stearic acid to mol/L stearic acid.

$C_{18}H_{36}O_2 + 26O_2 \rightarrow 12CO_2 + 18H_2O$

$$\frac{2\text{ g COD}}{\text{L}} \times \frac{\text{mol } O_2}{32\text{ g}} \times \frac{1\text{ mol stearic acid}}{26\text{ mol } O_2} = 0.0024 \frac{\text{mol stearic acid}}{\text{L}}$$

Next, the moles of acetate and H_2 that will be generated from 0.002 mol/L of stearic acid per 0.18 L bottle was calculated. Using the following reaction, it was determined that 9 moles of acetate are generated per 1 mole of stearic acid and 16 moles of H_2 are generated per 1 mole of stearic acid.

$C_{18}H_{36}O_2 + 16H_2O \rightarrow 9C_2H_4O_2 + 16H_2$

$$\frac{0.0024\text{ mol stearic acid}}{\text{L}} \times \frac{9\text{ mol acetate}}{1\text{ mol stearic acid}} = 0.022 \frac{\text{mol acetate}}{\text{L}}$$

$$\frac{0.0024\text{ mol stearic acid}}{\text{L}} \times \frac{16\text{ mol acetate}}{1\text{ mol stearic acid}} = 0.0384 \frac{\text{mol acetate}}{\text{L}}$$

Based on acetoclastic methanogenesis, the following reaction and equations can be used to calculate mL of methane generated from the acetate produced.

$C_2H_4O_2 \rightarrow CO_2 + CH_4$

$$\frac{0.022\text{ mol acetate}}{\text{L}} \times \frac{0.18\text{ L}}{\text{bottle}} \times \frac{1\text{ mol CH4}}{1\text{ mol acetate}} \times \frac{16.04\text{ g}}{\text{mol}} \times \frac{\text{mL}}{0.00067\text{ g}} = 93.23.\text{mL CH4}$$

Based on hydrogenotrophic methanogenesis, the following reaction and equations can be used to calculate mL of methane generated from the hydrogen produced.

$CO_2 + 4H_2 \rightarrow CH_4 + 2\ H_2O$

$$\frac{0.0384\ \text{mol}\ H_2}{\text{L}} \times \frac{0.18\ \text{L}}{\text{bottle}} \times \frac{1\ \text{mol CH4}}{4\ \text{mol}\ H_2} \times \frac{16.04\ \text{g}}{\text{mol}} \times \frac{\text{mL}}{0.00067\ \text{g}} = 23.31\ \text{mL CH4}$$

Based on acetoclastic and hydrogenotrophic methanogenesis, 116.5 mL of methane was predicted in the 2 g/L stearic acid assays. x

B. Appendix B

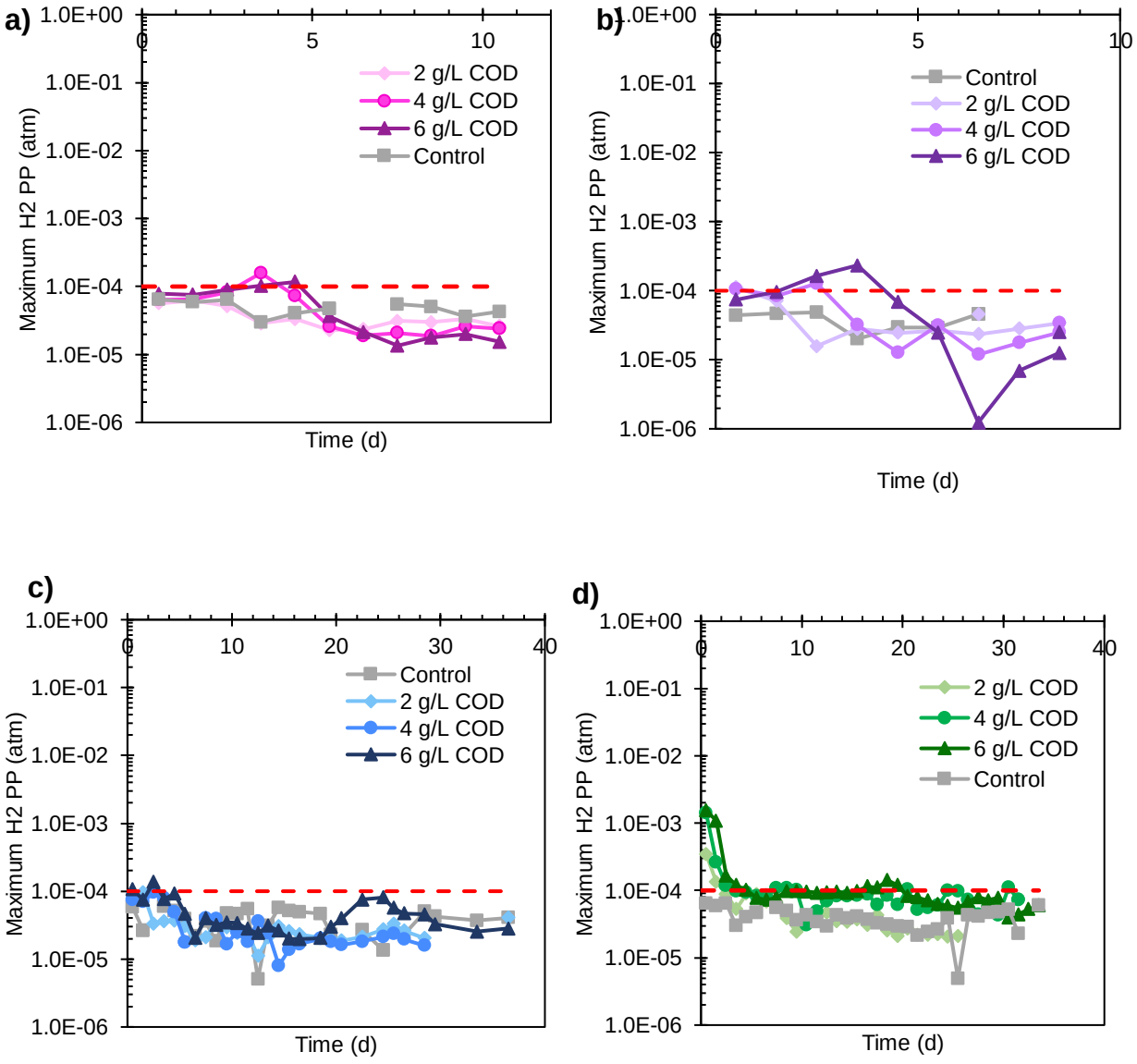
a)
1.0E+00
1.0E-01
1.0E-02
1.0E-03
1.0E-04
1.0E-05
1.0E-06
Maximum H2 PP (atm)
0
5
10
Time (d)
2 g/L COD
4 g/L COD
6 g/L COD
Control
b)
1.0E+00
1.0E-01
1.0E-02
1.0E-03
1.0E-04
1.0E-05
1.0E-06
Maximum H2 PP (atm)
0
5
10
Time (d)
Control
2 g/L COD
4 g/L COD
6 g/L COD
c)
1.0E+00
1.0E-01
1.0E-02
1.0E-03
1.0E-04
1.0E-05
1.0E-06
Maximum H2 PP (atm)
0
10
20
30
40
Time (d)
Control
2 g/L COD
4 g/L COD
6 g/L COD
d)
1.0E+00
1.0E-01
1.0E-02
1.0E-03
1.0E-04
1.0E-05
1.0E-06
Maximum H2 PP (atm)
0
10
20
30
40
Time (d)
2 g/L COD
4 g/L COD
6 g/L COD
Control

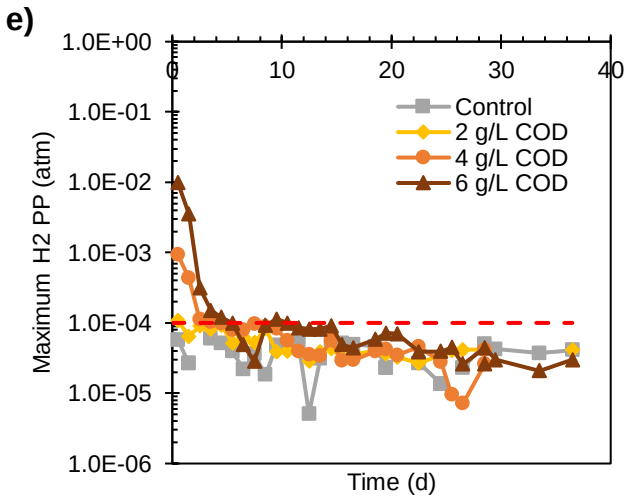

Figure B.1: Maximum hydrogen partial pressure of a) stearic acid, b) palmitic acid, c) myristic acid, d) linoleic acid, and e) oleic acid assays. The partial pressure should stay below the red dashed line to maintain thermodynamically favorable conditions.

C. Appendix C

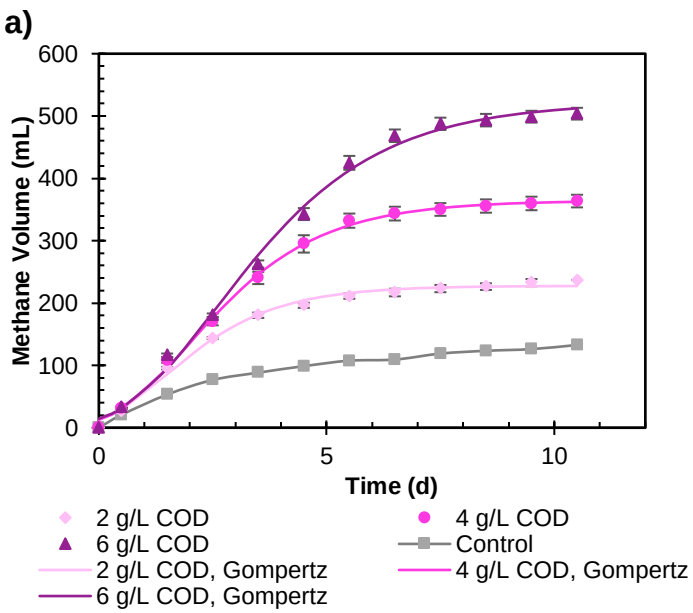
a)
Methane Volume (mL)
Time (d)
2 g/L COD
4 g/L COD
6 g/L COD
Control
2 g/L COD, Gompertz
4 g/L COD, Gompertz
6 g/L COD, Gompertz

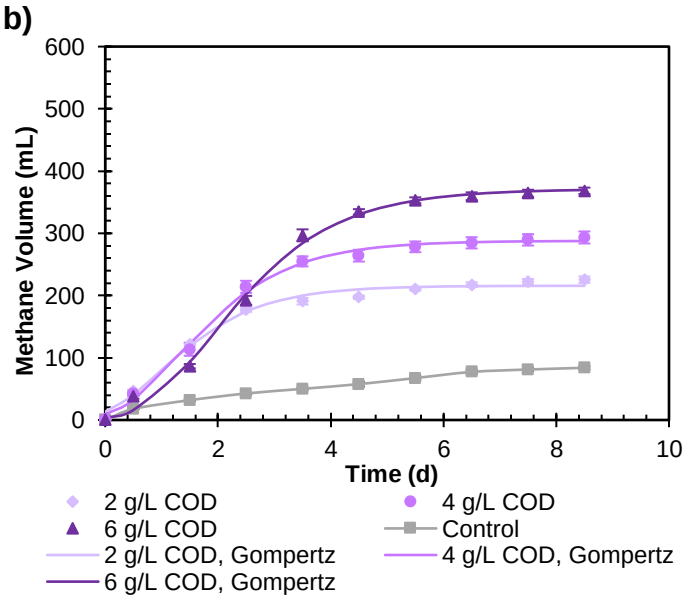
b)
Methane Volume (mL)
Time (d)
2 g/L COD
4 g/L COD
6 g/L COD
Control
2 g/L COD, Gompertz
4 g/L COD, Gompertz
6 g/L COD, Gompertz

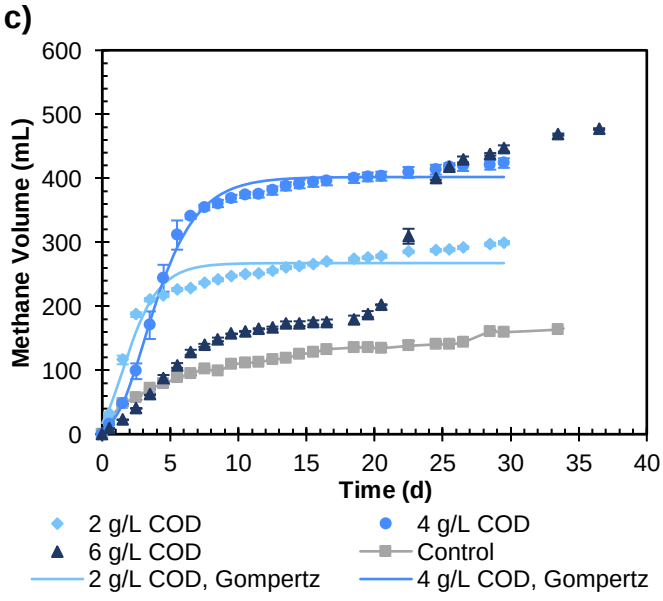
c)
Methane Volume (mL)
Time (d)
2 g/L COD
4 g/L COD
6 g/L COD
Control
2 g/L COD, Gompertz
4 g/L COD, Gompertz

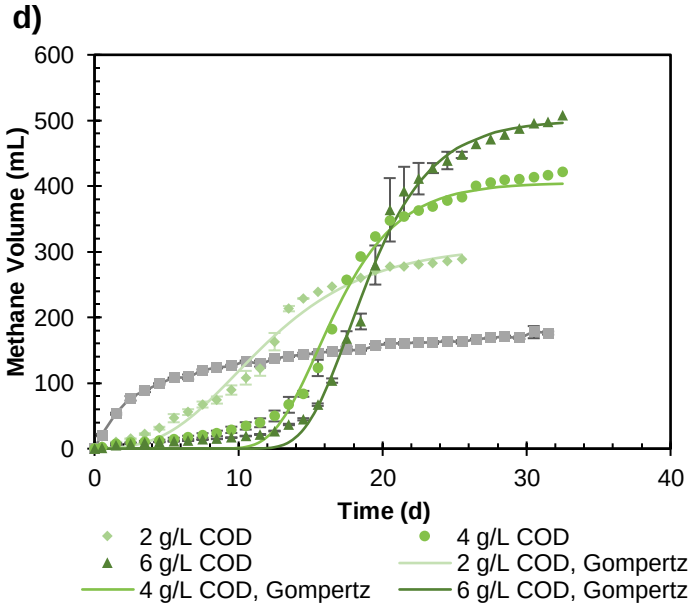
d)
Methane Volume (mL)
Time (d)
2 g/L COD
4 g/L COD
6 g/L COD
2 g/L COD, Gompertz
4 g/L COD, Gompertz
6 g/L COD, Gompertz

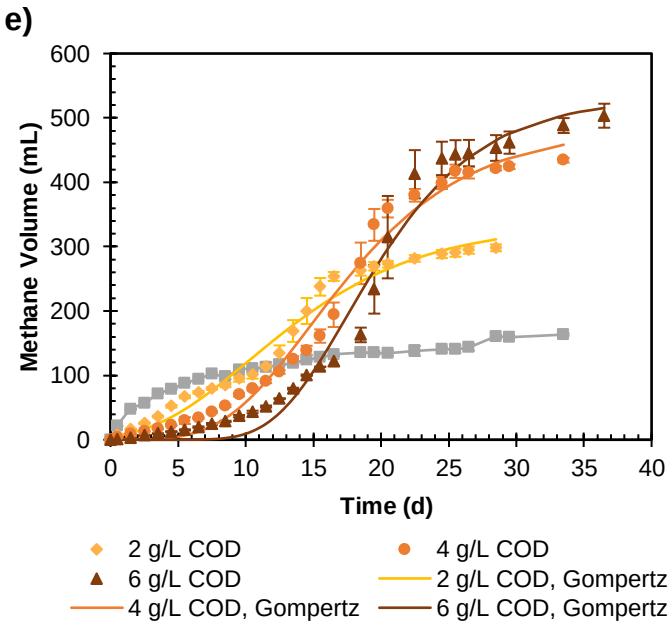

Figure C.1: Methane production volume fitted to Gompertz model for assays spiked with a) stearic acid, b) palmitic acid, c) myristic acid, d) linoleic acid, and e) oleic acid All curves were fit with $R2 \geq 0.94$.

D. Appendix D

ANOVA tests were performed to determine the statistical significance when comparing lag times and apparent degradation rates. The summary and ANOVA statistics tables for the lag times, grouped by acid are shown in Table D.1 and Table D.2. These two tables were generated using ANOVA: Single Factor data analysis tool in excel. Since p-value was less that 0.05 a post-ANOVA analysis was required. The post-ANOVA analysis results for the lag times grouped by acid are shown in Table D.3. The absolute mean difference is the difference in means between the averages of the two acids being compared. The $Q_{\text{critical value}}$ was calculated using the following formula

$$Q_{\text{critial value}} = Q \times \sqrt{s^2_{\text{pooled}}/_{\text{n.}}}$$

Q = value from studentized range Q table

s^2_{pooled} = pooled variances among all groups

n. = sample size for a given group

If the absolute difference in means is greater than the $Q_{\text{critical value}}$, then the difference in means is statistically significant.

Table D.1: Summary table of lag times grouped by acid.

Groups	*Count*	*Sum*	*Average*	*Variance*
Linoleic Acid	3	4.1650	1.3883	0.4467
Oleic Acid	3	4.7278	1.5759	0.5591
Stearic Acid	3	0.6500	0.2167	0.0004
Palmitic Acid	3	1.9071	0.6357	0.0024
Myristic Acid	3	1.9000	0.6333	0.1975

Table D.2: ANOVA statistics output for lag times grouped by acid, including p-value.

Source of Variation	*SS*	*df*	*MS*	*F*	*P-value*	*F crit*
Between Groups	683.51	4	170.88	33.73	0.00	3.48
Within Groups	50.65	10	5.07			
Total	734.17	14				

Table D.3: Post-ANOVA analysis results for comparison of mean lag times based on acid.

Comparison	Abs. Mean Diff	Q Critical Value	Significant?
Linoleic vs Oleic	1.16	12.90	No
Linoleic vs Stearic	14.28	12.90	Yes
Linoleic vs Palmitic	15.03	12.90	Yes
Linoleic vs Myristic	14.32	12.90	Yes
Oleic vs Stearic	13.11	12.90	Yes
Oleic vs Palmitic	13.87	12.90	Yes
Oleic vs Myristic	13.16	12.90	Yes
Stearic vs Palmitic	0.76	12.90	No
Stearic vs Myristic	0.04	12.90	No
Palmitic vs Myristic	0.10	12.90	No

Using the same method described above, the mean lag times were statistically compared based on concentration. The summary and ANOVA statistics tables for the lag times, grouped by concentration are shown in Table D.4 and Table D.5. These two tables were generated using ANOVA: Single Factor data analysis tool in excel. Since the p-value was greater than 0.05, post-ANOVA analysis was not required.

Table D.4: Summary table of lag times grouped by concentration.

Groups	*Count*	*Sum*	*Average*	*Variance*
2 g/L COD	5	22.79	4.56	33.79
4 g/L COD	5	32.41	6.48	56.54
6 g/L COD	5	37.75	7.55	87.47

Table D.5: ANOVA statistics output for lag times grouped by concentration, including p-value.

Source of Variation	*SS*	*df*	*MS*	*F*	*P-value*	*F crit*
Between Groups	22.98	2	11.49	0.19	0.83	3.89
Within Groups	711.19	12	59.27			
Total	734.17	14				

Using the same method described above, the apparent degradation rate constants were statistically compared based on acid. The summary and ANOVA statistics tables for the apparent degradation rate constants, grouped by acid are shown in Table D.6 and Table D.7. These two tables were generated using ANOVA: Single Factor data analysis tool in excel. Since the p-value was less than 0.05, post-ANOVA analysis was required. The post-ANOVA analysis results for the apparent degradation rate constants grouped by acid are shown in Table D.8. The same equation described above was used for these calculations.

Table D.6: Summary table of apparent degradation rate constants grouped by acid.

Groups	*Count*	*Sum*	*Average*	*Variance*
Linoleic Acid	3	4.17	1.39	0.4467
Oleic Acid	3	4.73	1.58	0.5591
Stearic Acid	3	0.65	0.22	0.0004
Palmitic Acid	3	1.91	0.64	0.0024
Myristic Acid	3	1.90	0.63	0.1975

Table D.7: ANOVA statistics output for apparent degradation rate constants grouped by acid, including p-value.

Source of Variation	*SS*	*df*	*MS*	*F*	*P-value*	*F crit*
Between Groups	3.91	4	0.98	4.05	0.03	3.48
Within Groups	2.41	10	0.24			
Total	6.32	14				

Table D.8: Post-ANOVA analysis results for comparison of apparent degradation rate constants based on acid.

Comparison	Abs. Mean Diff	$Q_{\text{Critical Value}}$	Significant?
Linoleic vs Oleic	0.19	0.61	No
Linoleic vs Stearic	1.17	0.61	Yes
Linoleic vs Palmitic	1.39	0.61	Yes
Linoleic vs Myristic	0.76	0.61	Yes
Oleic vs Stearic	1.36	0.61	Yes
Oleic vs Palmitic	1.58	0.61	Yes
Oleic vs Myristic	0.94	0.61	Yes
Stearic vs Palmitic	0.22	0.61	No
Stearic vs Myristic	0.42	0.61	No
Palmitic vs Myristic	0.00	0.61	No

E. Appendix E

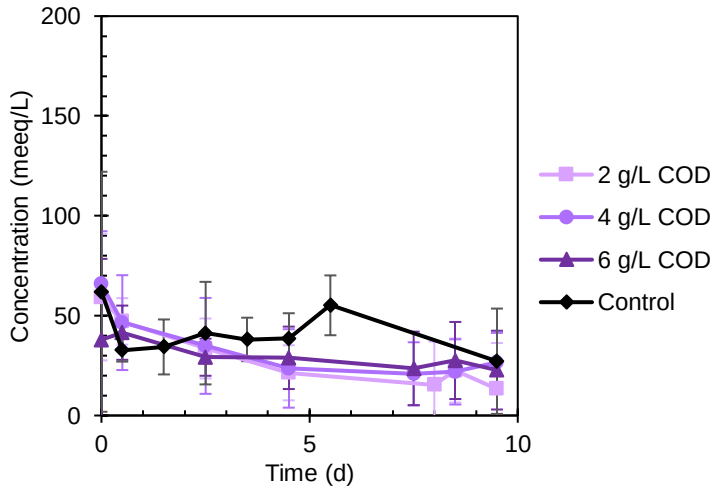

Figure E.1: Palmitic acid data from the stearic acid assays and the control.

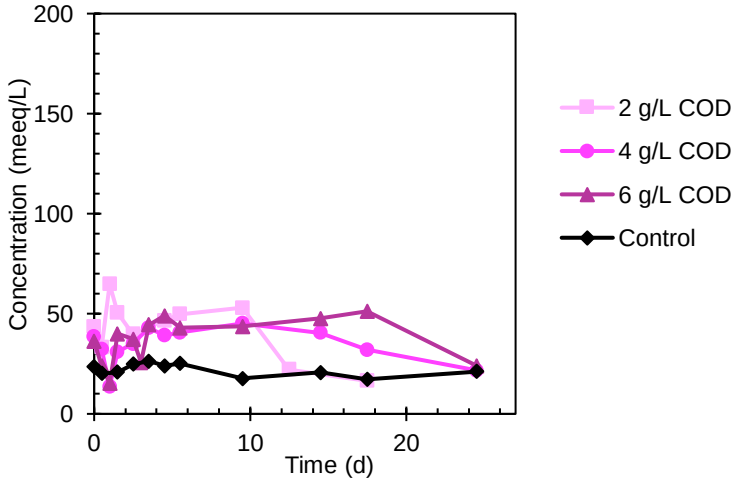

Figure E.2: Stearic acid data from the linoleic acid assays and the control.

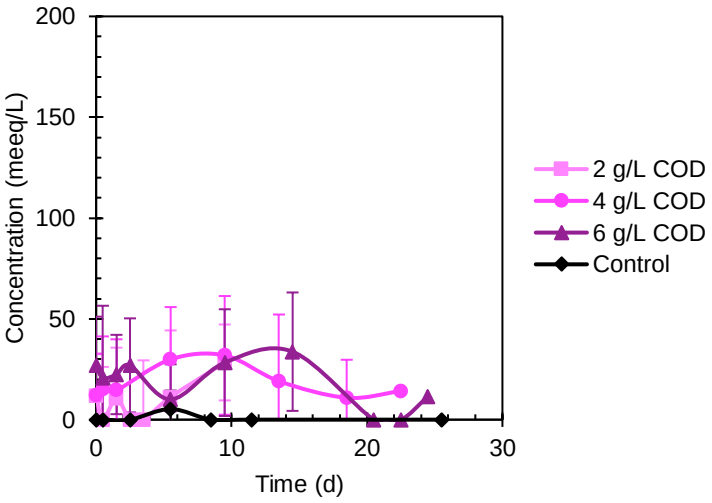

Figure E.3: Stearic acid data from the oleic acid assays and the control.

F. Appendix F

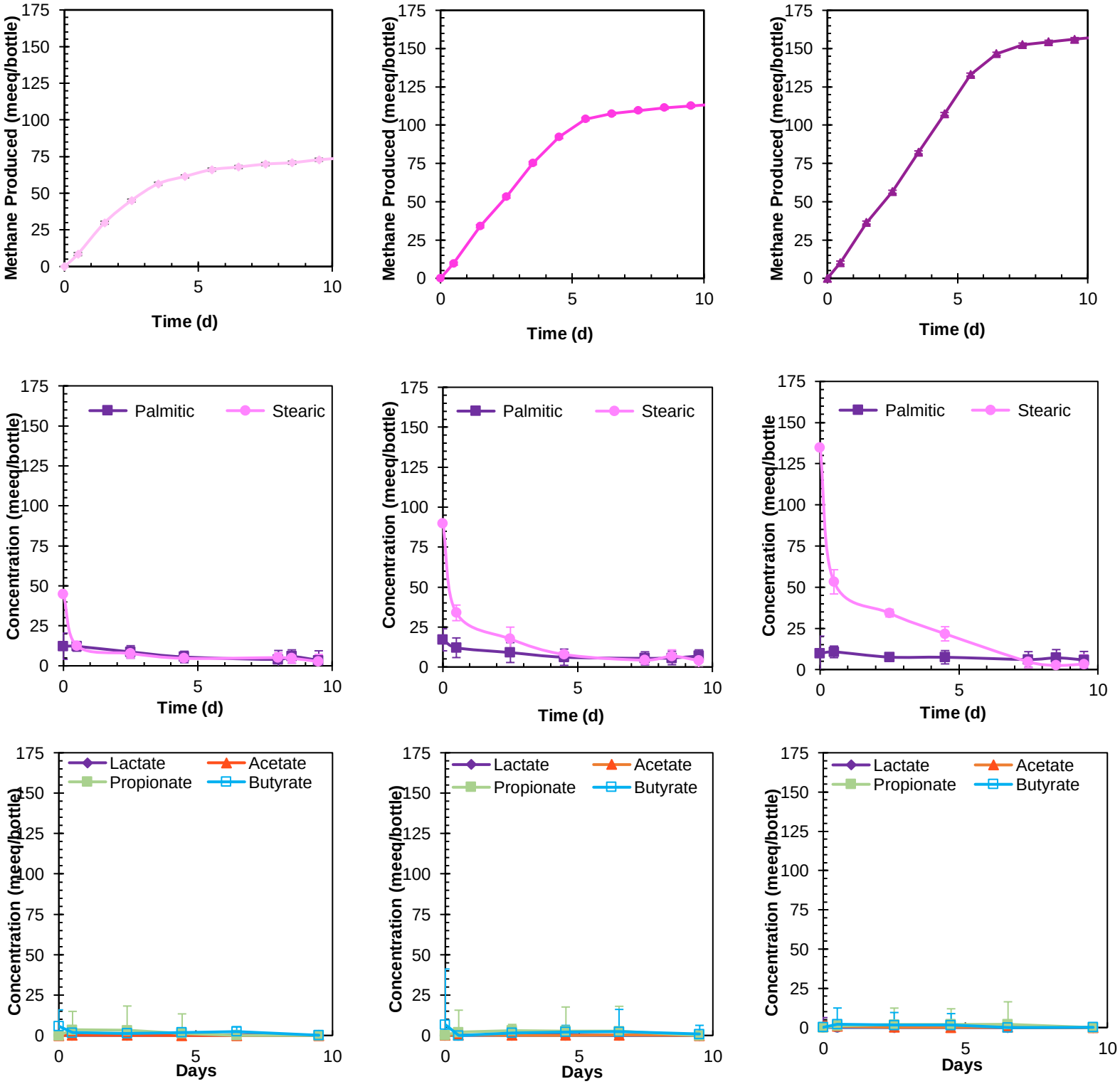

Figure F.1: All methane (row 1), LCFA (row 2), and VFA (row 3) data in meeq/bottle for stearic acid 2 g/L COD (column 1), 4 g/L COD(column 2), and 6 g/L COD(column 3).

G. Appendix G

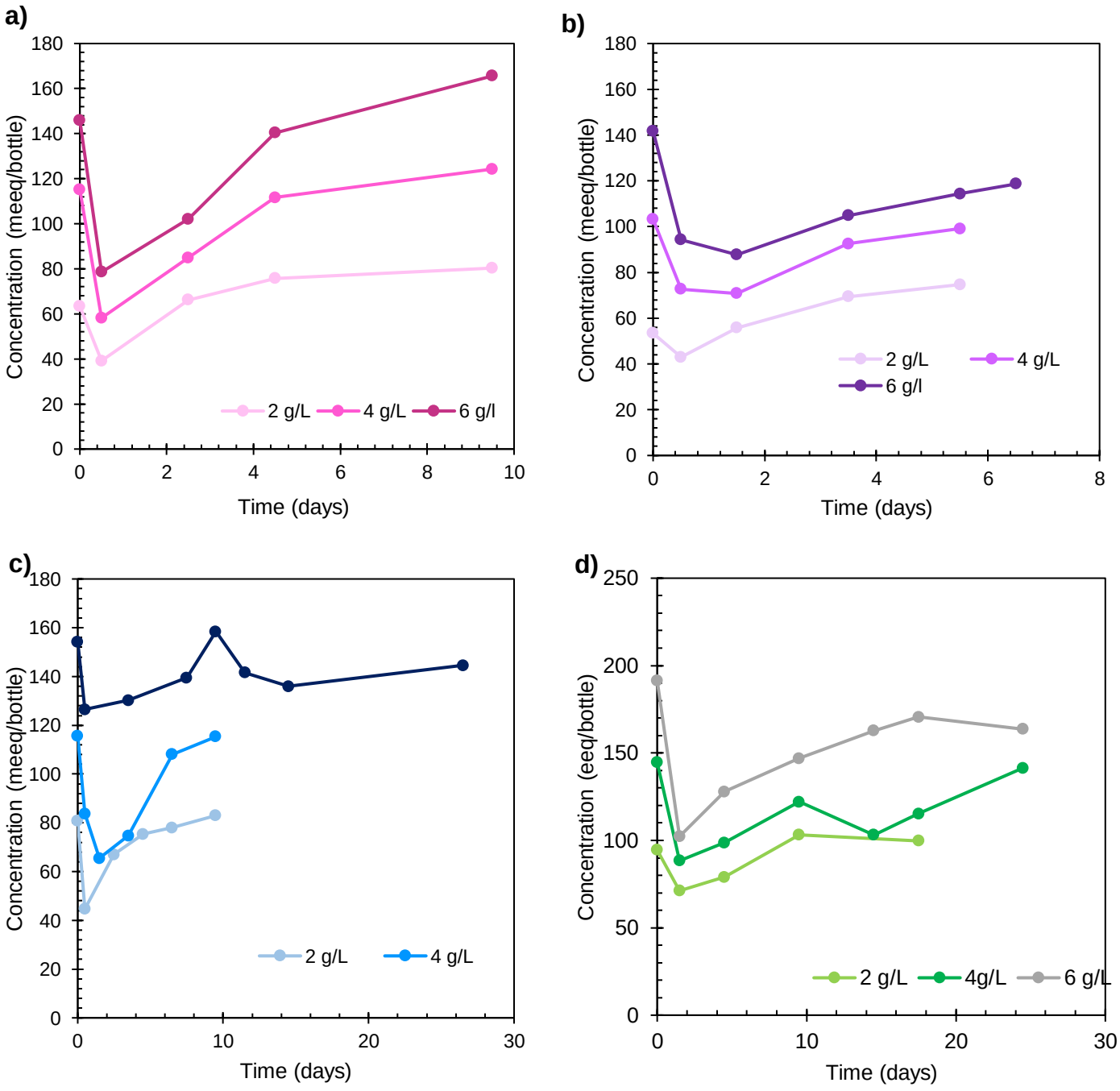
a)
Concentration (meeq/bottle)
Time (days)
2 g/L
4 g/L
6 g/l
b)
Concentration (meeq/bottle)
Time (days)
2 g/L
4 g/L
6 g/l
c)
Concentration (meeq/bottle)
Time (days)
2 g/L
4 g/L
d)
Concentration (eeq/bottle)
Time (days)
2 g/L
4g/L
6 g/L

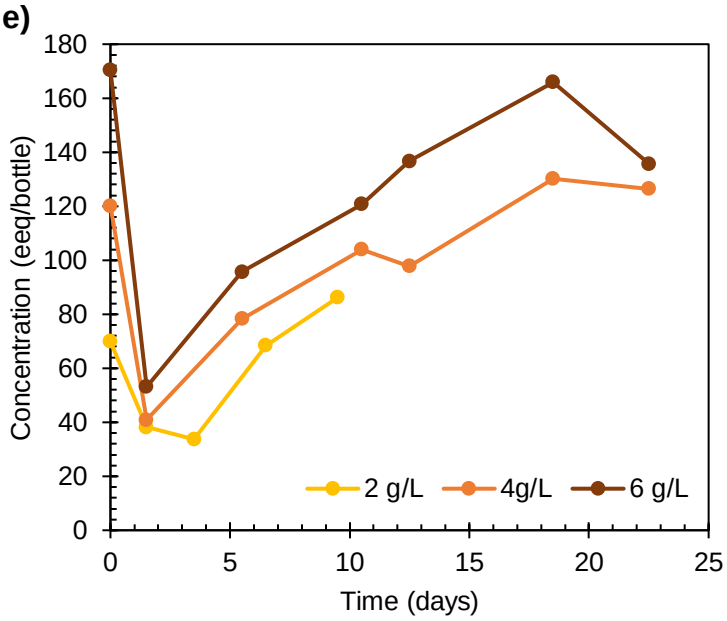

Figure G.1: The total eeq/bottle in a) stearic, b) palmitic, c) myristic, d) linoleic, and e) oleic assays. Eeq/bottle includes methane, LCFA, and VFA eeq.